CALIFORNIA PATH PROGRAM
INSTITUTE OF TRANSPORTATION STUDIES
UNIVERSITY OF CALIFORNIA, BERKELEY

Development and Evaluation of Selected Mobility Applications for VII

Steven E. Shladover, Xiao-Yun Lu, Christopher Nowakowski, and Dongyan Su

California PATH Research Report

UCB-ITS-PRR-2011-09

Disclaimer

This document is disseminated in the interest of information exchange. The contents of this report reflect the views of the authors who are responsible for the facts and accuracy of the data presented herein. The contents do not necessarily reflect the official views or policies of the State of California. This publication does not constitute a standard, specification or regulation. This report does not constitute an endorsement by the Department of any product described herein. For individuals with sensory disabilities, this document is available in Braille, large print, audiocassette, or compact disk. To obtain a copy of this document in one of these alternate formats, please contact: the Division of Research and Innovation, MS-83, California Department of Transportation, P.O. Box 942873, Sacramento, CA 94273-0001.

July 2011

CALIFORNIA PARTNERS FOR ADVANCED TRANSPORTATION TECHNOLOGY

Development and Evaluation of Selected Mobility Applications for VII

PATH Research Report on
Contract 65A0351

July 2011

Steven E. Shladover, Xiao-Yun Lu, Christopher Nowakowski,
and Dongyan Su

Abstract

This report describes the development of two of the three mobility applications that PATH has developed and evaluated under the sponsorship of the FHWA Exploratory Advanced Research Program, with cost share funding provided by Caltrans Contract 65A0351. These applications are intended to use DSRC wireless communications among vehicles and between vehicles and the roadway infrastructure to improve mobility on limited-access highways. The first application combines ramp metering with variable speed limits to enhance control of traffic so that traffic flow breakdowns can be deferred or avoided at bottleneck locations. The second application uses vehicle-vehicle communication to improve the performance of adaptive cruise control systems so that they can operate safely with smaller longitudinal gaps and vehicle-roadside communication to provide adjustments to their set speed and gap settings to adapt to changes in local traffic conditions.

Key Words: active traffic management, variable speed limits, adaptive cruise control, cooperative adaptive cruise control, DSRC applications

Executive Summary

This report describes the development of two of the three mobility applications that PATH has developed and evaluated under the sponsorship of the FHWA Exploratory Advanced Research Program, with cost share funding provided by Caltrans Contract 65A0351. These applications are intended to use DSRC wireless communications among vehicles and between vehicles and the roadway infrastructure to improve mobility on limited-access highways. The first application combines ramp metering with variable speed limits to enhance control of traffic so that traffic flow breakdowns can be deferred or avoided at bottleneck locations. The second application uses vehicle-vehicle communication to improve the performance of adaptive cruise control systems so that they can operate safely with smaller longitudinal gaps and vehicle-roadside communication to provide adjustments to their set speed and gap settings to adapt to changes in local traffic conditions.

Variable Speed Limits

The selection of variable speed limits (VSL) to reduce traffic breakdowns is based on careful modeling of the traffic dynamics and estimation of the probability of breakdown as a function of traffic speed and density. The work reported here extends the work that was reported earlier in the final report on PATH Task Order 6224, including microscopic as well as mesoscopic simulation, and leading to a real-time implementation using measured data collected along the I-80 corridor from Richmond to Emeryville, CA.

The VSL values chosen by the algorithm developed here were broadcast to a test vehicle driven along the I-80 corridor by 16 drivers from the general public, and their reactions to the VSL information were captured by recording data about their driving behavior and collecting their responses to a questionnaire. These results indicated that although the VSL concept is very promising, the implementation needs to provide for better filtering of noisy and inconsistent data so that drivers receive a display of VSL values that are stable in location and time and appear believable to the drivers.

Cooperative Adaptive Cruise Control

The initial results of the human factors experiment involving naïve drivers from the general public driving the production adaptive cruise control system and the new cooperative adaptive cruise control (CACC) system were reported in the TO 6224 final report. The combined results from the entire experiment are summarized here, in the distributions of the time gaps that the drivers selected when using both systems. The most significant of these results is that the mean time gap value when using CACC was 45% of the gap selected using ACC, indicating the potential for significant highway capacity increases.

The distributions of the time gaps that drivers selected using both systems were incorporated into a microscopic traffic simulation using the NGSIM oversaturated flow model for manually driven vehicles, in the Aimsun traffic simulation environment. The ACC and CACC car following

behaviors were modeled, and some of the manually driven vehicles were also represented as being capable of broadcasting their own status information ("Here I Am"), so that they could serve as leaders for CACC followers. The market penetrations of the four categories of vehicles were varied to show the trends in highway lane capacity that could be achieved for each scenario. The net result is that if all vehicles were equipped for CACC driving, the capacity could increase to 4000 vehicles per lane per hour, nearly doubling the effective capacity achieved today with manual driving. The increases at intermediate market penetrations are not as significant, but they can be helped to grow by the addition of "Here I Am" communication capabilities to other vehicles through inexpensive retrofit devices.

Applicability of Results to Transportation Problems

It appears, based on our simulation results, that variable speed limits have significant promise as a strategy to help delay or avoid traffic breakdowns, and they should be seriously considered for a full-scale field test to demonstrate how they would work in practice. The input data describing real-time traffic conditions need to be accurate and reliable in order to produce VSL values that will be credible enough to induce drivers to adjust their own driving speeds, so attention needs to be given to how to improve these data and how to filter and smooth data that have problems.

Drivers are very comfortable with the shorter gap settings provided by the CACC system, which means that widespread use of CACC offers the possibility of significantly increasing the capacity of a highway lane and reducing shock wave disturbances in traffic.

Table of Contents

Abstract i
Key Words: i
Executive Summary iii
List of Figures vii
List of Tables ix
1. Introduction to Traffic Control Issues 1
2. Literature Review 3
2.1 Ramp Metering 3
2.2 VSL Strategies 3
2.3 Combined VSL and RM 4
2.4 Microscopic Traffic Modeling and Simulation 5
2.4.1 Microscopic Traffic Model 5
2.4.2 Calibration of the Car-following Model 5
2.4.3 Traffic Simulation for VSL and CRM 5
3. Higher Level Control Strategy 7
3.1 Recurrent Bottleneck Characteristics 7
3.2 Control Objective and Strategy 8
4. Tightly Coupled VSL and Coordinated Ramp Metering 9
4.1 Modeling 9
4.2 Constraints 9
4.3 Objective Function 10
4.4 MPC Design for VSL 10
4.5 Model Calibration and Simulation 11
4.6 Further Remarks 13
5. Combined VSL and Coordinated Ramp Metering 15
5.1 Overall System Structure 15
5.2 VSL Design 17
5.2.1 Design VSL Upstream of Congestion Tail to Harmonize Traffic 17
5.2.2 Determine Critical VSL and L_{dis} 19
5.2.3 Determine $(V_{st}, \rho_{st}, L_{st})$ for Stage 2 20
5.2.4 Discharge Section Clearing 20
5.3 CRM Design with MPC 21
5.3.1 Modeling 21
5.3.2 Constraints 22
5.3.3 Objective Function 23
5.4 Integrated Traffic Control Simulation Platform (ITCSP) Development 23
5.4.1 Overall System Structure 23
5.4.2 Microscopic Traffic Modeling for Simulation 24
5.4.3 Model of I-80W PM Peak Traffic 27
5.4.4 Simulation Setup 28
5.4.5 Control Scenarios and Results 30
6. Field Testing of VSL Display in Vehicles 35
6.1 Experiment Protocol 35
6.1.1 Overview 35

6.1.2 Test Participants 35
6.1.3 VSL Experiment Test Route 36
6.1.4 Test Vehicle 38
6.1.5 Test Procedures 41
6.2 Experimental Results 42
6.2.1 Overview 42
6.2.2 Time in Zone & Advisory Speed Stability 43
6.2.3 Advisory Speed Profile 48
6.2.4 Driver Acceptance of Advisory Speeds 51
6.2.5 VSL Survey Results 57
7. Concluding Remarks about VSL/VSA 59
8. Introduction to Adaptive Cruise Control and Cooperative Adaptive Cruise Control Simulation Study 61
9. Vehicle Types to be Simulated 63
10. The Microsimulation Platform 65
11. Control Algorithm of ACC/CACC Vehicles 67
12. Manual Driving Model 69
13. A Freeway Section Model with Simplified Road Geometry 71
14. Simulation Scenarios and Results 73
15. Concluding Remarks about Cooperative Adaptive Cruise Control 81
References 83
Appendix A – Consent Materials 87
Appendix B – Post-Experiment Questionaire 91
Appendix C – Driver Compliance with Advisory Speeds in Zones 1, 3, and 5 93

List of Figures

Figure 3.1 Bottleneck characteristics and control strategy 7
Figure 3.2 I-80 West PM peak section (L); 8
Figure 4.1 MPC scheme to determine VSL 11
Figure 4.2 BHL Section of I-80 with Two VSL Sign Locations 12
Figure 4.3 Comparison of Flows, Speeds and Densities With and Without VSL at Station 2 13
Figure 5.1 Flow chart of overall system: measurement and control design 15
Figure 5.2 Schematic VSL control strategy at Stage 1 (L), and Stage 2 (R) 18
Figure 5.3 Empirical traffic speed drop probability contour vs. flow contour 22
Figure 5.4 Overall Structure of ITCSP 24
Figure 5.5 Examples of Simulated and Observed Speed and Trajectory in the Calibration 26
Figure 5.6 Distribution of the RMSPe 27
Figure 5.7 I-80 westbound, the simulated segment 28
Figure 5.8 Software structure 29
Figure 5.9 Delay Performance of Control Strategies in Simulation 31
Figure 5.10 Total Travel Time Performance of Control Strategies in Simulation 31
Figure 5.11 Total Distance Traveled (VMT) Performance of Control Strategies in Simulation . 32
Figure 5.12 Speed Performance of Control Strategies in Simulation 32
Figure 6.1 VSL Experiment Test Route 36
Figure 6.2 Overall System Structure for Preliminary Experimental Implementation of VSL with Feedback to the Driver on the CACC Vehicle 37
Figure 6.3 Vehicle Interior, Showing Locations of Video Cameras. 38
Figure 6.4 Variable Speed Limit Display. 39
Figure 6.5 Example of video file content (left is front view, right is quad view) 39
Figure 6.6 ACC display and controls as illustrated in vehicle owner's manual 40
Figure 6.7 ACC displays (left) and controls (right) 40
Figure 6.8 Durations of Time in Zone and Time that the Advisory Speed was Constant. 44
Figure 6.9 Duration of Time in Zone 1 and Time that Advisory Speed was Constant in Zone 1. 44
Figure 6.10 Duration of Time in Zone 2 and Time that Advisory Speed was Constant in Zone 2. 45
Figure 6.11 Duration of Time in Zone 3 and Time that Advisory Speed was Constant in Zone 3. 45
Figure 6.12 Duration of Time in Zone 4 and Time that Advisory Speed was Constant in Zone 4. 46
Figure 6.13 Duration of Time in Zones 5, 6, and 7 and Time that the Advisory Speed was Constant in Each. 47
Figure 6.14 Advisory Speed by Zone. 48
Figure 6.15 Advisory Speed Change Step Sizes. 49
Figure 6.16 Advisory Speed Changes at Each Zone 50
Figure 6.17 Driver Compliance with Advisory Speeds Across All Zones. 52
Figure 6.18 Driver Compliance with Advisory Speeds in Zone 2. 53
Figure 6.19 Driver Compliance with Advisory Speeds in Zone 4. 54
Figure 6.20 Driver Compliance with Advisory Speeds in Zone 6. 55
Figure 6.21 Driver Compliance with Advisory Speeds in Zone 7. 56
Figure 13.1 Distribution of time gap settings for CACC and ACC chosen by drivers while car following in field test 72

Figure 14.1 Highway Lane Capacity (Vehicles/Hour) as a Function of Changes in ACC Market Penetration 73
Figure 14.2 Highway Lane Capacity (Vehicles/Hour) as a Function of Changes in CACC Market Penetration Relative to Manually Driven Vehicles 74
Figure 14.3 Highway Lane Capacity (Vehicles/Hour) as a Function of Changes in CACC Market Penetration Relative to "Here I Am" Vehicles and Unequipped Vehicles 75
Figure 14.4 Original Prediction of Lane Capacity Effects of ACC and CACC Driven at 0.5 s Time Gap from 2001 76
Figure 14.5 Updated Prediction of Lane Capacity Effects of ACC and CACC Driven at Time Gaps Chosen by Drivers in Field Test (With remaining vehicles manually driven) 76
Figure 14.6 Prediction of Lane Capacity Effects of HIA and CACC Driven at Time Gaps Chosen by Drivers in Field Test (With the remaining vehicles manually driven) 77
Figure 14.7 Prediction of Lane Capacity Effects of HIA and CACC Driven at Time Gaps Chosen by Drivers in Field Test (With the remaining vehicles being ACC) 78
Figure C.0.1 Driver Compliance with Advisory Speeds in Zone 1. 93
Figure C.0.2 Driver Compliance with Advisory Speeds in Zone 3. 94
Figure C.3 Driver Compliance with Advisory Speeds in Zone 5. 95

List of Tables

Table 4.1 Performance Comparison With and Without VSL 12
Table 5.1 Results of the Calibration 25
Table 5.2 Performance Comparisons 33
Table 6.1 Summary of Data Collected Per Driver. 43
Table 6.2 Overall Mean Compliance With Advisory Speeds. 51
Table 14.1 Updated Prediction of Lane Capacity Effects of ACC and CACC Driven at Time Gaps Chosen by Drivers in Field Test (With the remaining vehicles manually driven) 77
Table 14.2 Prediction of Lane Capacity Effects of HIA and CACC Driven at Time Gaps Chosen by Drivers in Field Test (With the remaining vehicles manually driven) 78
Table 14.3 Prediction of Lane Capacity Effects of HIA and CACC Driven at Time Gaps Chosen by Drivers in Field Test (With the remaining vehicles being ACC) 79

1. Introduction to Traffic Control Issues

Freeway traffic flow is limited by bottleneck flow. The causes of bottlenecks may vary from case to case. Here we consider traffic control for recurrent (but not non-recurrent) bottlenecks for simplicity. It is known that congested upstream traffic may drop the bottleneck flow 5~20% below its capacity flow depending on location and time *(1-7)*. The reasons for such drops are: (a) the feeding flow into the bottleneck is reduced when upstream is congested; and (b) flow conservation: bottleneck out-flow equals its in-flow. A logical way to maximize bottleneck flow is to create a discharging section immediately upstream and to regulate its flow such that the bottleneck's feeding flow is closer to its capacity flow. We use a combination of Variable Speed Limits (VSL) and Coordinated Ramp Metering (CRM) to achieve this.

Ramp metering (RM) is the most widely practiced strategy to control freeway traffic in the US, particularly in California. It is recognized that ramp metering can directly control the flow into the freeway (demand) and the average density immediately downstream, which indirectly affects the traffic upstream. After entering the freeway, the collective behaviors of the drivers are not controlled, which determines the traffic flow pattern. In addition, from the perspective of equity among the onramps along a corridor and the ramp queue length limits due to road geometry, ramp metering has to be switched off if the demand from that onramp is too high to avoid traffic spilling back onto arterials. Therefore, from a systems and control viewpoint, using ramp metering alone cannot fully control the freeway traffic in practice. This is the motivation for investigating combining RM with VSL. A recent FHWA report (8) summarizes the benefits of using VSL, RM and other traffic control strategies in Active Traffic Management (ATM).

The following acronyms are used: CTM – Cell Transmission Model; FD – Fundamental Diagram; TOPL (Tools for Operational Planning); SWARM - System Wide Adaptive Ramp Metering; TTT – Total Travel Time (or VHT); TTS - Total Time Spent; TTD – Total Traveled Distance (or VMT); MPC – Model Predictive Control.

This report focuses on mobility improvements along a stretch of freeway using combined VSL and RM. Several possible ways exist to combine VSL and RM. At each time step:

- RM rate is determined before determining VSL;
- Determine RM and VSL simultaneously with coupled speed and density dynamics model;
- Determine VSL first before determining RM rate.

RM was designed before VSL in *(9)*, which has some practical implications in the sense that many California highways have already implemented RM. Adding VSL is a natural extension. This paper uses the third approach to design a combined traffic control strategy for maximizing the recurrent bottleneck flow. It determines VSL for maximizing the bottleneck flow taking into account the following factors: mainline flow, onramp demand and length limit (storage capacity), and limits on speed variation over time and space for driver acceptance and safety. VSL has three parts: (a) the critical VSL upstream of the discharge section, which regulates the discharge flow to bottleneck capacity flow; three regulators based on flow, density and occupancy respectively are proposed; (b) VSL for the potentially congested (mainline storage) section if the

demand is too high for smoothing the traffic; (c) VSL upstream of the congestion tail, to reduce shockwaves by gradually decreasing the VSL. Such a higher level design leaves optimization to CRM. It accounts for the fact that VSL cannot change quickly without disturbing drivers but the CRM rate can. In this sense, it is sub-optimal but practical. With the designed VSL, the first order mainline flow model is linearized, which is then used for CRM design to minimize the difference between scaled TTT and the TTD. This is essentially a trade-off between maximizing mainline throughput and accommodating more vehicles. The weight selection depends on the traffic situation. With proper formulation of the constraints, the control design problem can be formulated as a Sequential Linear Program, which has efficient numerical solutions.

This report presents the overall control strategy for combining VSL and RM after literature review, followed by VSL design and CRM design. Then an Integrated Traffic Simulation is introduced: microscopic simulation, macroscopic traffic control design, online optimization and feedback control of microscopic traffic will be briefly introduced. Simulation results illustrating the expected effectiveness of the VSL and CRM strategies are presented, followed by the description and results of a preliminary field test of VSL values displayed to drivers in a test vehicle.

2. Literature Review

In recent years, several VSL and CRM algorithms have been developed and implemented, for which some were based on models but some were not. In the following, both approaches are briefly reviewed for RM, VSL and their combination.

2.1 Ramp Metering

Several RM strategies were reviewed and compared in *(10, 11)*. Reference *(12)* evaluated four ramp metering methods: ALINEA-local traffic responsive; ALINEA/Q with onramp queue handling; FLOW - a coordinated algorithm that tries to keep the traffic at a predefined bottleneck below capacity; and the Linked Algorithm, which is a coordinated algorithm that seeks to optimize a linear quadratic objective function. The most significant result was that ramp metering, especially the coordinated algorithms, was only effective when the ramps are spaced closely together. A coordination strategy (HERO) was developed in (13) for a stretch of freeway with local ALINEA Local traffic responsive ramp metering, which is simple and requires no model. The implementation of HERO is reported in (14). A hierarchical structure of CRM strategy for freeway networks is presented in (15), which could be considered a further extension of work in (14) for two layers. On top of that, the third layer includes traffic state and disturbance prediction.

2.2 VSL Strategies

Reference *(16)* presents two VSL algorithms for traffic improvement, combined with RM. The authors of *(16)* believe that VSL not only can improve safety and emissions, but also can improve traffic performance by increasing throughput and reducing time delay, primarily for work zones. Two control algorithms were presented. VSL-1 was for reducing time delay by minimizing the queue upstream of the work zone; and VSL-2 was for reducing TTS by maximizing throughput over the entire work zone area. Simulation results showed that VSL-1 may even outperform VSL-2 in speed variance reduction. Reference *(17)* designed VSL using the second order METANET model. It assumed that the onramp and off ramp flow are stochastic variables with known PDF with an optimal control approach. Then an Extended Kalman filter was used for traffic state estimation. Based on that, a VSL strategy was designed by minimizing an objective function. Several objective functions were proposed including TTT and throughput.
Reference *(18)* identified two functions of VSL: speed homogenization and prevention of traffic breakdown. Prevention of traffic breakdown avoids high density, which achieves density distribution control through VSL. As an example, a VSL strategy is used to suppress shockwaves considering the whole traffic network as a system.
Reference *(19)* used an empirical approach to investigate the effectiveness of reducing congestion at a recurrent bottleneck and improving driver safety by using feedback to the driver with advisory Variable Message Signs (VMS) on an 18 km highway stretch. The feedback includes: (a) speed limit (piecewise constant with 12 km/h increment); and (b) warning information (attention, congestion, and slippery). The VSL strategy was based on the traffic situation upstream and downstream of the bottleneck. Data analysis showed that driver response to the speed limit and messages on the VMS was reasonable, speed was regulated to some extent,

and safety was improved by 20%~30% incident/accident reduction, more significant than mobility improvements.

Papageorgiou *(20)* evaluated implemented VSL strategies based on data analysis. The paper summarizes available information on the VSL impact on FD-aggregate traffic flow behavior as follows:

- decrease the slope of the flow-occupancy diagram at under-critical conditions;
- shift the critical occupancy to higher values;
- enable higher flows at the same occupancy values in overcritical conditions.

It concluded that there was no clear evidence of improved traffic flow efficiency in operational VSL systems for the implemented VSL strategies.

A simple real-time merging traffic control concept was proposed *(21)* for efficient toll plaza management in cases where the total flow exiting from the toll booths exceeds the capacity of the downstream highway, bridge, or tunnel, leading to congestion and reduced efficiency due to capacity drop. The Merging Control strategy of Toll Plaza is similar to RM - ALINEA, which is different from the VSL physically since VSL do not completely stop the vehicles. RM using traffic signals decouples the platoons into individual vehicles while VSL intends to keep platoons intact.

2.3 Combined VSL and RM

An example use of the second order model for combined Variable Speed Limit and Coordinated Ramp Meter control design is reported in *(22)*. Reference *(23)* considered the combined effect of VSL and RM in reducing the risk of crashes and improving operational parameters such as speeds and travel times on congested freeways. Work in *(24)* adopted the METANET model adapted to different vehicle classes for combined VSL and CRM design with MPC. Reference *(25)* used a second order model for optimal VSL and RM plus extended Kalman filter for state estimation. Optimization was done by minimizing (or maximizing) an empirical mean cost function according to the Monte Carlo method. Reference *(26)* considered combined VSL and CRM with an optimal control approach. It claimed an algorithm feasible for large scale systems and showed by simulation that traffic flow significantly improved with combined VSL and CRM versus using each strategy alone.

Reference *(27)* considered combined RM and VSL based on the FD with MPC approach. It is believed that RM was effective only when the traffic demand from the combination of onramp and mainline does not significantly exceed downstream mainline capacity flow. Otherwise, flow would break down and RM has no use. The basic idea in *(27)* is that: when density is high, the following chain effect would result - Coordinated VSL upstream ➔ Reduce density downstream ➔ changing the shape of the FD ➔ allowing more vehicles to move in from onramp ➔ preventing or postponing traffic breakdown if there is large demand from on-ramp ➔ increase the effective range of RM. Just because of this, the VSL could reduce TTS. In this paper, the combined VSL and CRM design takes into account mobility, safety, equity and driver acceptance instead of just safety as in most previous VSL practice. However, results are sub-optimal from the overall system viewpoint.

Mainstream traffic flow control using combined VSL and CRM was investigated in (28, 29). These papers used an extended METANET model for tightly coupled VSL and CRM control design for freeway network traffic. A nonlinear optimization process was necessary at each time step.

2.4 Microscopic Traffic Modeling and Simulation

2.4.1 Microscopic Traffic Model

Many microscopic traffic models have been established and investigated in the past few years. In a microscopic traffic model, the car-following model determines the speed of a vehicle based on information about itself and its leading vehicle. The basic inputs of a car following model usually are the current speed of the considered vehicle and its leading vehicle, the spacing between the two vehicles, reaction time, acceleration and deceleration. Some car-following models use a set of equations to define the future speed (30), for example, the Gazis-Herman-Rothery model, Gipps's model, Newell's model, etc. Some other car-following models rely on thresholds, like Michaels's model. Based on whether the threshold is exceeded or not, the driver has different reactions. There are also car-following models using fuzzy logic to specify the driver response.

2.4.2 Calibration of the Car-following Model

To make the microscopic model reflect the actual driver behavior, we must carefully select the values of the basic parameters in the model. Thus before we use the model, we need to calibrate it to obtain a good estimation of the parameters. Plenty of work has been done on the calibration of each microscopic model. Because we use Gipps's model here, we only focus on the methods and results of this model. Mainly there are three methods for calibrating this model, trajectory based, double loop measurement based, and steady state behavior based. Trajectory based method is a widely used method when calibrating a car-following model. Ossen (31) used trajectory data extracted from digital camera photos to calibrate the model. The objective function of the calibration is both the speed error and position error. Brockfeld (32) used the Berkeley Highway Lab data, which is double loop measurements, to calibrate and compare different microscopic models. He averaged the five lane data into one lane, and tried to minimize the error between the simulated speed from the model and field measured speed. Wilson (33) analyzed the steady-state solutions and the stability of Gipps's model, and Rakha (34) gave the procedure of calibration for the model based on this result.

2.4.3 Traffic Simulation for VSL and CRM

Several simulations have been done on the impact of VSL or ramp metering on traffic. Abdel-Aty (35) evaluated the improvement of freeway safety by VSL in micro-simulation and gave recommendations for VSL implementation. Park (36) tested different variable speed limit control logic at work zones by VISSIM microscopic simulation. Carlson (29) demonstrated that VSL and ramp metering can improve traffic flow efficiency by macroscopic simulation. And Hasan (37) compared two ramp metering algorithms, ALINEA and FLOW, under a wide range of traffic conditions in a MITSIM simulation.

3. Higher Level Control Strategy

This section presents the main results. i.e., design of VSL based on a pre-specified RM strategy for a stretch of freeway as shown in Figure 1.1. The objective is to maximize the recurrent bottleneck flow to approach its capacity flow. The definition of "Cell" is referred to *(38)*. MPC terminologies are used in the discussion below, which are referred to *(27)*.

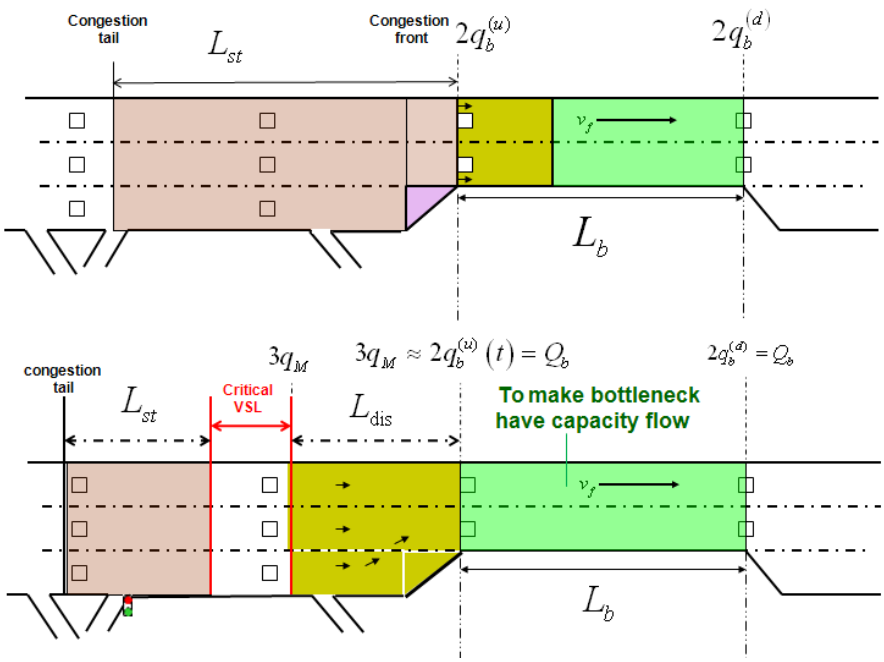

Figure 3.1 Bottleneck characteristics and control strategy

In Figure 1, Upper: the discharge flow of two lanes will be lower than the bottleneck capacity flow due to conservation if upstream is congested: $q = 2q_b^{(u)} < Q_b$; $q_b^{(u)}$ – feeding flow per lane into the bottleneck; Q_b – total bottleneck capacity flow; Lower: Control strategy: to maximize bottleneck flow by creating a discharge section upstream of the bottleneck.

3.1 Recurrent Bottleneck Characteristics

This analysis applies to a recurrent bottleneck that can be represented as a lane reduction. To understand bottleneck flow characteristics, the following concepts are crucial: *Bottleneck Capacity:* Physical capacity of the bottleneck or its observed maximum flow; *Bottleneck Discharge flow (exit flow)*; and *Bottleneck feeding flow*: the flow at the geometric starting point of the bottleneck. The following cases are not distinguished: (a) upstream is congested but there is no queue within the bottleneck; and (b) both upstream and part of the bottleneck stretch are congested with queue.

3.2 Control Objective and Strategy

The control objective is to maximize the bottleneck flow and reduce shockwaves upstream to improve safety and emissions. It can be proved that maximizing the bottleneck flow is equivalent to reducing the TTS under the assumption that all the traffic has to pass the bottleneck. Based on the traffic characteristics, the following control strategy is proposed: (a) if the demand upstream is below bottleneck capacity flow, upstream traffic is harmonized by VSL and CRM; and (b) if the demand is too high from both mainline upstream and onramp and congestion is unavoidable, then create a discharge section with adequate length (500~700 m) immediately upstream of the bottleneck, and use the critical VSL to control the traffic in the section upstream of the discharge section as shown in Figure 1 such that the feeding flow to the bottleneck is closer to the bottleneck capacity flow. This is possible if there is a geometric lane drop (such as work-zone or design) or *virtual lane drop* upstream of the bottleneck. A virtual lane drop can be considered as an effective capacity reduction from a weaving section, for example as shown in Figure 2. Because of the lane drop at the bottleneck and excess demand approaching it, the immediate upstream of the bottleneck is congested. Therefore the flow into the bottleneck drops below its capacity flow. The weaving and/or lane changing effect aggravate the situation.

Figure 3.2 I-80 West PM peak section (L);
Virtual lane drop and weaving at freeway diverge (R)

A practical example of virtual lane drop is the freeway diverge at I-80 West and I-880S & I-580E for PM peak traffic as shown in Figure 1.2. Some drivers destined to I-880S or I-580E use I-80W until the last second before changing to the proper lane since the traffic on I-80W is generally light in the PM peak hours.

4. Tightly Coupled VSL and Coordinated Ramp Metering

This section presents a tightly coupled control strategy for VSL and Coordinated Ramp Metering. A nonlinear second order model is used *(41)*.

4.1 Modeling

The model necessary for VSL control design needs to involve speed dynamics. Based on our analysis of the second order model, we select the model for this purpose:

$$\rho_m(k+1) = \rho_m(k) + \frac{T}{L_m \lambda_m}\left(\rho_{m-1}(k) v_{m-1}(k) - \rho_m(k) v_m(k) + r_m(k) - s_m(k)\right)$$

$$v_m(k+1) = v_m(k) + \frac{T}{\tau}\left(u_m(k) - v_m(k)\right) + \frac{T}{L_m} v_m(k)\left(v_{m-1}(k) - v_m(k)\right) - \frac{1}{\tau}\left(\frac{\nu T}{L_m}\frac{\rho_{m+1}(k) - \rho_m(k)}{\rho_m(k) + \kappa}\right) \tag{4.1}$$

$$m = 1, \ldots, M$$

where: v – speed; ρ – density; T- time step; L_m – length of link *m*; (τ, ν, κ) – model parameters. This is a simplified METANET model with two major modifications: (a) there is no further parameterization in the speed control variable $u_{m,i}(k)$; (b) there is no assumption of the FD. The advantages of doing so include:

- Speed control variable appears linearly;
- 2-DOF for control design: both VSL and RM rate;
- Effectively avoiding model mismatch caused by discrepancies between field data and the FD curve;
- Proper constraints will be added to the optimization problem from an empirical traffic flow drop probability analysis with respect to both speed and density (occupancy) *(42)*.

Here it is assumed that at each time step *k*, the RM rate

$$\hat{\mathbf{r}} = \left[r_1(k+1), \ldots, r_1(k+N_p), \ldots, r_m(k+1), \ldots, r_m(k+N_p), \ldots, r_M(k+1), \ldots, r_M(k+N_p) \right]^T \tag{4.2}$$

is independently determined by an RM strategy over the time horizon, which is necessary for the prediction over the same time horizon using the model above.

4.2 Constraints

For any given RM rate, the Critical VSL is determined by:

$$\lambda_M \rho_M \left(k+j+1\right) v_M \left(k+j+1\right) = Q_b$$
$$j = 1, \ldots, N_p \tag{4.3}$$

which is further relaxed as an inequality constraint:

$$Q_b - \varepsilon \le \lambda_M \rho_M \left(k+j+1\right) v_M \left(k+j+1\right) \le Q_b + \varepsilon$$
$$0 < \varepsilon \text{ is a small number.} \tag{4.4}$$

It is an implicit constraint on the control variable through the density dynamics in (4.1). Therefore it needs converting to direct constraints to the speed control variable by recursively using (4.1) starting from the initial condition at each time step *k* and over the predicted time horizon. Denote

$$\mathbf{u}_M = \left[\bar{u}_M \left(k+1\right), \ldots, \bar{u}_M \left(k+N_p\right)\right]^T \tag{4.5}$$

which are the critical VSL and can be calculated based on the RM rate. Based on considerations of safety, driver acceptance and traffic flow characteristics, the following constraints on the VSL control variable are adopted:

$$0 \le u_m \left(k\right) \le \bar{V}_m$$
$$-5 \le u_m \left(k-1\right) - u_m \left(k\right) \le 5$$
$$5 \le u_{m-1} \left(k\right) - u_m \left(k\right) \le 5 \tag{4.6}$$

The first one is the bounds for the VSL, and the second and the third are the speed increment/decrement limit over time and distance for driver acceptance and enforceability in mile per hour. The following inequality limits the feasible region in the speed and density plane

$$v_m + a\rho^2{}_m \left(k\right) + b\rho_m \left(k\right) \le \eta_m \tag{4.7}$$

where η_m is a design parameter to be tuned off-line. This constraint is from the following consideration: density and speed are upper bounded by a contour on the speed-density plane [33] where a and b are determined with field data.

4.3 Objective Function

The following objective function is used over the predictive time horizon:

$$J = T \sum_{j=1}^{N_p} \sum_{m=1}^{M} L_m \lambda_m \left[\alpha_{TTT} \rho_m \left(k+j\right) - \alpha_{TTD} v_m (k+j) \cdot \rho_m \left(k+j\right)\right] \tag{4.8}$$

The first term minimizes TTT (to maximize mainline flow); the second term maximizes the TTD (to accommodate more vehicles in mainline). $\left(\alpha_{TTT}, \alpha_{TTD}\right)$ =(55,1) are selected to match their units for trade-off.

4.4 MPC Design for VSL

MPC design is used here. For any given time starting from *k*, the control parameters are to be determined in the MPC procedure as the decision parameters for time *k+1*:

$$\mathbf{u} = \left[u_1(k+1), \ldots, u_1(k+N_p), \ldots, u_m(k+1), \ldots, u_m(k+N_p), \ldots, u_M(k+1), \ldots, u_M(k+N_p) \right]^T$$

The MPC mechanism works in logical order for each time step k as depicted in Figure 4.1. The numerical algorithm (44) and Matlab package for Nonlinear Sequential Programming (45) are used in simulation.

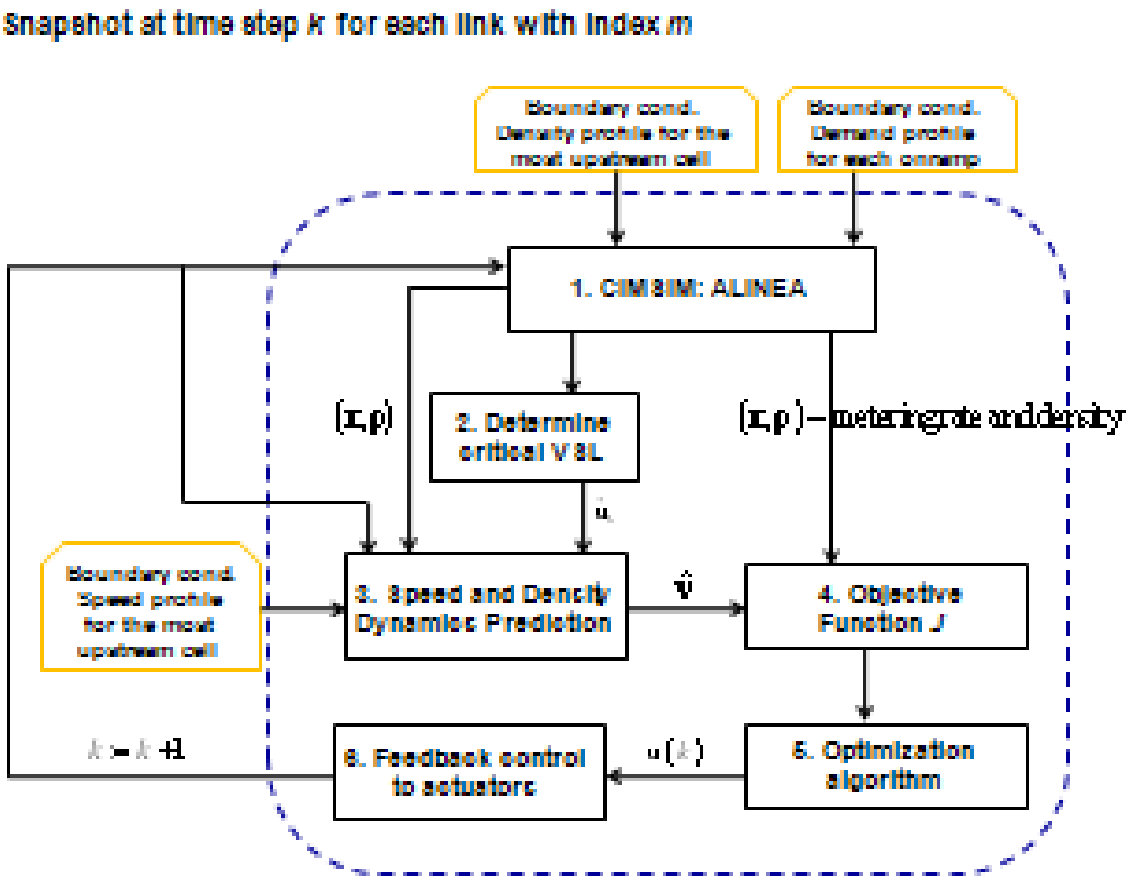

Figure 4.1 MPC scheme to determine VSL

4.5 Model Calibration and Simulation

To validate the proposed method, the above control algorithm has been implemented in simulation with the BHL *(46)* field data, which is a test site that covers 2.7 miles of I-80 eastbound immediately east of the San Francisco-Oakland Bay Bridge in California (Figure 4.4). Dual loop detector stations provide 60 Hz event data on individual vehicle actuations. Aggregated flow and speed information are extracted from the raw event data. In calibration, the model parameters have been chosen to minimize the quadratic errors between the model computed and the measured values of speed and flows. After the calibration procedure, the following parameter values are adopted for (3.2): $\tau = 0.02$, $\nu = 8.5$, and $\kappa = 32$.

The suggested two locations for VSL signs are between Station 1 and 2, and between 5 and 6 in Figure 4. The simulation starting time is 2:00 PM on December 1 2005, corresponding to the time index 0 on the X axis, and the ending time of simulation is 12:00 AM on December 2 2005, associated with the time index 600 minutes. From Figure 4.3 it should be noted that VSL control sometimes slows down the traffic flow, for example around the time index 60 (3:00 PM), but on

average its effects improve the performance with all the cost functions. The initial conditions of simulation are the same for both controlled and uncontrolled cases, coming directly from the measured BHL data. The deployment of the proposed control strategy is particularly effective against congestion. The VSL improved traffic stability, with more constant flow and a higher average speed as can be seen from Figure 4.3 comparing the traffic with and without VSL for the peak hours 3:00 PM -7:00 PM.

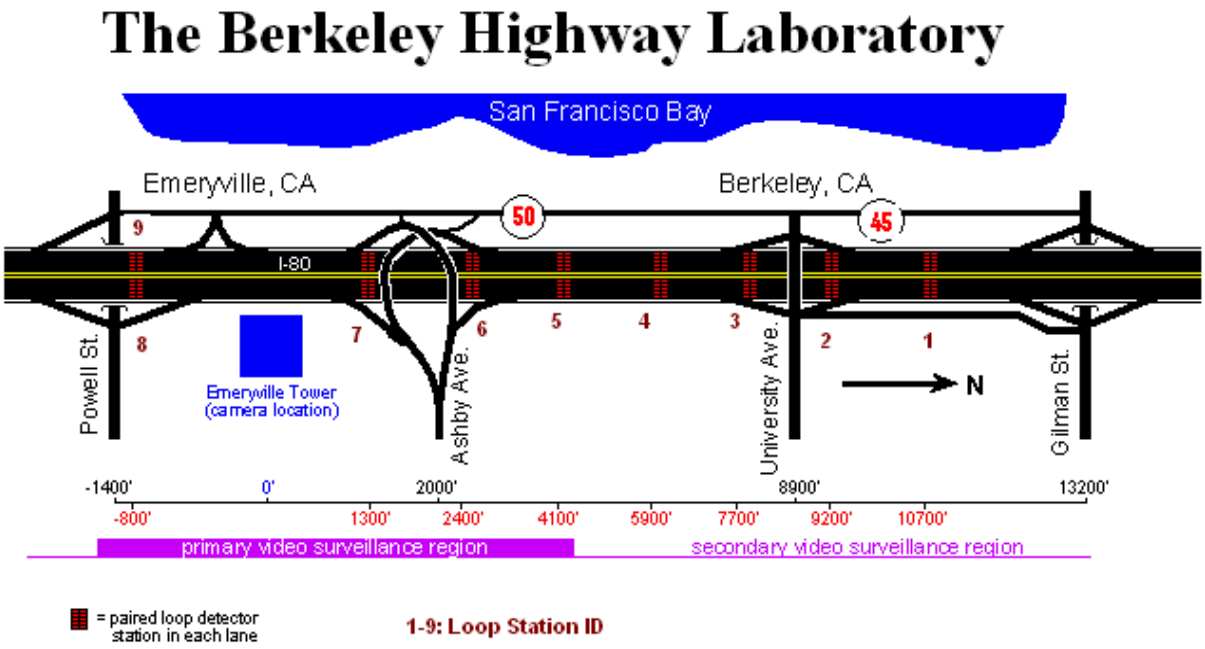

Figure 4.2 BHL Section of I-80 with Two VSL Sign Locations

The accumulated performance parameters (except the average flow) over the 10 hour simulation period and 5 lanes, showing the improvements with VSL, are summarized in Table 4.1.

Table 4.1 Performance Comparison With and Without VSL

Performance Measure	**Without VSL**	**With VSL**	**Improvement**
TTT (hours)	5,150	3,510	- 31.8%
TTD (vehicle miles)	157,385	177,645	+ 12.8%
Average Flow (veh/hr/lane)	1259	1421	+12.87%
Objective Function	125,865	15,405	- 87.8%

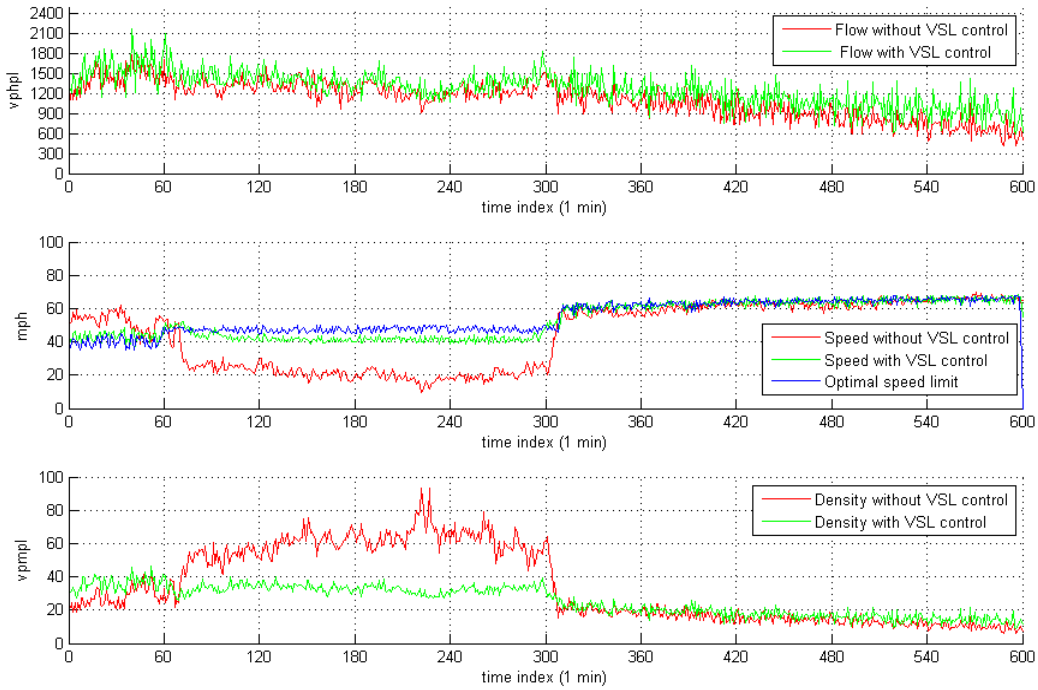

Figure 4.3 Comparison of Flows, Speeds and Densities With and Without VSL at Station 2

4.6 Further Remarks

The METANET model has been simplified by dropping the Fundamental Diagram assumption and the re-parameterization of the speed control variable. With the simplified METANET model involving speed and density dynamics and under the assumption that the RM rate is pre-determined by a separate approach at each time step *k*, VSL control has been designed using Finite Time Horizon MPC. Simulation has been conducted over the I-80 BHL section, showing that VSL alone improves traffic noticeably.

Since the density directly affects the traffic flow, even a local high density could cause a moving jam. It is necessary to investigate the spatiotemporal characteristics of density for optimal ramp metering.

5. Combined VSL and Coordinated Ramp Metering

For practical implementation, we propose a new approach for combining VSL and CRM.

5.1 Overall System Structure

The flow chart for the overall system including measurement and control design is depicted in Figure 5.1. The following factors need to be taken into account in the design:

- Driver equity to access the freeway from all onramps along a corridor, in the sense that the control strategy should not sacrifice the interests of drivers from downstream;
- TTS should be minimized, including the queue time at the onramps with or without ramp metering;
- TTD should be maximized – equivalent to saying that the freeway should accommodate more vehicles if demands from onramps are too high to avoid spillback to arterials;
- The overall control design strategy accounts for the fact that VSL cannot change quickly but the CRM rate can: the optimization process could generate different RM rates at each step.

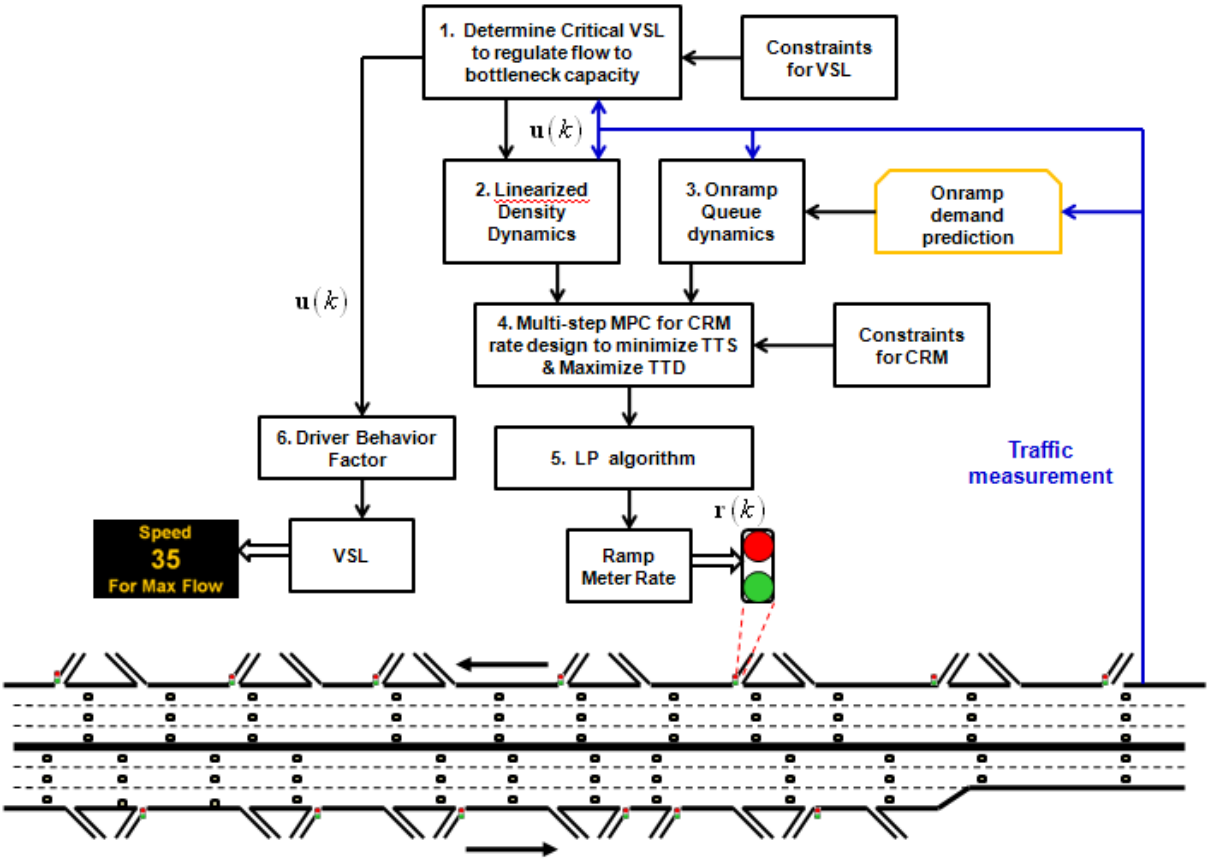

Figure 5.1 Flow chart of overall system: measurement and control design

In addition to higher weight for TTD in peak hours to avoid traffic spilling back, once the queue length at the onramp reaches a certain level, ramp metering is switched off to allow vehicles to get onto the freeway. In this case, VSL will play a major role because it is the only remaining control mechanism available.

The notations are grouped according to their functions:

Model Parameters

m – link index; M – Critical VSL Control link index; *M+1* discharge link index;

k – time index

L_m – length of link *m*

m_0 – index of the most upstream link affected by the bottleneck; m_0 could be a negative integer;

m_h – link index of the congestion head

m_t – link index of the congestion tail

γ – gain parameter to be determined in simulation

N_p – prediction steps for each *k* in Model Predictive Control

State and Control Variables

q_{M+1}, v_{M+1} – flow and speed at the discharge section

u_m – desired VSL at link *m*, to be designed

$q_m(k)$ - estimated mainline flow at time *k*

$\rho_m(k)$ – density of link *m* at time *k*

$u_M(k)$ – Critical VSL immediately above the discharge link, control variable

$r_m(k)$ – metering flow rate (veh/hr), control variable

Measured or Estimated Traffic State Parameters

$\overline{q}_m(k-1)$ – flow at time *k-1,* measured

$\overline{v}_m(k)$ – speed of link *m* at time *k,* measured

$u_0(k)$ – speed in the most upstream link, measured

$\overline{\rho}_{M+1}$ – discharge link density, measured/estimated

$s_m(k)$ – total off-ramp flow of a link (veh/hr), measured

d_m – demand from onramp *m*, measured or estimated

$V_{st}(k), \rho_{st}(k)$ – speed and density of storage section upstream of Critical VSL, TBD

$L_{st}(k)$ – length of the storage section upstream of Critical VSL, TBD

Q_m – mainline capacity of link *m*, known

Q_b – bottleneck capacity flow, known

$Q_{m,o}$ – onramp *m* capacity, known

$L_{m,o}$ – onramp *m* length, known;

V_f – free-flow speed, known

O_c – critical occupancy, known

ρ_c – critical density, known

It is possible to further divide a link into cells *(26, 18)* in theory. Here, each link is considered as one cell for simplicity. It is assumed that each link has exactly one on-ramp but may contain more than one off-ramp.

5.2 VSL Design

VSL design is divided into three parts: (i) design VSL from the most upstream to the congestion tail along the corridor to the critical VSL point to harmonize traffic; and (ii) design the critical VSL to maximize bottleneck flow; and (iii) determine the V_{st} in the storage section. Three relevant problems are also addressed: (a) length of the discharge section; (b) length of the potential congestion/storage section (or the congestion tail); and (c) handling the case if the bottleneck is already congested.

5.2.1 Design VSL Upstream of Congestion Tail to Harmonize Traffic

This VSL strategy is designed in two stages according to the traffic. Using m_t and m_h denote the cell index of congestion tail and head respectively. Their determination will be discussed later. Then,

$$m_0 \le m_t \le m_h \le M$$

Stage 1: (congestion beginning) It can be characterized by the measured flow exceeding a threshold. The congestion tail and head are the same $m_0 = m_t = m_h = M$ (Figure 5.2). The VSL for each link in the potential influence zone could be determined as:

$$\begin{aligned}
&u_{m-1}(k) = u_m(k) + \\
&\max\left\{-5, \min\left\{\left(\eta\alpha_m(k) + (1-\eta)\beta_m\right)\left[u_M(k) - u_{m_0}(k)\right], 0\right\}\right\} \\
&m_0 < m_h = m_t = M \\
&u_0(k) = V_f \\
&q_m(k) = \bar{q}_{m-1}(k-1) + R_m(k) - s_m(k) \\
&R_m(k) = \min\left\{d_m(k), Q_{m,o}, Q_m - \bar{q}_{m-1}(k-1)\right\} \\
&\alpha_m(k) = H\left(Q_m - q_m(k)\right) \\
&\beta_m = H\left(1/L_{m,o}\right) \\
&0 \le \eta \le 1
\end{aligned} \tag{5.1}$$

where $\alpha_m(k)$ reflects the demand from onramp and $\beta_m(k)$ the onramp length, and η is to balance the priorities between onramp demands and storage capacity along the corridor for equity. The recursive algorithm is the first in Equation 5.1. Negative 5 in the braces is the limit for VSL changes over time to encourage driver acceptance. The Harmonic function $H(\cdot)$ is defined as: Let $\mathbf{x} = [x_1, x_2, ..., x_n]$ be a real vector. Then

$$H\left(x_m\right)=\frac{\frac{1}{x_m^2}}{\sum_{\mu=1}^{M}\frac{1}{x_\mu^2}}=\frac{\prod_{\mu=1,\mu\neq m}^{M}x_\mu^2}{\sum_{\mu=1}^{M}\prod_{\eta=1,\eta\neq\mu}^{M}x_\eta^2} \tag{5.2}$$

The following properties are straightforward:

$$\begin{aligned}&\sum_{m=1}^{M}\alpha_m\left(k\right)=1, \qquad \sum_{m=1}^{M}\beta_m=1\\ &\sum_{m=1}^{M}\left(\eta\alpha_m\left(k\right)+\left(1-\eta\right)\beta_m\right)=1\end{aligned} \tag{5.3}$$

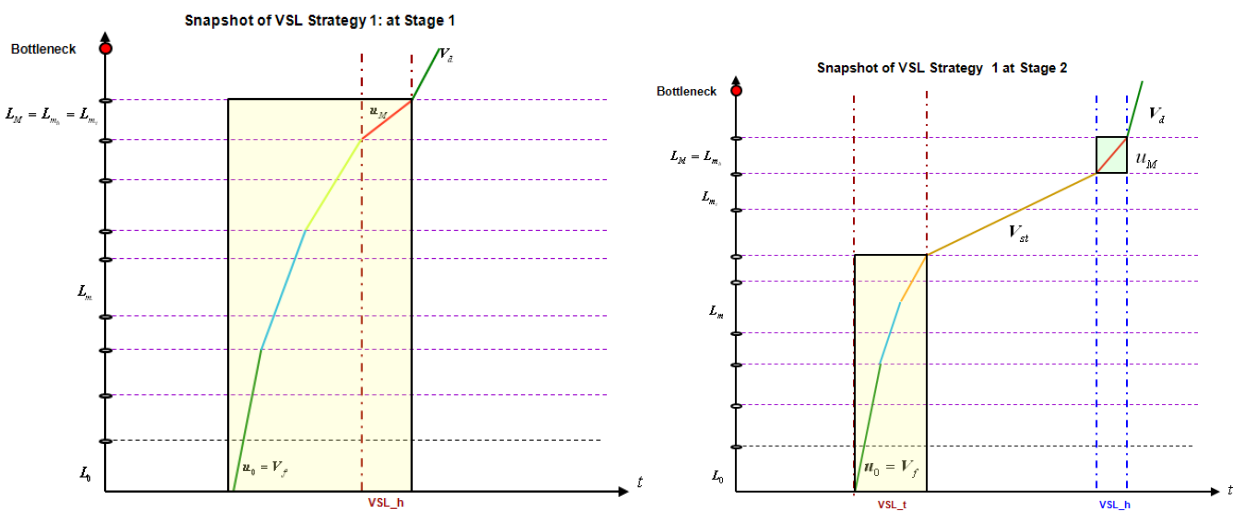

Figure 5.2 Schematic VSL control strategy at Stage 1 (L), and Stage 2 (R)

The algorithm determines $u_m\left(k\right)$ by interpolating $u_0\left(k\right)$ and $u_M\left(k\right)$. The coefficients for the interpolation are determined by: mainline acceptance capability, onramp demand and physical length. The algorithm can be explained as: the VSL is monotone decreasing from the most upstream link (cell) of the affected zone with free-flow speed to the congestion tail; if the onramp demand is higher, the speed reduction at that link will be greater to allow more vehicles to be injected from the onramp; short onramp length leads to more VSL reduction at that link for similar reason.

Stage 2: After applying the VSL for traffic at Stage 1, it is possible that a congestion section upstream of the critical VSL could further back propagate if the demand from upstream is high, which is the case for I-80W in peak hours. This is called Stage 2 (Figure 5.2- R). It is characterized as $m_0 \le m_t < m_h = M$ and can be identified with criteria

$$\rho_m\left(k\right) > \rho_{st}$$

The density threshold ρ_{st} is to be determined later. The VSL algorithm for Stage 2, the VSL for each link downwards to the congestion tail ($0 \le m \le m_t$) can be specified as:

$$
\begin{aligned}
& u_m(k) = u_{m-1}(k) + \\
& \max\left\{-5.0, \min\left\{\left(\eta\alpha_m(k) + (1-\eta)\beta_m\right)\left[V_{st}(k) - u_{m_0}(k)\right], 0\right\}\right\} \\
& u_{m_0}(k) = V_f \\
& q_m(k) = q_{m-1}(k-1) + R_m(k) - s_m(k) \\
& R_m(k) = \min\left\{d_m(k+1), Q_{m,o}, Q_m - q_{m-1}(k-1)\right\} \\
& \alpha_m(k) = H\left(Q_m - q_m(k)\right) \\
& \beta_m = H\left(1/L_{m,o}\right) \\
& 0 \le \eta \le 1
\end{aligned}
\tag{5.4}
$$

The explanation of the algorithm is similar to the above. $V_{st}(k)$ is the VSL in the congested section, which will be determined later.

5.2.2 Determine Critical VSL and L_{dis}

Two methods are presented based on integral control to determine $u_M(k)$.

(a) Flow based Regulator to regulate the bottleneck feeding flow to the capacity flow:

$$
u_M(k) = u_M(k-1) + \gamma \cdot \min\left\{\left(Q_b - \overline{q}_{m-1}(k)\right),\ \overline{v}_{M+1}(k) \cdot \left(\rho_c - \overline{\rho}_{M+1}(k)\right)\right\} \tag{5.5}
$$

(b) Density Based Regulator

$$
u_M(k) = u_M(k-1) + \begin{cases} \varsigma_1 \cdot \left(\rho_c - \overline{\rho}_{M+1}\right), & \text{if} \quad \overline{\rho}_{M+1} < \rho_c \\ \varsigma_2 \cdot \left(\rho_c - \overline{\rho}_{M+1}\right), & \text{if} \quad \overline{\rho}_{M+1} > \rho_c \end{cases} \tag{5.6}
$$

The two control gains may be different to adapt to differences in the traffic situation. Such flexibility can also be used in anti-windup strategy to avoid control oscillation. In practice, the density can be replaced with occupancy, and the critical density replaced with critical occupancy:

$$
u_M(k) = u_M(k-1) + \begin{cases} \varsigma_{o1} \cdot \left(O_c - o_{M+1}\right), & \text{if} \quad o_{M+1} < O_c \\ \varsigma_{o2} \cdot \left(O_c - o_{M+1}\right), & \text{if} \quad o_{M+1} > O_c \end{cases} \tag{5.7}
$$

VSL algorithms Equation 5.1 and 5.4 need the length of the discharge section. The discharge section length L_{dis} is determined by the distance required for the vehicle to accelerate from zero speed (the worst case) to the desired speed:

$$
L_{dis} = \frac{V_{tgt}^2}{2a_{ave}} + 200 \tag{5.8}
$$

a_{ave} – average acceleration

V_{tgt} – desired speed at the bottleneck.

The added 200 m takes into account other important effects such as weaving and lane changing.

5.2.3 Determine $(V_{st}, \rho_{st}, L_{st})$ for Stage 2

Implementation of the VSL algorithm in Equations 5.1 and 5.4 needs the estimation of the congestion tail (Figure 5_2-R). For saturated traffic, the shockwave back-propagation speed is nearly constant *(39)*. With VSL, it is expected that the shockwave will be diminished or even avoided. Therefore, the speed of the congestion tail propagation is expected to be smaller than the shockwave speed without control. It depends on:

- measured upstream mainline flow
- flow from onramp or RM rate
- roadway storage capacity
- VSL for the congested section

The VSL in this section can be specified as follows:

$$\begin{aligned} &V_{st}(k) \cdot \rho_{st}(k) \geq Q_b \\ &\rho_c \leq \rho_{st}(k) \leq \rho_J \end{aligned} \tag{5.9}$$

where ρ_{st} is specified first based on historical data or the operator's experience. The worst case is $\rho_{st} = \rho_J$. However, one could operate at density levels $\rho_{st} < \rho_J$ depending on traffic. $V_{st}(k)$ is then determined based on Equation 5.9 and a static FD relationship for saturated traffic *(42)*. After the expected density is determined for the storage section, one can determine if a link upstream should be added to the storage section. This could be done using real-time data jointly with density dynamics for one step prediction:

$$\rho_m(k+1) = \rho_m(k) + \frac{T}{L_m \lambda_m}\left(\lambda_m \rho_{m-1}(k) u_{m-1}(k) - \lambda_m \rho_m(k) u_m(k) + r_m(k) - s_m(k)\right) \tag{5.10}$$

At time step *k*, after implementing VSL $u_m(k-1)$ and ramp metering $r_m(k-1)$, the right hand side of Equation 5.10 can be estimated based on measurements. If $\rho_m(k) \geq \rho_{st}(k)$, then link *m* is considered to be added to the storage section: $L_{st}(k) := L_{st}(k-1) + 1$; otherwise $L_{st}(k) := L_{st}(k-1)$.

5.2.4 Discharge Section Clearing

If the bottleneck is already congested, it is necessary to recover the flow in the bottleneck and restore the discharge section to free flow to maximize the bottleneck flow. This can be achieved by first limiting the bottleneck feeding flow at the critical VSL point. The time required to restore the discharge section to free flow can be estimated. It is assumed that the physical capacity of the bottleneck Q_b is a known constant. The potential queue length from the congested section can be modeled as follows:

L_b - bottleneck section length (assumed known)
$\lambda_b -$ number of lanes at bottleneck
$\lambda_{dis} -$ number of lanes in discharge section
L_{dis} calculated as in previous section.

The storage capacities of those two sections are:

$$\left(\lambda_{dis} L_{dis} + \lambda_b L_b\right)\rho_J$$

To optimize the traffic flow, it is necessary to reduce the traffic to the desired density:

$$\rho_b = \frac{Q_b}{V_b} \tag{5.11}$$

$V_b -$ the desired speed for traffic at capacity flow Q_b in the bottleneck; and ρ_b the corresponding density (as an example, $\rho_b \le \rho_J$) are assumed known.

A constant discharging flow $Q_b \cdot (1 - x\%)$ is further assumed for the bottleneck. The time T_{dis} required to recover density from ρ_J to ρ_b would be:

$$\begin{aligned} T_{dis} &= \frac{T_{dis}\lambda_{dis} u_M \rho_M + \left(\lambda_{dis} L_{dis} + \lambda_b L_b\right)\left(\rho_J - \rho_b\right)}{Q_b \cdot (1 - x\%)} \\ \Rightarrow T_{dis} &= \frac{\left(\lambda_{dis} L_{dis} + \lambda_b L_b\right)\left(\rho_J - \rho_b\right)}{\left(Q_b \cdot (1 - x\%) - \lambda_{dis} u_M \rho_M\right)} \end{aligned} \tag{5.12}$$

u_M, ρ_M are desired speed and density at the critical VSL point satisfying

$$u_M \rho_M << Q_b \tag{5.13}$$

It is clear from Equation 5.12 that smaller $V_M \rho_M$ will lead to shorter discharging time; and smaller capacity drop in the bottleneck will generate similar results. Suppose that the bottleneck flow maximization control strategy starts (at time t_0) after both the bottleneck and discharge section recover to their capacity.

5.3 CRM Design with MPC

In MPC design, at time step *k*, RM rate is to be determined over the predicted time horizon $k+1, \ldots, k+N_p$:

$$r = \left[r_1(k+1), \ldots, r_1(k+N_p), \ldots, r_M(k+1), \ldots, r_M(k+N_p)\right]^T \tag{5.14}$$

5.3.1 Modeling

The following linearized density and onramp queue dynamics model are adopted:

$$\begin{aligned} \rho_m(k+1) &= \rho_{m-1}(k) + \frac{T}{L_m \lambda_m}\left(\lambda_m \rho_{m-1}(k) u_{m-1}(k) - \lambda_m \rho_m(k) u_m(k) + r_m(k) - s_m(k)\right) \\ w_m(k+1) &= w_m(k) + T \cdot \left[d_m(k) - q_{m,o}(k)\right] \end{aligned} \tag{5.15}$$

The first is the conservation of flow *(38)*. It is linear since the speed variables $u_{m-1}(k)$ and $u_m(k)$ are already the designed VSL values. This can be justified because (a) for strictly enforced VSL, the actual speed will be close to the designed VSL; (b) for advisory VSL, if the density is high enough, even 30% driver compliance will compel speed reductions by the rest of the drivers. Such linearization and decoupling bring great advantages to control design.

5.3.2 Constraints

The following constraints (Equation 5.16) are adopted for CRM design.

$$\begin{aligned} &0 \le w_m(k) \le L_m^{(r)} \cdot \rho_J \\ &0 \le r_m(k) \le \min\left\{d_m(k), Q_{m,o}, \lambda_m\left(Q_m - \bar{q}_{m-1}(k)\right), \lambda_m u_m(k)\cdot\left(\rho_J - \bar{\rho}_m(k)\right)\right\} \\ &0 \le \rho_m(k) \le \min\left\{\rho_J, \varphi\left(u_m(k)\right)\right\} \end{aligned} \tag{5.16}$$

The first is the onramp queue length limit; the second is the direct constraints on RM rate, which is the minimum of the four terms in the braces: the onramp demand, onramp capacity; the last two terms are space available in the mainline. $\lambda_m\left(Q_m - \bar{q}_{m-1}(k)\right)$ is likely assumed in free-flow case, and $\lambda_m u_m(k)\cdot\left(\rho_J - \bar{\rho}_m(k)\right)$ is likely assumed in congestion. This consideration is motivated by *(38)*. The third is an indirect constraint on RM rate through the density dynamics. $\varphi\left(u_m(k)\right)$ is the curve of a specified traffic speed drop probability contour as indicated in Figure 5.3, with three flow contours for reference. For a given acceptable traffic drop probability, the contour gives an upper bound for the feasibility region *(42)*.

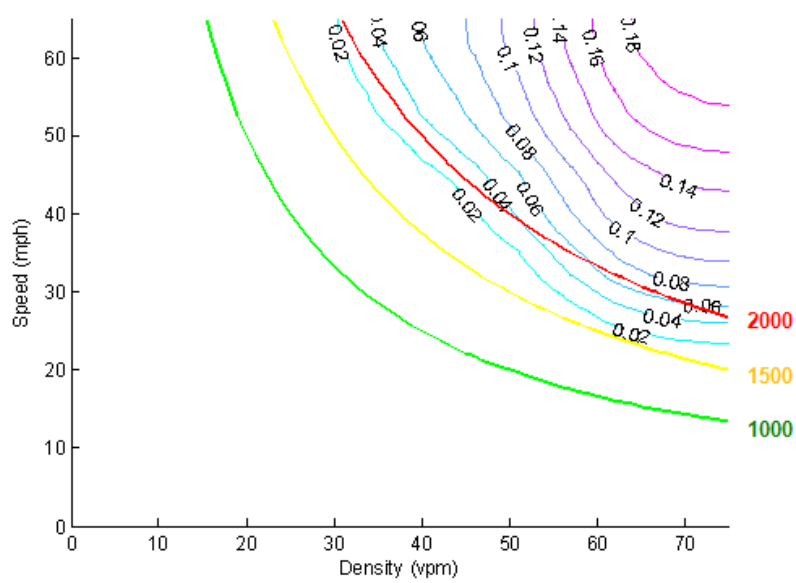

Figure 5.3 Empirical traffic speed drop probability contour vs. flow contour

5.3.3 Objective Function

The following objective function is used at time step k over the predictive time horizon:

$$
\begin{aligned}
& J = TTS - TTD \\
& TTS = T\sum_{j=1}^{N_p}\sum_{m=1}^{M} L_m \lambda_m \rho_m \left(k+j\right) \qquad \text{(TTT)} \\
& +T\sum_{j=1}^{N_p}\sum_{o} w_o \left(k+j\right) \quad \text{(Time Delay Due to Onramp Queue)} \qquad (5.17) \\
& TTD = \alpha_{TTD,0} T\sum_{j=1}^{N_p}\sum_{m=1}^{M-1} \lambda_m L_m q_m \left(k+j\right) + \alpha_{TTD,M} T\sum_{j=1}^{N_p} \lambda_M L_M q_M \left(k+j\right) \\
& \alpha_{TTD,M} >> \alpha_{TTD,0} > 0
\end{aligned}
$$

Minimizing J minimizes TTS (or density), and maximizes TTD (to maximize mainline flow). Choosing $\alpha_{TTD,M} >> \alpha_{TTD,0}$ emphasizes maximizing the flow on link M.

5.4 Integrated Traffic Control Simulation Platform (ITCSP) Development

An Integrated Traffic Control Simulation Platform (ITCSP) has been developed in Aimsun with API, which includes: (i) a 7-link network representation of 10 km of I-80 W from Carlson to the diverge of I-80 and I-580E & I-880S (with HOV lane ignored) (Figure 3.2); (ii) aggregated field data on traffic speed, flow and density (occupancy) for feeding into a calibrated macroscopic traffic model; (iii) combined VSL and CRM design using the macroscopic model; (iv) feedback control at the microscopic level with VSL and CRM; and (v) performance evaluation for comparison of different control scenarios.

5.4.1 Overall System Structure

The overall simulation structure is depicted in Figure 5.4. It considers a scenario with a combination of lane reduction (virtual lane reduction) and weaving upstream of a diverge leads to capacity drop type of bottleneck. The basic simulator is the Aimsun microscopic traffic simulation model. The microscopic traffic data are aggregated in 20 s intervals across lanes, and then used for VSL design and ramp metering design. The key in the VSL design is to create a discharge section by setting the critical speed limit to keep the bottleneck section close to its capacity flow. The ramp metering design tries to minimize total time spent (VHT) and maximize total travel distance (equivalent to VMT) by the Model Predictive Control approach.

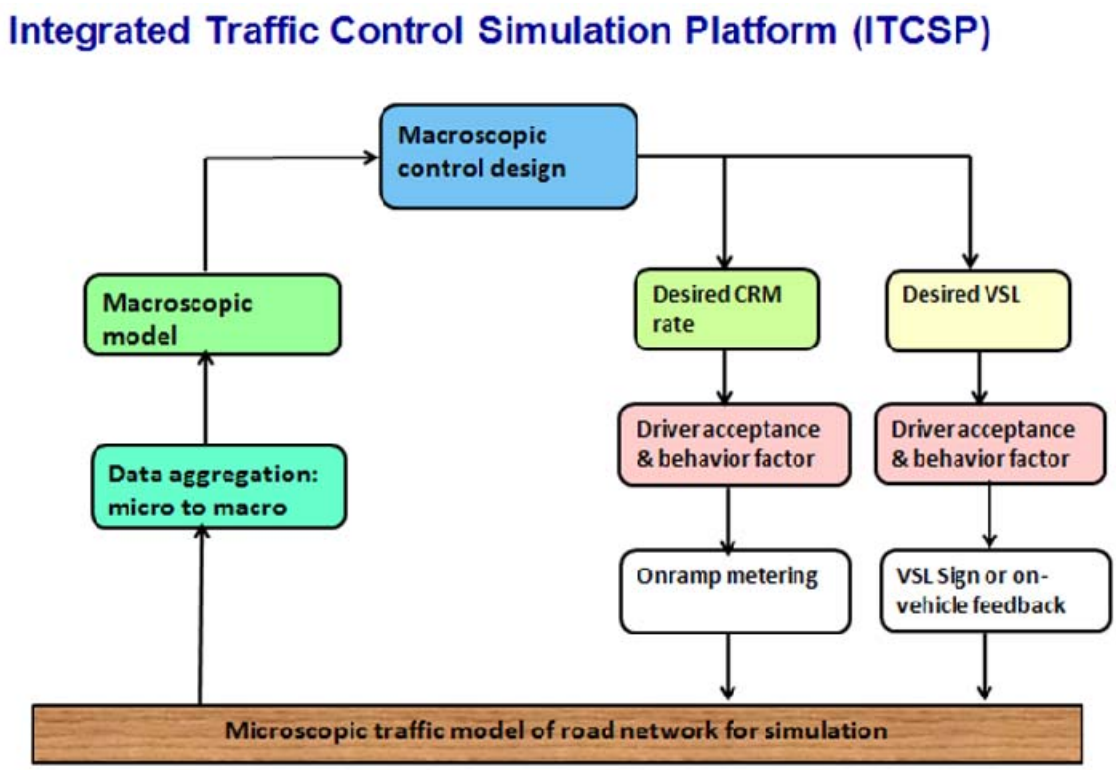

Figure 5.4 Overall Structure of ITCSP

5.4.2 Microscopic Traffic Modeling for Simulation

The car following model we use is Gipps's car following model *(47)*. As shown in Equations (5.18) ~(5.21), at time $t+T$, the speed of the nth vehicle $V(n,t+T)$ is dependent on the relation between the $(n-1)^{th}$ and the nth vehicle. Here T is the reaction time, $a(n)$ is the maximum acceleration of the nth vehicle, V^* is the desired speed, $d(n)$ is the maximum deceleration of the nth vehicle, $d'(n-1)$ is the deceleration estimation of the $(n-1)^{th}$ by the driver of the nth vehicle, α is the sensitivity factor, $s(n-1)$ is the length of the $(n-1)^{th}$ vehicle, and $x(n-1,t)$ and $x(n,t)$ are the current positions of the vehicles. So the calibration variables are T, $a(n)$, $V^*(n)$, $d(n)$ and α.

The data we use for calibration is the NGSIM data *(48)*. This data, as part of the Federal Highway Administration Next Generation Simulation project, was collected on Interstate 80 eastbound in Emeryville, California on April 13, 2005. It is a 6 lane freeway, the observed segment covers 1650 feet and there is an onramp in this segment. The vehicle-by-vehicle trajectory tracking data is derived from digital camera video, and it includes the speed and position information of each vehicle with 0.1s resolution. In the calibration, to eliminate the effect of lane changing, we only choose vehicles that did not change lanes during their travel in the observed section, and whose leading vehicle also stayed in the same lane.

$$V_a(n,t+T) = V(n,t) + 2.5a(n)T\left(1 - \frac{V(n,t)}{V^*(n)}\right)\sqrt{0.025 + \frac{V(n,t)}{V^*(n)}} \tag{5.18}$$

$$V_b(n,t+T) = d(n)T + \sqrt{d(n)^2T^2 - d(n)\Big[2(x(n-1,t) - s(n-1) - x(n,t)) - V(n,t)T -} \tag{5.19}$$

$$V(n,t+T) = \min\{V_a(n,t+T), V_b(n,t+T)\} \tag{5.20}$$

$$d'(n-1) = d(n-1)\alpha \tag{5.21}$$

The objective function of the calibration is to minimize the root mean square percentage error (RMSPe) of the simulated speed relative to the observed speed, that is

$$RMSPe = \sqrt{\frac{1}{N}\sum_{t=1}^{N}\left(\frac{V^{obs}(t) - V^{sim}(t)}{V^{obs}(t)}\right)^2}$$

The calibration result is shown in Table 5.1. Figure 5.5 is an example of the simulated speed and observed speed, simulated trajectory and observed trajectory of one vehicle. We can see that the two trajectories are almost overlapped. Figure 5.6 is the RMSPe distribution of all the calibrated vehicles. In this calibration, 80.5% of the vehicles have an RMSPe less than 0.1, 77.45% of them are less than 0.05, and 71.62% less than 0.01. The result for trucks seems to be not so favorable. This might due to the shortage of truck data in the data set. We only have 25 trucks in the data set, compared with more than 700 cars.

We need to notice that although we calibrate $V^*(n)$, if the advisory speed limit from the VSL control is less than this $V^*(n)$, the driver takes the smaller value as his desired speed in the simulation.

Table 5.1 Results of the Calibration

	car	truck
T (second)	1.12	1.05
a (m/s^2)	1.57	1.28
V^* (km/h)	108	109
d (m/s^2)	-2.29	-2
α	1.45	1.23

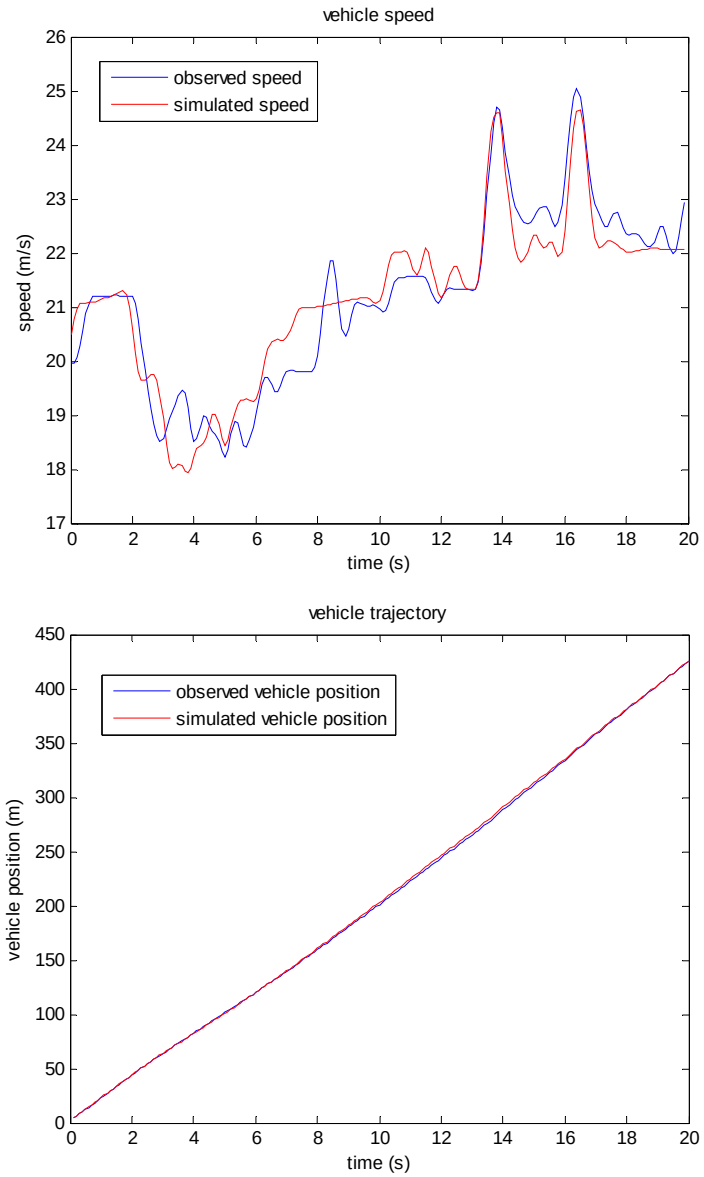

Figure 5.5 Examples of Simulated and Observed Speed and Trajectory in the Calibration

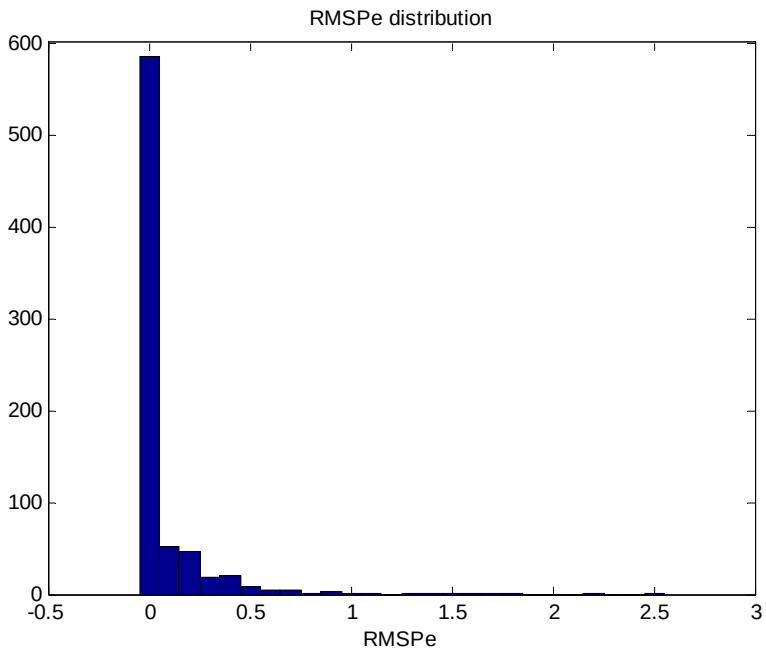

Figure 5.6 Distribution of the RMSPe

5.4.3 Model of I-80W PM Peak Traffic

A network was built to model I-80 westbound from Carlson Blvd to the diverge point of I-80 and I-580, as shown in Figure 5.7. There are 7 onramps, 7 off-ramps, and one freeway to freeway connector. At the diverge point, the 6 lane freeway splits into two 3 lane freeways (I-580EB and I-880SB, I-80WB). The demands for this section on I-80WB and I-580EB and I-880SB are usually high. And some drivers in the direction of I-580EB and I-880SB take advantage of less traffic on I-80WB during the PM peak in the right-most lane and change to the desired (left exiting) lane at the last second. Thus from the onramp at Powell to the diverge point of I-80WB and I-580EB and I-880SB, there are a lot of vehicles changing lane. To the three-lane ramp leading to I-580EB and I-880SB, there is a virtual lane drop. The weaving effect at this section greatly reduces the flow, and together with the high demand, it causes severe congestion. This is a typical example of a virtual lane drop from the weaving effect.

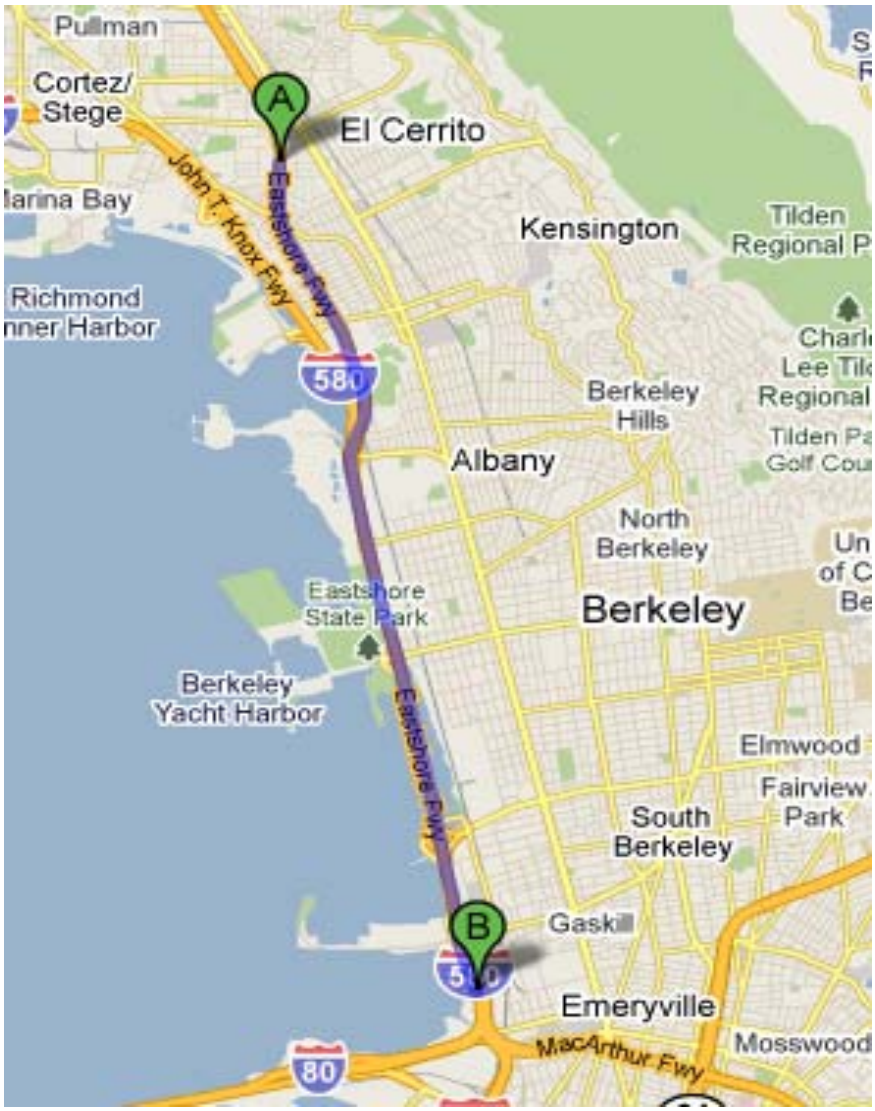

Figure 5.7 I-80 westbound, the simulated segment

5.4.4 Simulation Setup

We use the traffic simulation software Aimsun (49) to test our control strategy. Aimsun is a traffic simulation environment developed by TSS. It contains microscopic and mesoscopic simulators, and also offers extended tools for advanced investigation, such as Aimsum API which allows the user to incorporate any application program. The car-following model implemented in Aimsun is the Gipps's model described above. In the simulation test, we collect the real-time measurements of each link every 20 s, and then calculate the speed limit and ramp metering rate. Advisory speed limit and ramp metering rate are updated every minute in the simulation. This is done by use of the Aimsun API. Figure 5.8 shows the software structure.

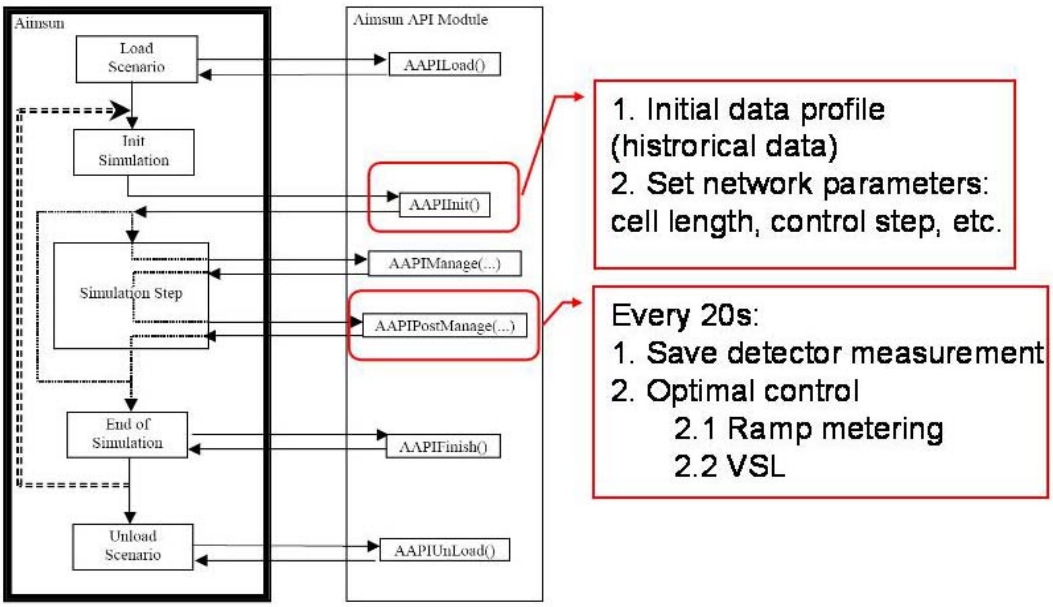

Figure 5.8 Software structure

Due to the lack of detectors on the ramps and therefore lack of the actual on-ramp demand data and split ratio for the off-ramp and diverge, a virtual demand is used for our simulation test. The simulation time is 5 hours. The first hour is in high demand, and in the remaining four hours, 25% of the demand of the first hour is used for all the onramps and the upstream mainline. In the first hour about 7700 vehicles need to pass the diverge point, and 60% of them go to I-580EB and I-880SB. It is observed that many of the vehicles need to change lane after the onramp at Powell. The car to truck ratio in the demand is 20:1. This section of freeway has one HOV lane, but it is ignored in the simulation.

In the simulation model, we have detectors upstream of each onramp. Those detectors are in the same location as the field installed detectors in PeMS (50). By doing this, we can use the existent detectors for field implementation in the future. And the corridor is discretized into links to use the dynamics model. The link is from some distance upstream of one onramp to upstream of the next one, except the link of Powell and the link for the critical speed limit. The distance to the onramp is 100 to 200 meters, and it is necessary to include the detector into that link. The link of the discharge section is 500 m and the advisory speed limit sign is placed at the merge point of each onramp. So the speed instruction is activated from one onramp to the next one. We also have ramp metering at each onramp. But the freeway to freeway connector (I-580 and I-80 merge point) does not have ramp metering.

The calibration result mentioned above is used to define the vehicle characteristics at the microscopic level and the information about vehicle length and width is also derived from the NGSIM data. Initially, the simulated network is empty. In the MPC, the demand from onramp and upstream is assumed known exactly. In practice, this can come from historical data.

Six control scenarios are simulated in our test: 1) All time VSL, in which VSL control is on from the beginning of the simulation; 2) all time combined, in which both VSL and ramp metering are

activated; 3) switched VSL, in which VSL is switched on only when the detected occupancy is over the specified threshold and is switched off when traffic recovers to free flow; 4) switched combined; 5) all time metering, in which only ramp metering is implemented; 6) all time VSL 30% compliance, in which only 30% of drivers follow the speed limit posted. Scenarios 1~5 assume 100% driver compliance with the posted values of VSL.

5.4.5 Control Scenarios and Results

The simulation results are shown in Figures 5.9 – 5.12. It can be observed that ramp metering alone improves traffic performance, but VSL control can improve more. Table 5.2 shows that if we use VSL control, total travel time can decrease to less than half, and delay drops to around one third. Figure 5.12 also shows that the vehicle speed at the diverge point is greatly increased by the VSL control. The differences between VSL and VSL combined with ramp metering, all time control and switched control, are not significant. However, it shows that all time VSL is slightly better than combining VSL and ramp metering control, which seems to be contradictory to our feeling that ramp metering can improve traffic performance. A reason for this is the short onramps in this section don't leave enough queue storage space, so that ramp metering can't hold many vehicles back before they cause queuing on arterials or require queues to be flushed out by turning ramp meters green. This is supported by the fact that switched combined control has better performance than switched VSL control, which indicates the complementary effects of VSL and CRM.

A possible explanation for all time control performing better than switched control is that the control is switched on too late and it takes more time for the discharge section to recover to free flow. Therefore, the choice of threshold for control to switch on needs further consideration. It is also observed that the ramp metering at the congested section is often switched off in the simulation. This is because the mainline is too congested and queues on the ramps exceed the storage capacity. Under those circumstances, only VSL is in action.

Furthermore, the result also shows that 30% driver compliance with the advisory speed limit can yield a similar result with 100% compliance. This may be explained as: due to the density being rather high for saturated traffic, if 30% of the drivers follow the posted VSL, all the other drivers are compelled to follow since there is no space for them to maneuver around the vehicles complying with the VSL.

In Figures 5.9 – 5.12, the speed under control is oscillatory in the first part. This phenomenon may be caused by (a) total delay which includes measurement delay, delay in VSL feedback, delay in driver's response; and (b) errors which include measurement error, feedback roundup error, and driver response error. In control theory, this phenomenon is called windup. Special techniques will be necessary to address those oscillations, which will be one of the topics to be investigated in future extensions of this work.

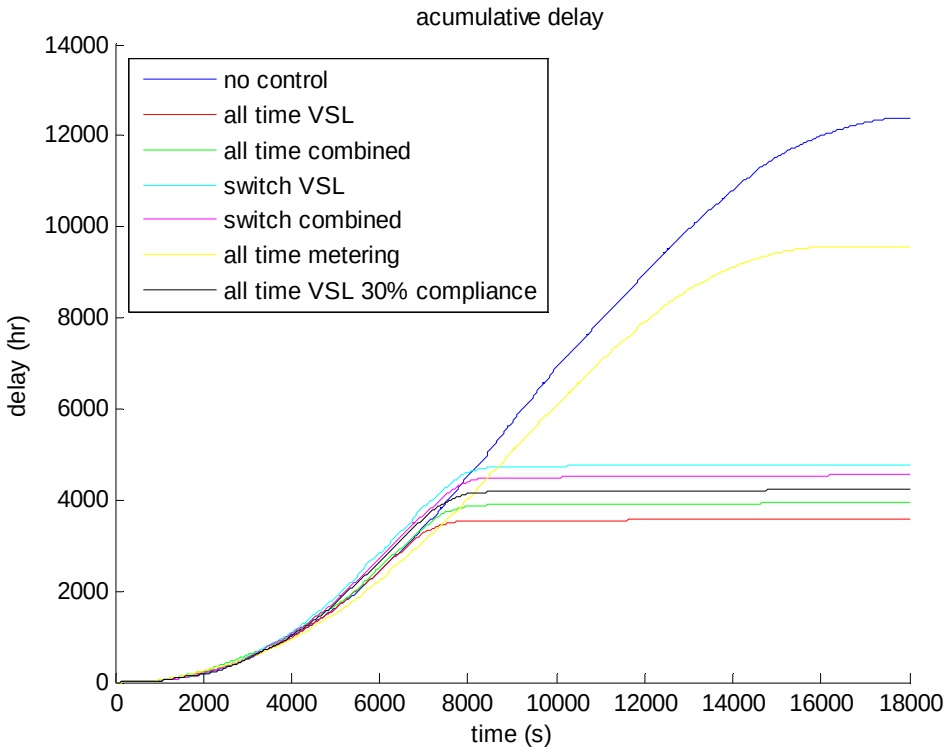

Figure 5.9 Delay Performance of Control Strategies in Simulation

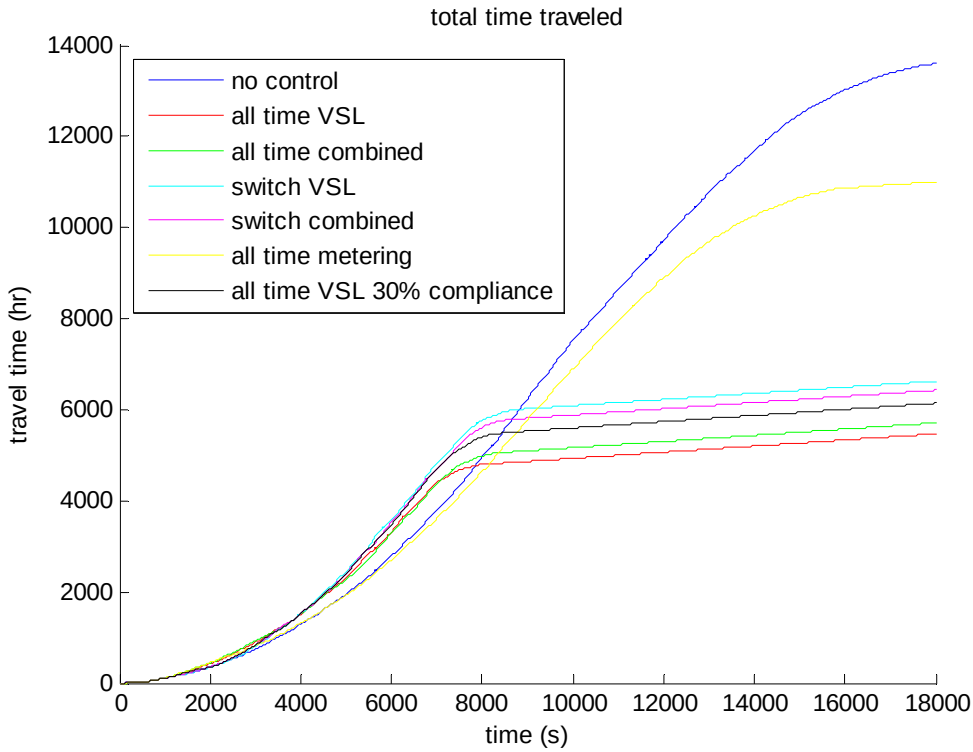

Figure 5.10 Total Travel Time Performance of Control Strategies in Simulation

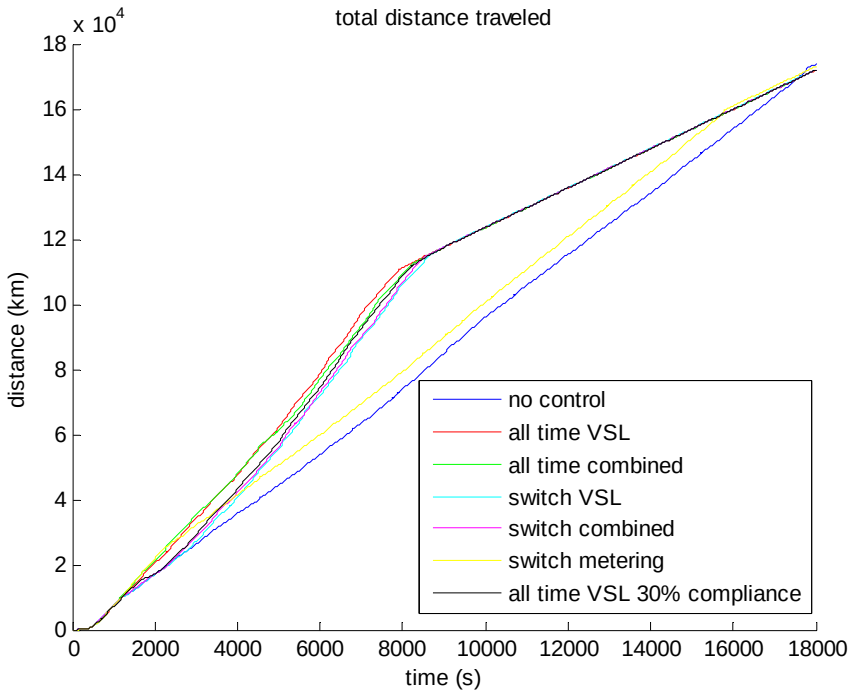

Figure 5.11 Total Distance Traveled (VMT) Performance of Control Strategies in Simulation

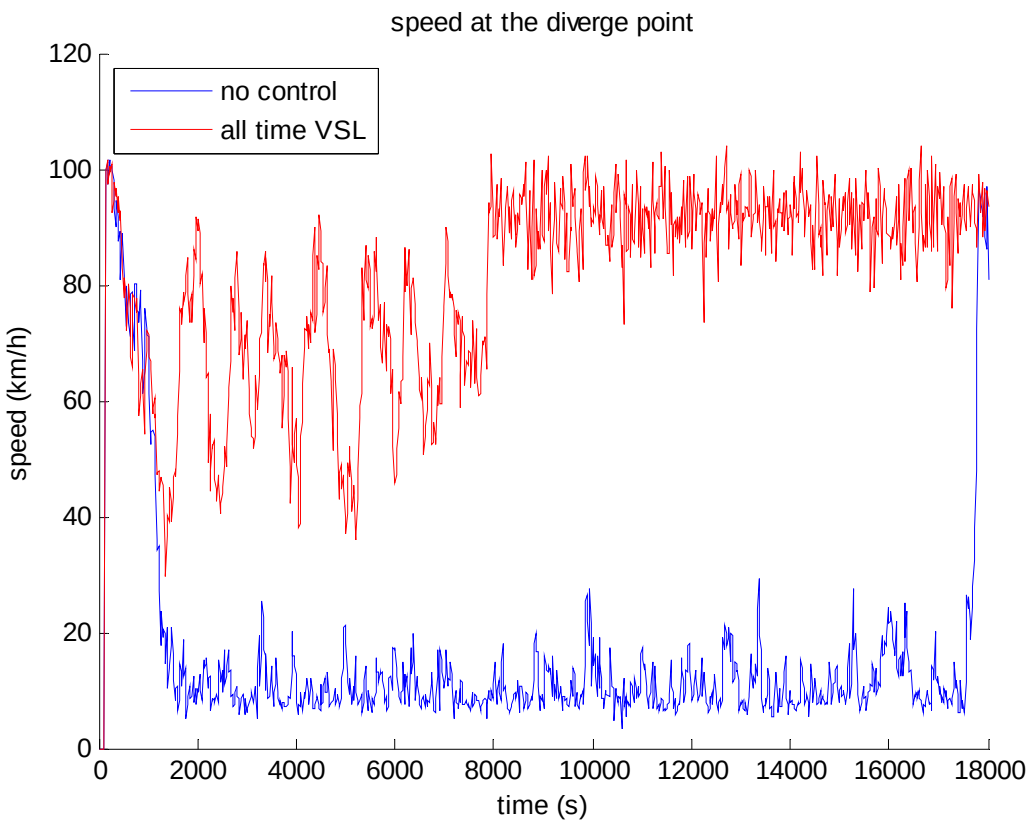

Figure 5.12 Speed Performance of Control Strategies in Simulation

Table 5.2 Performance Comparisons

	No control	All time VSL	All time combined	Switch VSL	Switch combined	Switch metering	All time VSL 30% compliance
TTS $(\times 10^3 \text{veh} \cdot \text{h})$	13.6	5.47	5.71	6.63	6.43	11.0	6.14
$\frac{\text{TTS with control}}{\text{TTS withouth control}}$	100	40.2	42.0	48.8	47.3	81.0	45.2
Delay $(\times 10^3 \text{veh} \cdot \text{h})$	12.4	3.59	3.95	4.79	4.56	9.56	4.23
$\frac{\text{Delay with control}}{\text{Delay withouth control}}\%$	100	29.0	31.9	38.6	36.7	77.1	34.1

The simulation results show the control method should be able to improve traffic performance quite significantly in the case of either 100% or 30% driver compliance.

6. Field Testing of VSL Display in Vehicles

6.1 Experiment Protocol

6.1.1 Overview

The experiment protocol was designed to evaluate both the technical suitability of the variable speed limit algorithm that was implemented and the perceived acceptability of the speed recommendations from the point of view of a driver. The most important consideration in evaluating the results of this experiment is that the test participant was the only vehicle on the road receiving the recommended speeds generated by the variable speed limit algorithm. The rest of the drivers on the roadway were unaware of either the speed recommendation or the fact that an experiment was in progress.

Since none of the test participants were familiar with the concept of variable speed limits, they were given a brief overview of the variable speed limit concept prior to the experiment. The participants were then told that the system being tested was a very early draft of a variable speed limit algorithm, and it was not ready for deployment. This stressed the fact that the participants were there to provide feedback about the concept of variable speed limits, rather than focusing on the behavior of this particular algorithm.

6.1.2 Test Participants

The test participants were recruiting using a combination of prior research subject email lists, U.C. Berkeley departmental email lists, and an advertisement placed on Craigslist.org. To be eligible to participate in this study, potential candidates needed to meet the following four criteria:

1. Be between the ages of 21 and 65
2. Have a valid California driver's license
3. Have a clean driving record with no moving violations within in the last 3 years and no DUIs
4. Be available from approximately 2 pm to 5 pm on the day of the experiment

First, an experimenter typically validated a candidate participant's eligibility over the phone, and second, the experimenter obtained consent to electronically check the candidate's DMV records using the Volunteer Select Plus service available from LexusNexis Risk & Information Analytics Group, Inc. Candidates who passed the DMV records screening were scheduled for a time and date to participate in the experiment.

A total of 16 volunteer drivers participated in the experiment. However, the sample as analyzed was only composed of 15 participants, 9 male and 6 female, due to data collection failures during one of the trips. The ages of the drivers ranged from 21 to 61 with a mean driver age of 40 years old (SD 15 years). All of the participants were familiar with conventional cruise control, but none of the participants had experienced driving with an ACC equipped vehicle before participating in this study. Additionally, none of the participants expressed any familiarity with the concept of variable speed limits.

6.1.3 VSL Experiment Test Route

The VSL experiment was conducted on an 8-mile stretch of Interstate 80 travelling westbound from Solano Ave (Richmond, CA) to Powell Street (Emeryville, CA). (See **Error! Reference source not found.**.) This section of freeway is monitored using Caltrans loop detectors, the FastTrak toll tags, and various third party sensors. The data are aggregated under the California Freeway Performance Measurement System (PeMS) which has been in operation since 1999 (51). All PeMS data are freely available to the public in archival format (http://pems.dot.ca.gov/). However, for this project, the data were needed in real time, and a live feed was made available for the test section from PeMS to a server at California PATH's Richmond Field Station location.

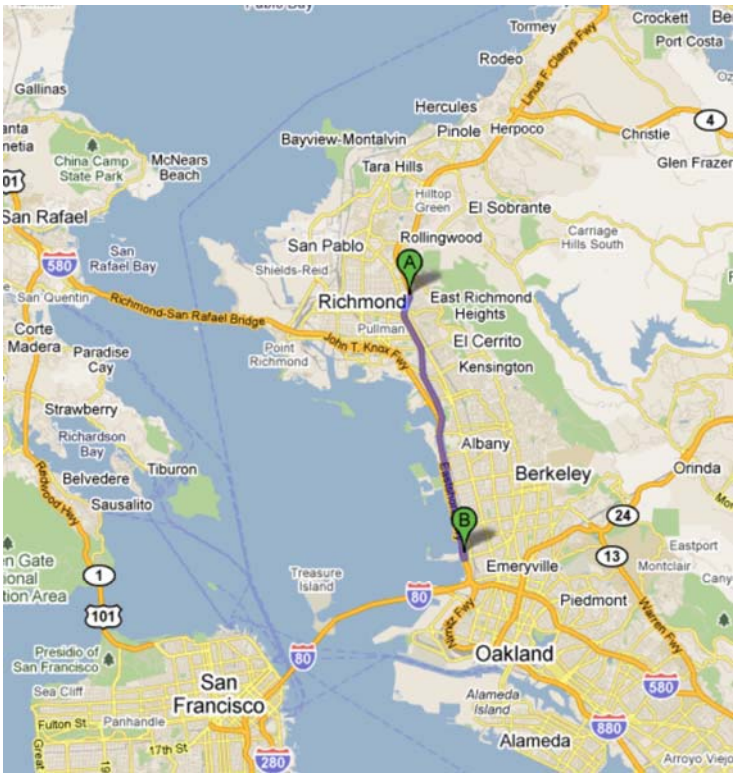

Figure 6.1 VSL Experiment Test Route

The test route was divided into 8 sections, each approximately 1 mile long. The VSL server processed the raw data obtained from PeMS and computed the recommended speed limit for each section of the test route. The server then provided a web service to the test vehicle, so that the test vehicle could query the recommended speeds for the test section through a cellular modem data connection.

The architecture of the combined infrastructure and vehicle system for providing the VSL information to the drivers is shown in Figure 6.2.

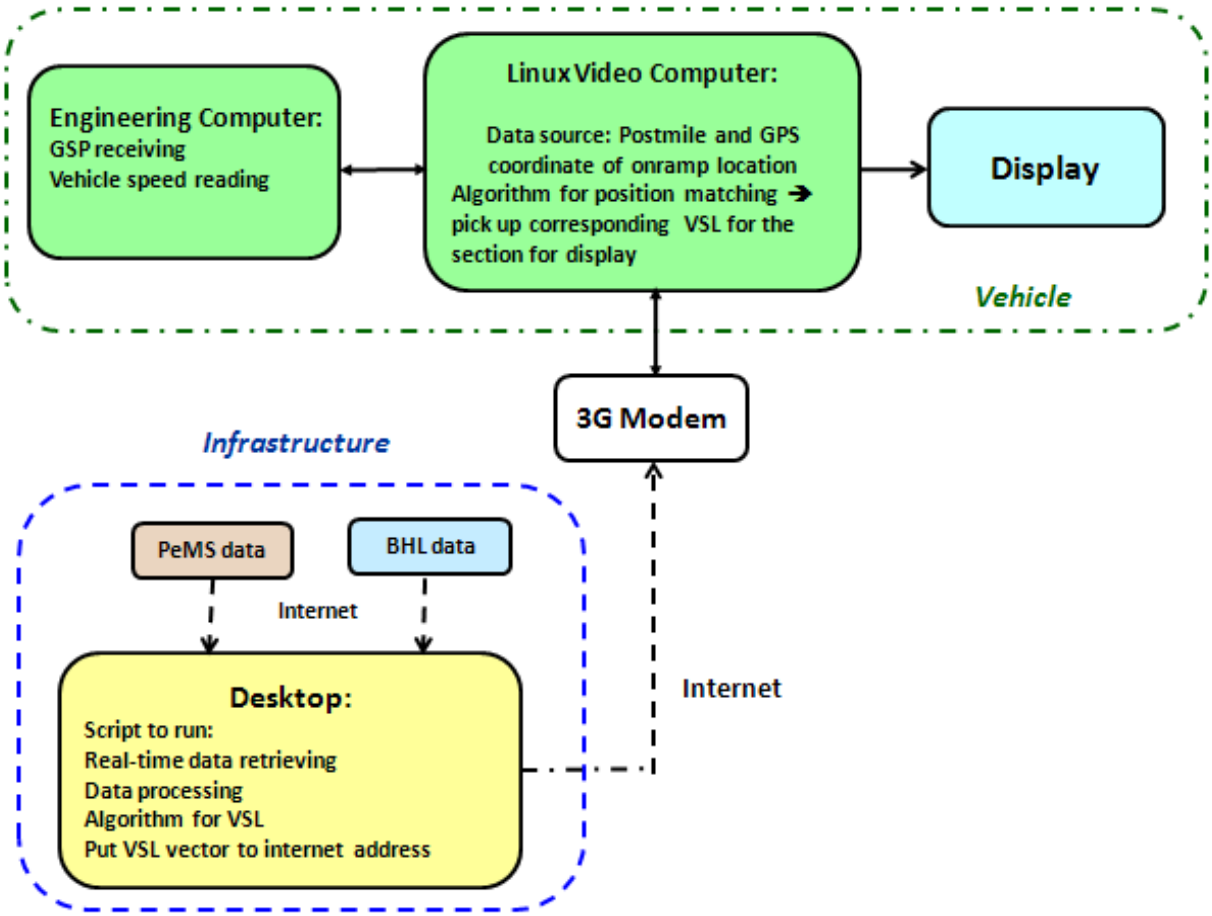

Figure 6.2 Overall System Structure for Preliminary Experimental Implementation of VSL with Feedback to the Driver on the CACC Vehicle

As shown in Figure 6.2, the overall system is composed of the following parts:

- Real-time traffic data collection and processing and traffic state parameter estimation
- VSL calculation on a desktop computer on the infrastructure
- Communication between the desktop computer and the engineering computer on the CACC vehicle
- CACC vehicle location determination
- Display to the driver of the VSL for that section according to the current location of the CACC vehicle.

The VSL calculation is conducted on the desktop computer based on the algorithm described in previous sections. Communication between the desktop computer and the engineering computer on the CACC vehicle is accomplished using a 3G modem. The calculated VSL array (for all the cells in the selected freeway section) is passed to the CACC vehicle every 30 s. The CACC vehicle location is determined in real time based on the combination of GPS data and wheel speed measurements for dead reckoning. Both the postmile and GPS location of the freeway onramp for each section are stored in the computer on the CACC vehicle. By comparing the GPS information with the stored data, it is possible to determine which section the vehicle is

currently occupying. With this information, the corresponding VSL value for that section is picked up and displayed to the driver.

6.1.4 Test Vehicle

The test vehicle used for the variable speed limit experiment was a 2004 Infiniti FX 45 equipped with a factory installed Adaptive Cruise Control (ACC). The vehicle was outfitted with a Data Acquisition System (DAS) and a video recording system. The complete architecture of DAS and video recording system on the test vehicle is more thoroughly described in Nowakowski, Shladover, Cody, et al. (52); however, a brief overview is provided in this report. The data acquisition system recorded a variety of engineering variables to characterize the motions of the vehicles, the driver actions, the functioning of the ACC system, and the speed limit recommended by the VSL algorithm. The video recording system recorded 5-channels of video data to provide additional information about the driving environment. The recommended speed limit was displayed to the driver on a 3.5" LCD display located on the top of the dashboard in the center of the vehicle (see Figure 6.3).

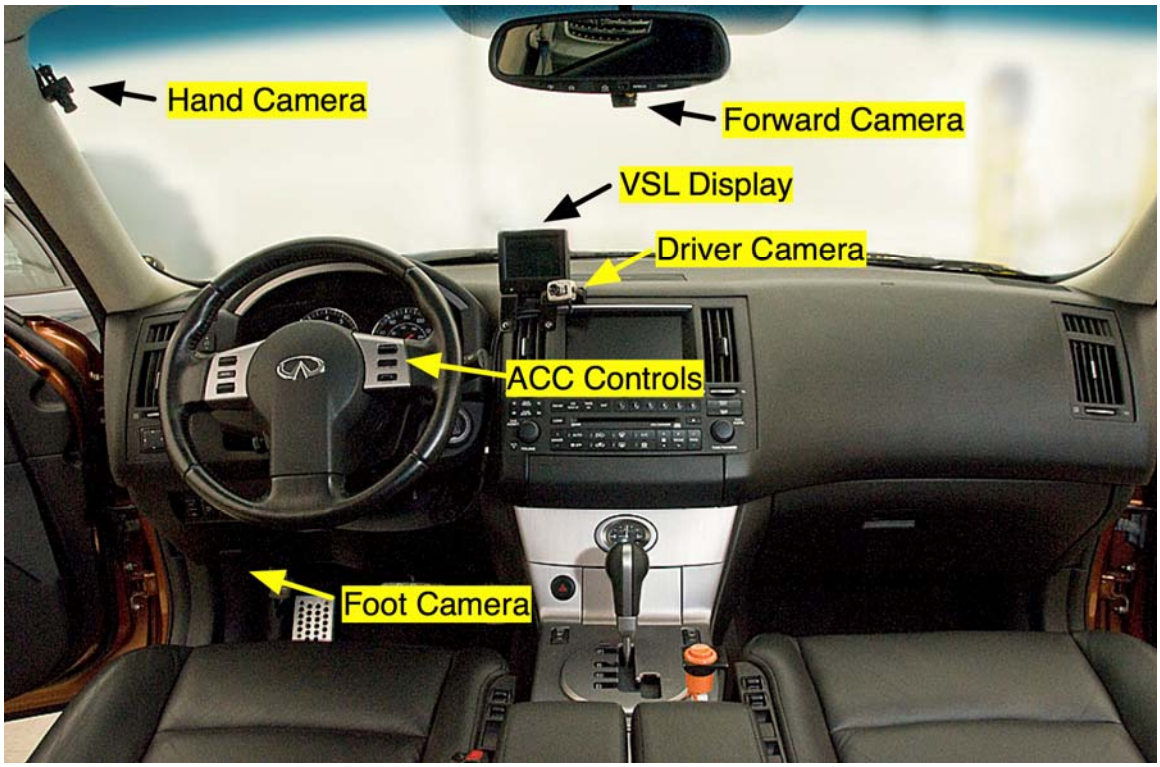

Figure 6.3 Vehicle Interior, Showing Locations of Video Cameras.

The VSL display, as shown in Figure 6.4, simply indicated the recommended speed limit in miles per hour. The recommended speed limits for each of the eight sections of the test route were obtained by the vehicle through a cellular data modem connection. The vehicle polled the server at California PATH for the recommended speed limits every 30 seconds, and using the vehicle's GPS location, it displayed the recommended speed limit for the current freeway segment. Changes in the recommended speed limit were accompanied by a "Beep Beep" composed of two short 2000 Hz tones. The wireless icon on the display indicated that the

recommended speed limits being received by the vehicle were less than 2 minutes old, and the grey integer in the lower right corner indicated the freeway segment (for the experimenter).

Figure 6.4 Variable Speed Limit Display.

For this experiment, the important parameters recorded by the vehicle DAS included the following:

- Timestamp
- Vehicle Speed & Braking
- ACC System Status, Set Speed, and Gap Setting
- Lead Vehicle Range & Relative Speed
- GPS Location
- VSL Algorithm Recommended Speed

The output of the video recording system is shown in Figure 6.5. Two MPEG files were recorded, the first containing the forward road scene, and the second containing a quad-split recording of the rear road scene, the driver's face, the driver's hands, and the driver's feet.

Figure 6.5 Example of video file content (left is front view, right is quad view)

Although the ACC system usage was not the focus of the VSL experiment, the drivers were asked to use the ACC system whenever possible. The ACC Driver Vehicle Interface (DVI) consisted of a set of four buttons located on the right side of the steering wheel and two visual displays located on the dashboard. Figures 6.6 and 6.7 depict the dashboard displays and the steering wheel controls. The main ACC display is located at the bottom of the tachometer dial

on the instrument panel, adjacent to the transmission gear indicator, as shown in Figure 6.7. This picture shows how the display looks when the ACC has first been activated, but the set speed has not yet been selected and there is no lead vehicle present.

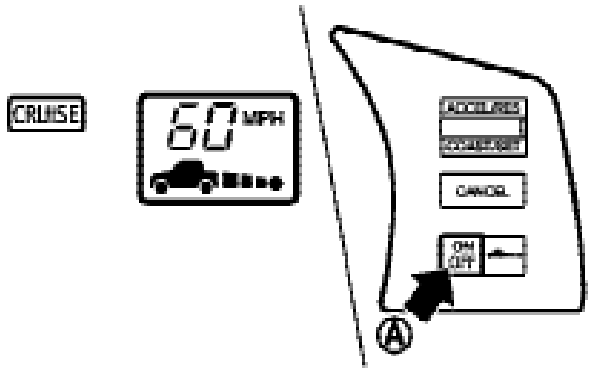

Figure 6.6 ACC display and controls as illustrated in vehicle owner's manual

Figure 6.7 ACC displays (left) and controls (right)

The first visual display is the "CRUISE" indicator light, located along the left side of the instrument cluster, which is activated with a green background when the on/off switch is pushed down. In case of system malfunction, this display background turns to orange. This light only indicates that the cruise control system has been turned on, and not that it is currently active and controlling the vehicle speed.

The second, and main, ACC display is located within the tachometer to the left of the current gear indication ("P" in Figure 6.7). This display shows the current ACC set speed (for example, 60 mph in Figure 6.6). The display also shows the current gap setting. Each square between the vehicle and dot represents an increasing gap setting. If all squares are visible, the longest gap has been selected. When the shortest gap has been selected, only the square closest to the dot is present. Finally, this display indicates whether or not a lead vehicle has been detected by the system. If no lead vehicle has been detected, there is no car icon to the left of the current gap

setting (as shown in Figure 6.7). If a lead vehicle has been detected, there is a car icon to the left of the current gap setting (as shown in Figure 6.6).

The driver controls the ACC with four buttons. The ACC is activated by the driver pushing the "on/off" button (the left side of the middle button on the steering wheel), as shown in Figures 6.6 and 6.7. The set speed is selected by toggling the top button down, and then toggling it up or down to increase or decrease the set speed. Short toggles produce changes of 1 mph in set speed, while holding the button in the up or down position for about one second produces a change of 5 mph in the corresponding direction. The bottom button ("Cancel") is used to interrupt the ACC action at any time the user chooses, analogous to hitting the brake pedal, but retaining the set speed value for the next time the system action is resumed by toggling the top button up.

The only important characteristics of the ACC system to note for this experiment are the facts that the minimum set speed was 25 mph, and below 20 mph, the ACC system automatically disengaged. Thus, when either the recommended speed limit or the speed of traffic was below 25 mph, the ACC system could not be used.

6.1.5 Test Procedures

The experiment began at the California PATH Richmond Field Station facility and lasted anywhere between 2 and 2.5 hours, depending on traffic conditions. There were four general parts to the experiment:

1. Read and Sign consent forms at California PATH (10 minutes)
2. Vehicle Familiarization at Richmond Field Station (10 minutes)
3. Speed Recommendation Testing on I-80 (90-120 minutes)
4. Survey and subject payment at California PATH (10 minutes)

The consent form (Appendix A) consisted of three parts. The first of the consent forms (obtained verbally by phone and later signed by the participants) was the consent to check the participant's DMV records. The second part of the consent form described the experiment, and the third part of the consent form was a photograph/video release form. Participants read the consent materials and asked the experimenters any questions that they might have had. The photograph/video release form was optional. Participants were not obligated to release their photographic or video images as a prerequisite for the participation in the experiment.

The vehicle familiarization took place in the parking lot at the Richmond Field Station and during the drive to the start of the freeway test route. Participants were given time to adjust the seat and mirrors, and then they were given a brief tutorial on the use of the ACC system by the experimenter. On the way to the start of the freeway test route, the experimenter talked the participant through engaging the ACC system, changing the set speed, and changing the gap setting. The experimenter continued to act as a reference regarding the ACC operation throughout the experiment.

The target of the experiment was to obtain four runs through the freeway test section as the freeway traffic was building from free-flow to congested. On Mondays and Tuesdays, this

necessitated starting around 3:00 PM, and on Wednesdays and Thursdays it necessitated starting around 2:00 PM. On Fridays there was almost always some congestion on the freeway test section, so free-flow conditions were unobtainable. Each run through the freeway test section began as the participants entered I-80 westbound at Solano Ave., and participants had about a half-mile to merge onto the freeway and activate the ACC system before entering the first section of the freeway where a recommended speed was provided. A nominal run in free-flowing traffic lasted about 10 minutes, while the longest run in congestion lasted about 20 minutes.

Each time a new recommended speed was provided on the display, the experimenter prompted the participant to set the ACC system set speed as close to the recommendation as the participant felt comfortable travelling. Thus, the ACC system set speed represented a conscious decision by the driver as to what speed he or she felt comfortable travelling on that section of freeway. The actual speed travelled by the vehicle may have been lower at times due to merging or exiting traffic. Drivers were free to make comments to the experimenter about the recommended speed or the behavior of the VSL algorithm.

After the test drives were completed, the participant and experimenter returned to the California PATH Richmond Field Station, and the participants were given a short post-experiment questionnaire to fill out (See Appendix B). After finishing the questionnaire, the participants were thanked for their time and paid a stipend of $55.

6.2 Experimental Results

6.2.1 Overview

A total of 16 drivers participated in the experiment, but the amount of data gathered from each driver varied as shown in **Error! Reference source not found.**. Typically each driver completed four runs through the freeway test section, but in some cases there were either more or fewer runs gathered for a driver. If traffic was light, more runs were gathered during the 2-hour test period, and if traffic was heavy, fewer runs were gathered. For driver 13, although four runs were collected, the resulting data were corrupted due to a DAS system failure, and the data could not be analyzed.

Additionally, some of the analyses described in this section examined the driver's behavior with the speed advisory system with respect to the current mean traffic speed. However, the mean freeway speed calculations were not transmitted to or recorded on the test vehicles. The mean freeway speeds were recalculated in post-processing using the raw PeMS data (which was originally used to provide the test vehicle with the speed advisory.) As shown in **Error! Reference source not found.**, any analysis with respect to the mean freeways speeds was based on fewer participants because there were errors in the saving of or the post-processing of the raw PeMS data needed to recompute the mean freeway speeds during the time when the test participant was travelling through the freeway test section.

Table 6.1 Summary of Data Collected Per Driver.

Driver	Gender	Runs	Day	Freeway Speed Data
1	Male	4	Wednesday	Yes
2	Female	4	Tuesday	Yes
3	Male	5	Wednesday	Yes
4	Male	4	Thursday	Yes
5	Male	4	Friday	No Data
6	Male	6	Monday	No Data
7	Female	2	Tuesday	Yes
8	Female	3	Wednesday	Yes
9	Male	3	Thursday	Yes
10	Male	2	Friday	Yes
11	Female	4	Monday	Yes
12	Male	4	Tuesday	Yes
13	Male	No Data	Wednesday	No Data
14	Female	2	Thursday	Yes
15	Male	4	Monday	Yes
16	Male	4	Tuesday	Partial Data

6.2.2 Time in Zone & Advisory Speed Stability

The freeway test section was divided into seven, mile-long zones, where each zone should have a decreasing advisory speed leading up to the bottleneck point at the end of the test section. As shown on the left side of Figure 6.8, the distribution of times spent in each zone during each run ranged from about 40 seconds to greater than 5 minutes (depending on the particular zone and traffic conditions). Overall, the mean time spent driving in a zone was 79.5 (SD 61.2) seconds. On the right side of Figure 6.8 is shown the distribution of times that the advisory speed displayed to the driver was constant (within a zone). Although the distribution shapes are roughly similar, a fairly large portion of the advisory speeds were shown to the driver for less than 30 to 40 seconds (corresponding to the advisory speed data update rate on the test vehicle). This indicates that the advisory speed frequently changed on the driver before the driver exited a zone.

Additionally, there was a large difference in the performance of the speed advisory system between zones. In the first zone, Figure 6.9, the mean time spent in the zone was 75.7 (SD 4.2) seconds, and the advisory speed was almost always constant. In contrast, in the second zone, Figure 6.10, the mean time spent in the zone was only 30.2 (SD 2.1) seconds because the second zone was slightly shorter in length. Furthermore, about 20 to 25 percent of the time, the driver was presented with an advisory speed change within the zone, i.e., the advisory speed for the zone started at one value, and changed to a different value within 30 seconds and before exiting the second zone.

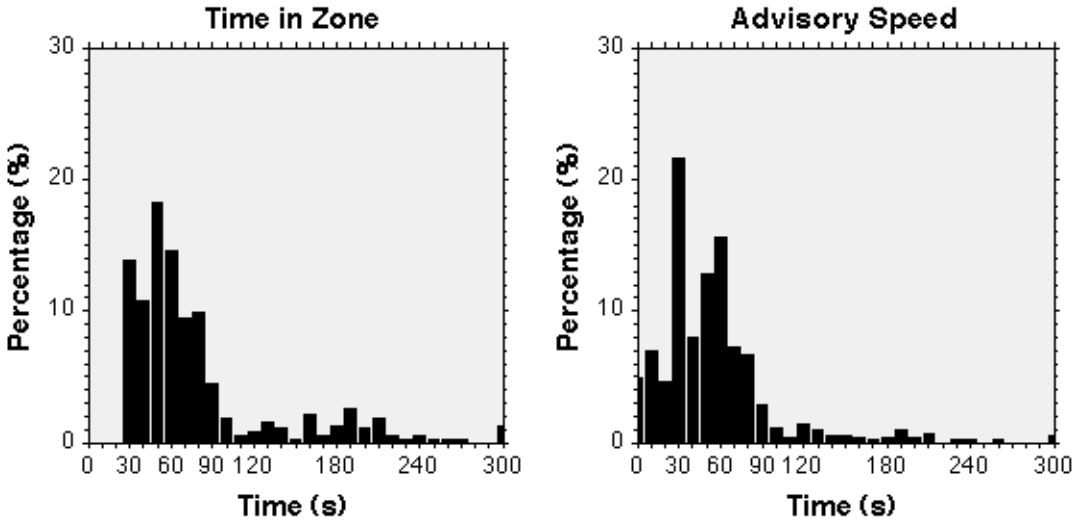

Figure 6.8 Durations of Time in Zone and Time that the Advisory Speed was Constant.

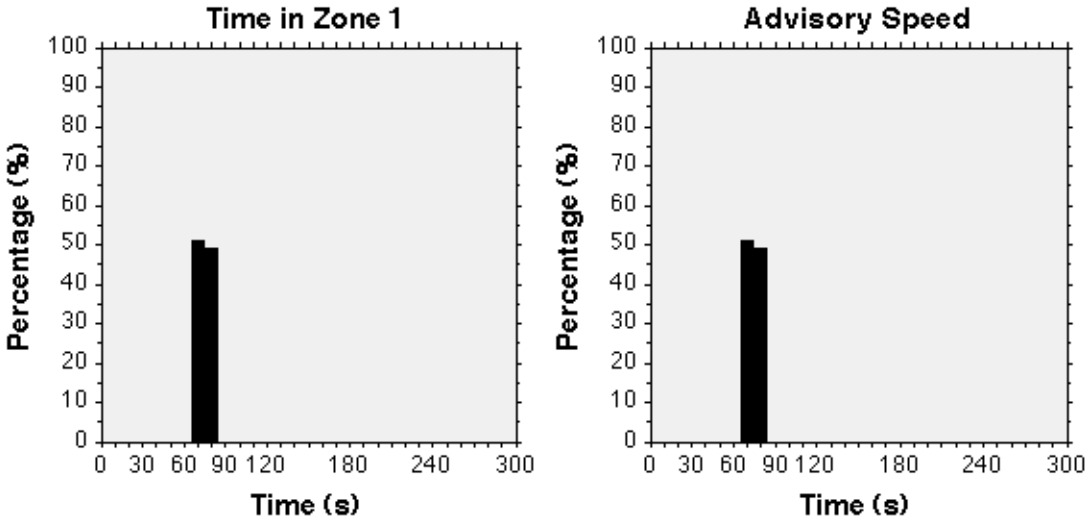

Figure 6.9 Duration of Time in Zone 1 and Time that Advisory Speed was Constant in Zone 1.

A similar trend to Zone 2 was seen in Zone 3, Figure 6.11, where the mean time to traverse the zone was 46.6 (SD 4.7) seconds, and nearly 15 to 20 percent of the trails in Zone 3 resulted in the driver seeing a speed change before exiting the zone. Interestingly, Zone 4, Figure 6.12, does break from the trend slightly. The mean time to traverse Zone 4 was 62.2 (SD 25.9) seconds, but advisory speed changes within the zone occurred less than 10 percent of the time.

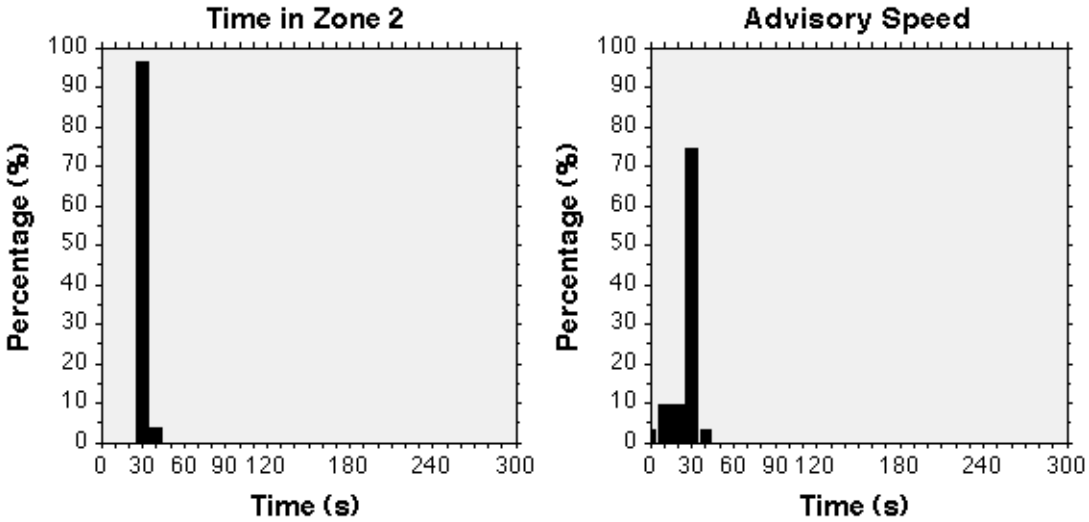

Figure 6.10 Duration of Time in Zone 2 and Time that Advisory Speed was Constant in Zone 2.

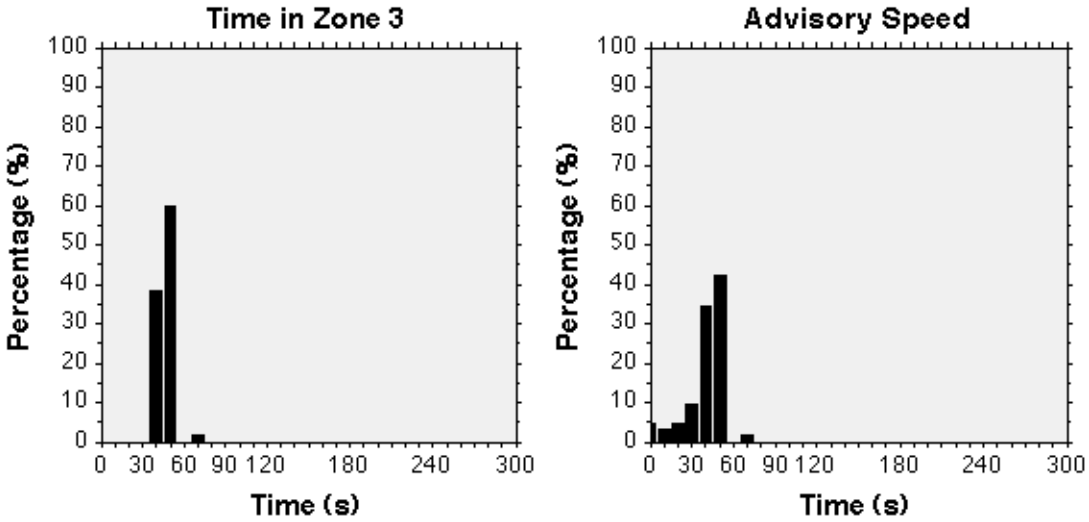

Figure 6.11 Duration of Time in Zone 3 and Time that Advisory Speed was Constant in Zone 3.

The mean times spent in Zones 5, 6, and 7 (see Figure 6.13) were far more variable because these zones were closer to the breakdown in traffic flow, and thus, these zones were often more congested. The mean times to traverse these zones were 99.0 (SD 76.9), 70.0 (SD 36.8), and 174.2 (SD 72.6) seconds for Zones 5, 6, and 7, respectively. In each of these zones, the speed advisory value changed at intervals of 30 seconds or less, or on each update received by the vehicle, on between 15 and 35 percent of the trials.

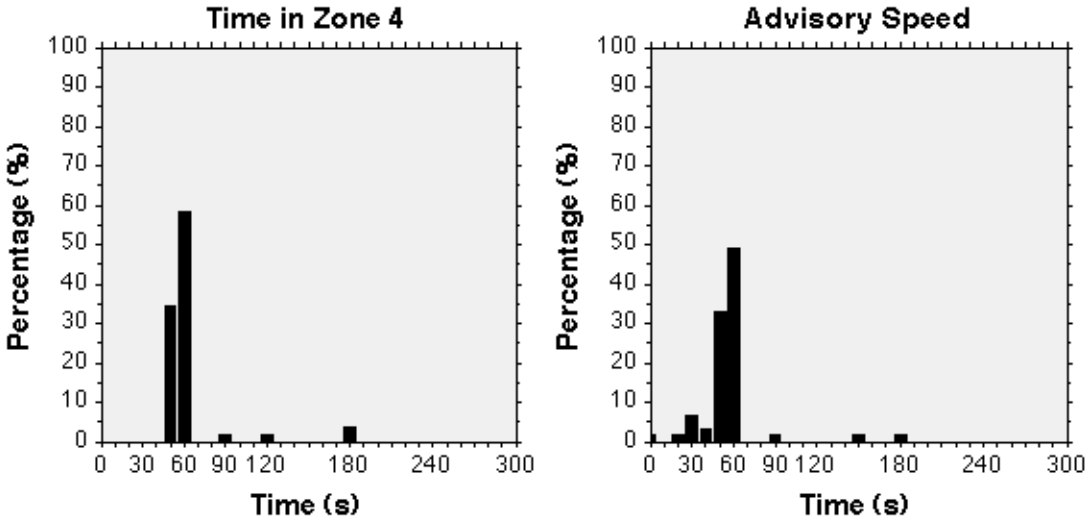

Figure 6.12 Duration of Time in Zone 4 and Time that Advisory Speed was Constant in Zone 4.

Overall, the analysis and graphs shown in this section indicate that the speed advisory system did not appear to be stable to the participants. Because of the asynchronicity of data updates to the test vehicle, there were cases when the driver entered a zone and the system recommended one speed, but then the recommended speed changed within 5 seconds because the system received a new updated speed for that zone. Additionally, there were cases noted when the advisory speed oscillated between two speeds, e.g., 30 and 35 mph, every 30 seconds or so when new information was received by the vehicle. These situations prompted participants to frequently make comments along the lines of not trusting the advisory speed because it changed too frequently.

Thus, the experiment results clearly indicated that perception of stability of the speed advice was a concern among the drivers, and a question was specifically asked in the post-experiment questionnaire regarding the desired frequency of advisory speed updates. However, the answers put forth by the drivers to this survey question were not that helpful. The answers ranged from ¼ mile to 1 mile, which translates to about 15 to 60 seconds based on the distribution of time required to traverse each zone in the experiment. Based on all of the feedback of the participants, both during the experiment and on the post-experiment questionnaire, it would seem that updates every 1 mile or 60 seconds would be about the fastest that one would want the advisory speed to change in order to maintain confidence in the advice.

Furthermore, there are a number of filtering strategies that could be implemented to ensure that the in-vehicle advisory speed system does not update too frequently. The simplest filter might be modeled on having a roadside sign at the entrance to each zone, and thus, the advisory speed for the zone is calculated once as the vehicle enters the zone, and is then maintained until the vehicle reaches the next zone.

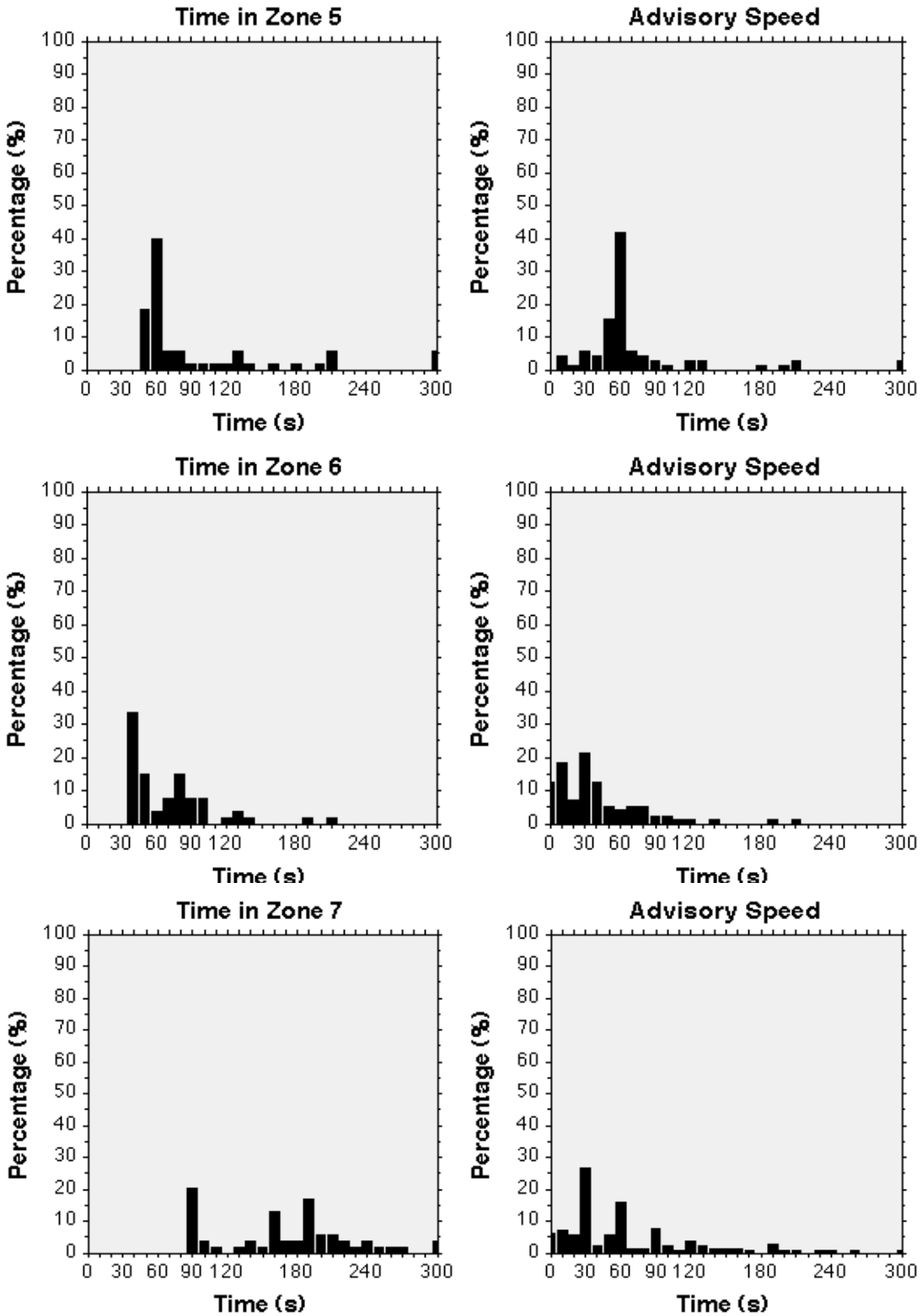

Figure 6.13 Duration of Time in Zones 5, 6, and 7 and Time that the Advisory Speed was Constant in Each.

6.2.3 Advisory Speed Profile

The advisory speed from the VSL algorithm varied by both the freeway segment and the traffic conditions during the test participant's run. As shown in Figure 6.14, the maximum advisory speed given for any of the seven freeway segment zones was 65 mph or the speed limit through the freeway test section. This recommendation was given when there was little to no traffic. The minimum advisory speed given by the VSL algorithm was 15 mph, but this recommendation was generally only given in the most congested zones at the most congested times. The minimum recommended speeds seen during the experiment were 65 mph for Zone 1, 45 mph for Zone 2, 20 mph for Zone 3, and 15 mph for the remaining zones. The mean advisory speed for each zone as shown in Figure 6.14 was obtained by averaging across all participants and all trials.

Although the mean advisory speed appears to decrease smoothly when traversing the seven zones, the participants often expressed dissatisfaction with the magnitude of the individual changes in the advisory speed. The advisory speed could change either between zones or within a zone (since the data for a zone was refreshed on the vehicle every 30 seconds). As shown in Figure 6.15, the changes in the advisory speed, either between or within zones, were frequently greater than 10 mph (almost 25 percent of the time) and sometimes as high as 50 mph (indicating a recommended speed change from 65 mph to 15 mph).

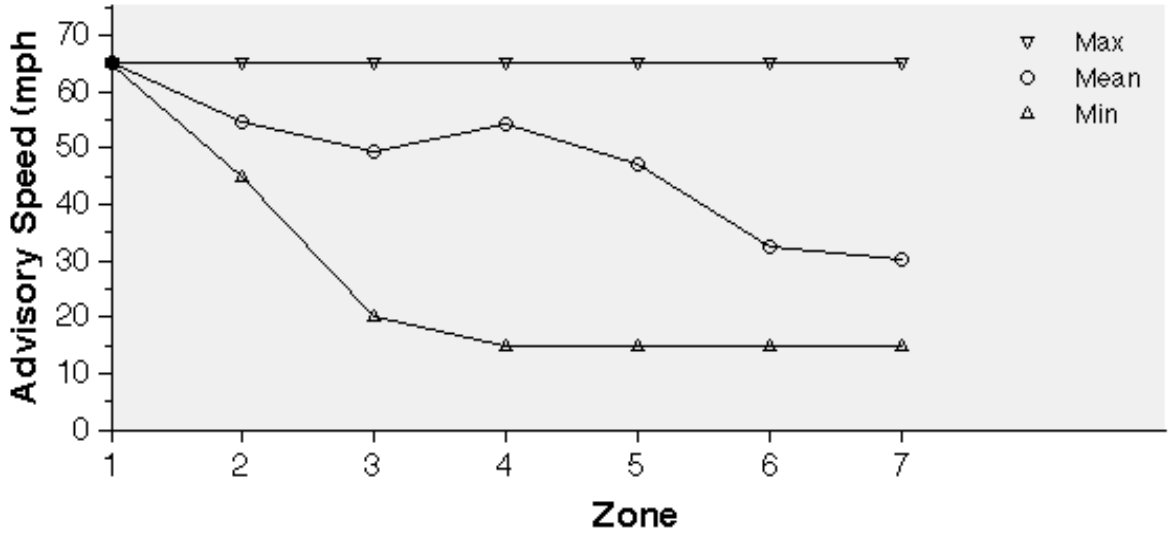

Figure 6.14 Advisory Speed by Zone.

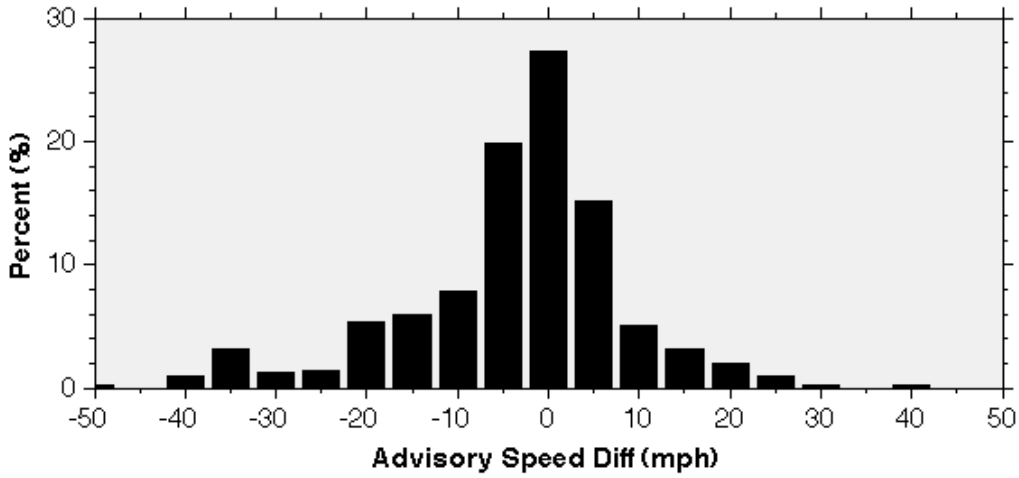

Figure 6.15 Advisory Speed Change Step Sizes.

There was variability in the advisory speed changes based on the freeway segment or zone, which is detailed in Figure 6.16. Zone 1 always displayed an advisory speed of 65 mph (the speed limit), and about 27 percent of the time, this value carried over to Zone 2. The reduction in speed requested in Zone 2 was less than 10 mph only about 17 percent of the time, while 40 percent of the time, the requested reduction in speed was either 15 or 20 mph. The graph for Zone 3 looked slightly better. Over 85 percent of the time, there was a requested reduction in speed of less than 10 mph when entering Zone 3.

Although there was generally a decrease in the mean advisory speed progressing from Zone 1 to Zone 7, there was typically an anomaly in the VSL algorithm when entering Zone 4. As shown in Figure 6.16, almost 60 percent of the time the advisory speed increased by 5 to 20 mph upon entering Zone 4. Many of the participants did notice this increase and commented about it while driving with the speed advisory system.

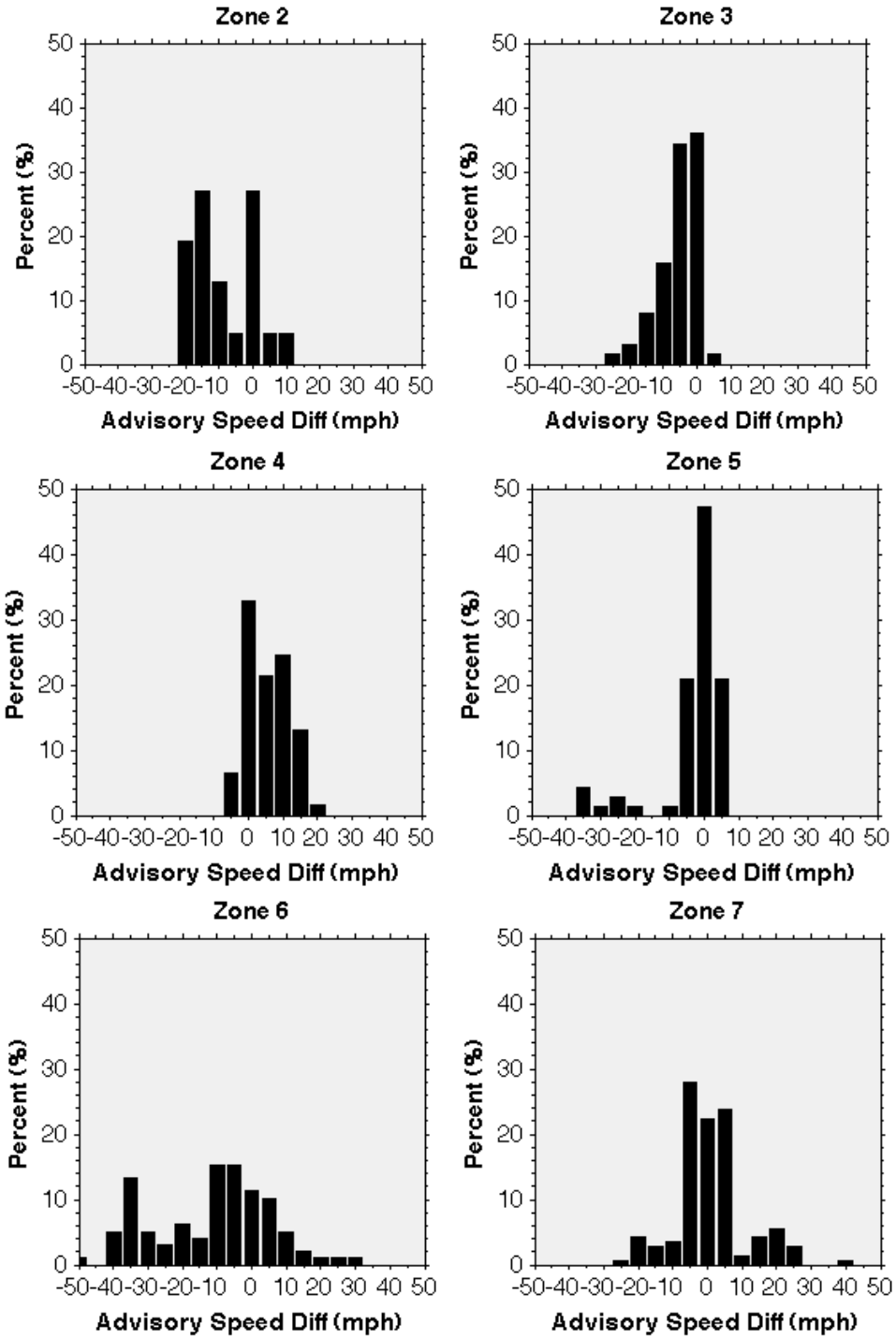

Figure 6.16 Advisory Speed Changes at Each Zone.

Unfortunately however, the increased advisory speed in Zone 4 was often followed by very large decreases in the advisory speed in Zones 5 and 6. Almost 10 percent of the time in Zone 5 and 30 percent of the time in Zone 6, the advisory speed was decreased by 20 to 50 mph. The participants almost unanimously commented that such large decreases in the advisory speed were not acceptable from their point of view. There was one post-experiment survey question

regarding the desired intervals for changes in the advisory speed which shed some light on this subject. Most of the participants answered the question saying that the speed changes should be no more than 5 to 10 mph at a time.

Finally, one aspect of the VSL algorithm that can be seen in the graphs in this section was the oscillation of the advisory speed between two values. These oscillations were typically noted in Zones 5, 6, and 7, where the advisory speed increased by 5 mph between 10 and 24 percent of the time. The 5 mph increases in the advisory speed in these zones were matched by 5 mph decreases in the speed at about the same rate, indicating that the advisory speed was changing up and down by 5 mph every 30 seconds or so. Examining the data for the VSL algorithm, these oscillations were typically due to rounding errors when the algorithm was suggesting a speed somewhere between the two values and minor changes in the moment by moment traffic data would push the advisory speed up or down to the nearest 5 mph increment. The participants definitely noticed these oscillations and commented on their annoyance with them.

6.2.4 Driver Acceptance of Advisory Speeds

The driver acceptance of the advisory speeds was measured in two ways. First, the driver was asked to make a conscious decision regarding their desired travel speed by setting the ACC (Adaptive Cruise Control) set speed each time the advisory speed changed. The instructions to the participants were to set the ACC speed as close to the advisory speed as the participant felt comfortable travelling. Second, the actual speed of the test vehicle was examined because the participants may have consciously indicated one speed using the ACC set speed at the time of the recommended speed change, but the prevailing traffic conditions may have dictated that the vehicle travel at a slower speed later during the run.

Table 6.3 and Figure 6.17 show the participants' compliance as a function of the advisory speed averaged across all of the zones. During testing, the mean freeway speed averaged across all zones ranged from 43 to 51 mph. Overall, it appeared that drivers did lower their ACC set speed and the mean vehicle speed did decrease in response to lower advisory speeds, but there was generally not strict compliance with the advisory speed.

Table 6.2 Overall Mean Compliance With Advisory Speeds.

Advisory Speed	Mean ACC Set Speed	Mean Vehicle Speed	Mean Freeway Speed
65	65	61	45
60	61	57	51
55	61	55	45
50	62	53	41
45	60	51	43
40	57	48	43
35	47	34	45
30	42	28	48
25	45	27	49

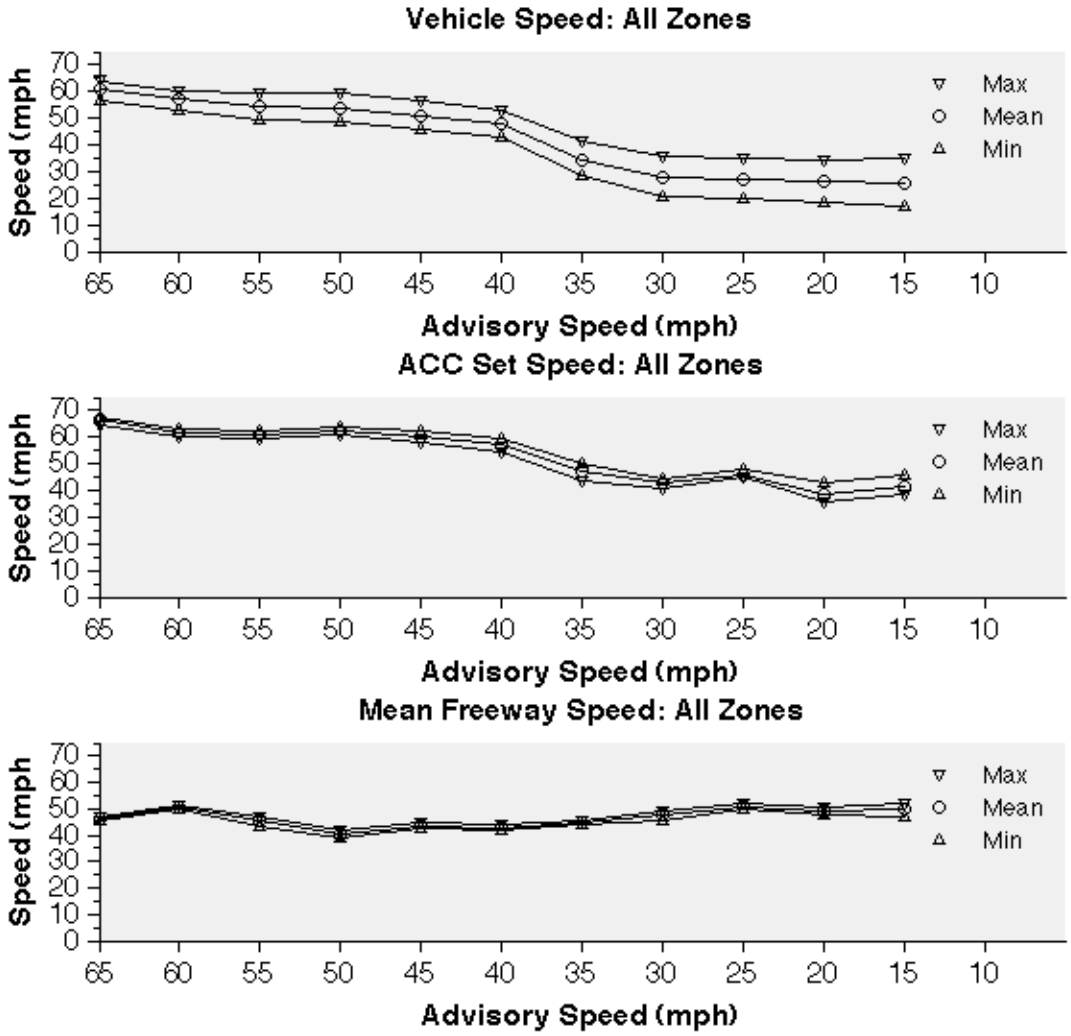

Figure 6.17 Driver Compliance with Advisory Speeds Across All Zones**.**

To further understand the typical driver compliance with the advisory speeds, the data must be examined with respect to both the advisory speed and the prevailing traffic conditions in the zone. As an example, in Zone 2, Figure 6.18, the freeway was typically free-flowing at 55 to 65 mph. The advisory speeds ranged from 65 to 45 mph, and the estimates based on the infrastructure sensor data suggested that the mean traffic speed in the zone was typically around 45 mph. (It should be noted that the freeway speeds in Zone 2 were probably estimated using single loop detector stations, and the VSL algorithm was conscious of the fact that the infrastructure sensing of the speed was typically low in this zone.) The ACC set speed ranged from 60 to 65 mph, and mean vehicle speed generally ranged from 55 to 60 mph. Thus, in Zone 2, it can be assumed that traffic was mostly free-flowing from 55 to 65 mph, and the participants were only willing to travel about 5 mph slower than the prevailing traffic around them. This behavior was also typical for Zones 1 and 3 which can be found in Appendix C.

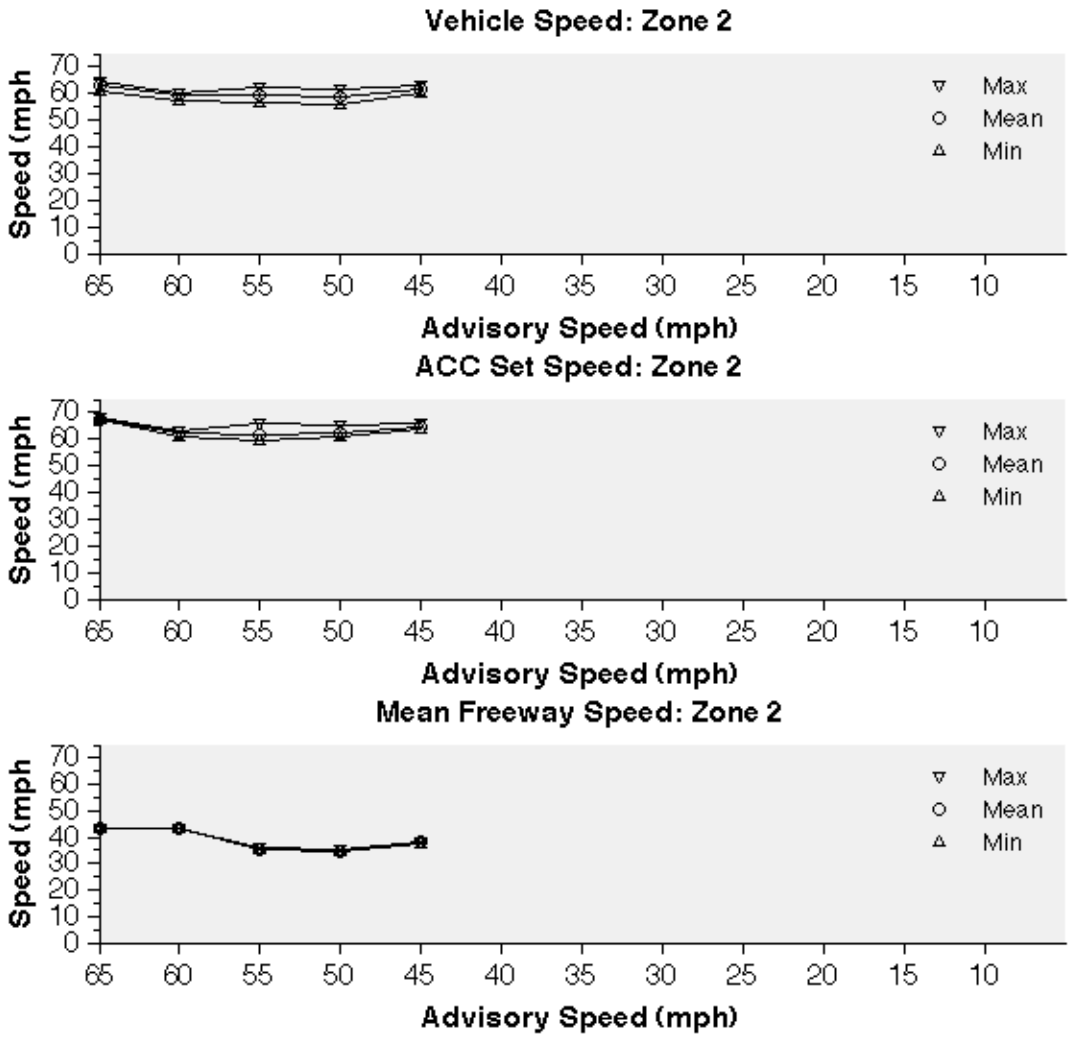

Figure 6.18 Driver Compliance with Advisory Speeds in Zone 2.

In the second example, Zone 4 is interesting because it represented a transition case. (See Figure 6.19.) Most of the time, Zone 4 contained free-flowing traffic, and the advisory speed ranged from 50 to 65 mph. When the traffic speed in the zone was free-flowing, the minimum set speed that drivers were comfortable using was 60 mph, or about 5 mph less than the perceived speed of the prevailing traffic. The minimum vehicle speeds were a little less than 55 mph through the same stretch.

However, in Zone 4 there were also cases when the traffic flow started to break down, and the advisory speed was between 40 and 45 mph. In these two situations, the ACC set speed became irrelevant since the participants left the set speed somewhere between 55 and 65 mph, but the vehicle speed dropped to about 20 mph in the Zone. Interestingly, the mean vehicle speeds were actually less than the advisory speeds in these situations. When the VSL algorithm recommended 45 mph, the mean vehicle speed was actually only 35 mph, and when the VSL

algorithm recommended 40 mph, the mean vehicle speed was actually only 25 mph. These two cases probably represent conditions when the traffic breakdown occurred faster than the VSL algorithm could compensate. However, the important driver behavior to note was the fact that the participants more or less ignored an advisory speed that was 10 to 20 mph slower than the current traffic speed until they actually saw the traffic jam and were slowed due to its effects. Zone 5 was also very similar to Zone 4, and the details for Zone 5 can be found in Appendix C.

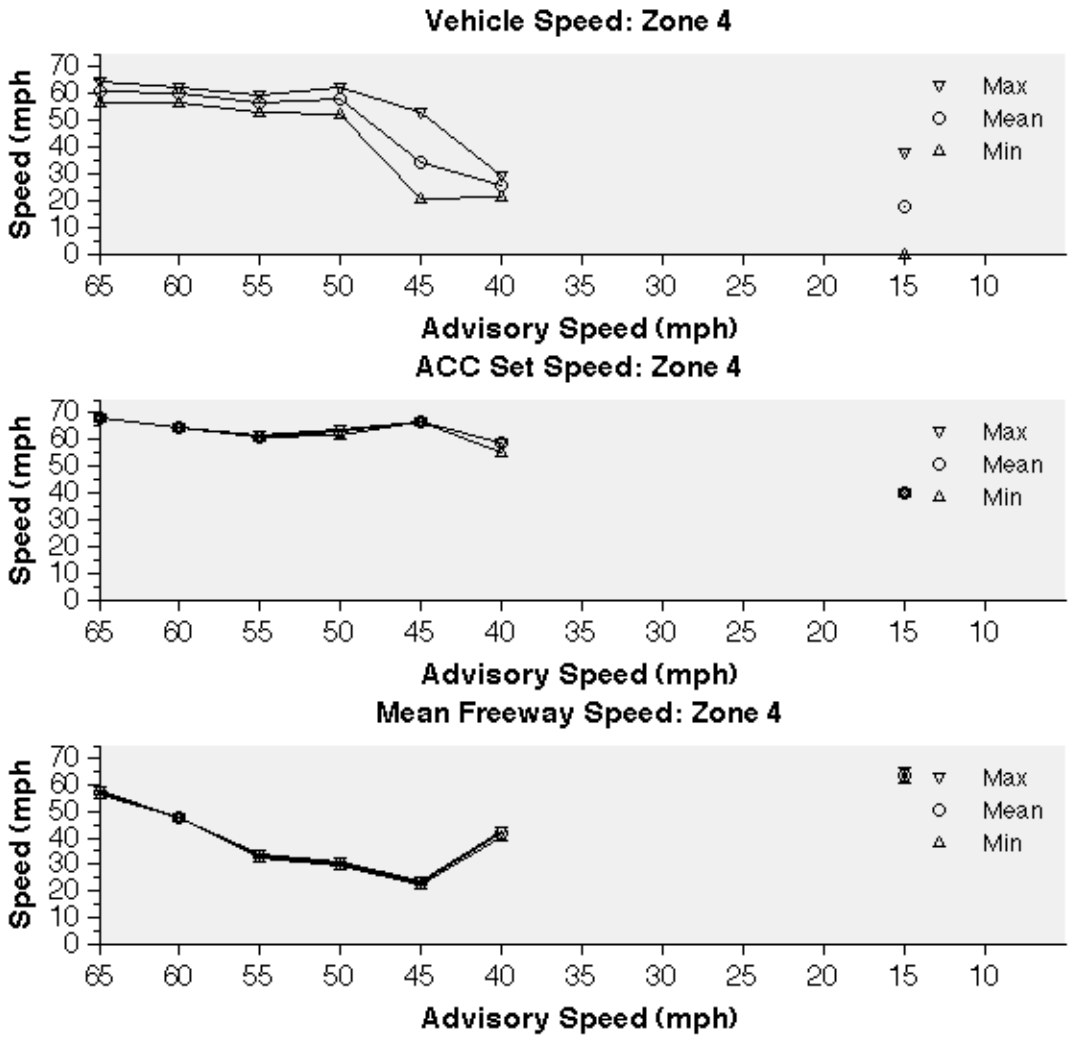

Figure 6.19 Driver Compliance with Advisory Speeds in Zone 4.

In Zone 6, the participants were about 2 miles from the main bottleneck. Since the experiment was geared to allow the participants to drive through this section of freeway multiple times while traffic was building, it was not surprising to find that the range of both advisory speeds and vehicle speeds in Zone 6 spanned the entire range from 15 to 65 mph as shown in Figure 6.20. On some runs, the advisory speed was high, above 50 mph and the freeway and vehicle speeds

were also high. On other runs, the traffic was building to breakdown and the advisory speeds ranged from 15 to 45 mph. The most interesting data points in Zone 6 were when the advisory speed was between 30 and 45 mph, and the surrounding traffic had slowed from free-flowing speeds. When the advisory speed was between 40 and 45 mph, the mean vehicle speed was 50 mph, and the ACC set speed was about 55 mph. Whereas at higher speeds, the participants were willing to set the ACC system to 5 mph below the speed of traffic, in this transition range, the participants were reluctant to lower the ACC set speed even though the mean vehicle speed was about 5 mph slower than the set speed.

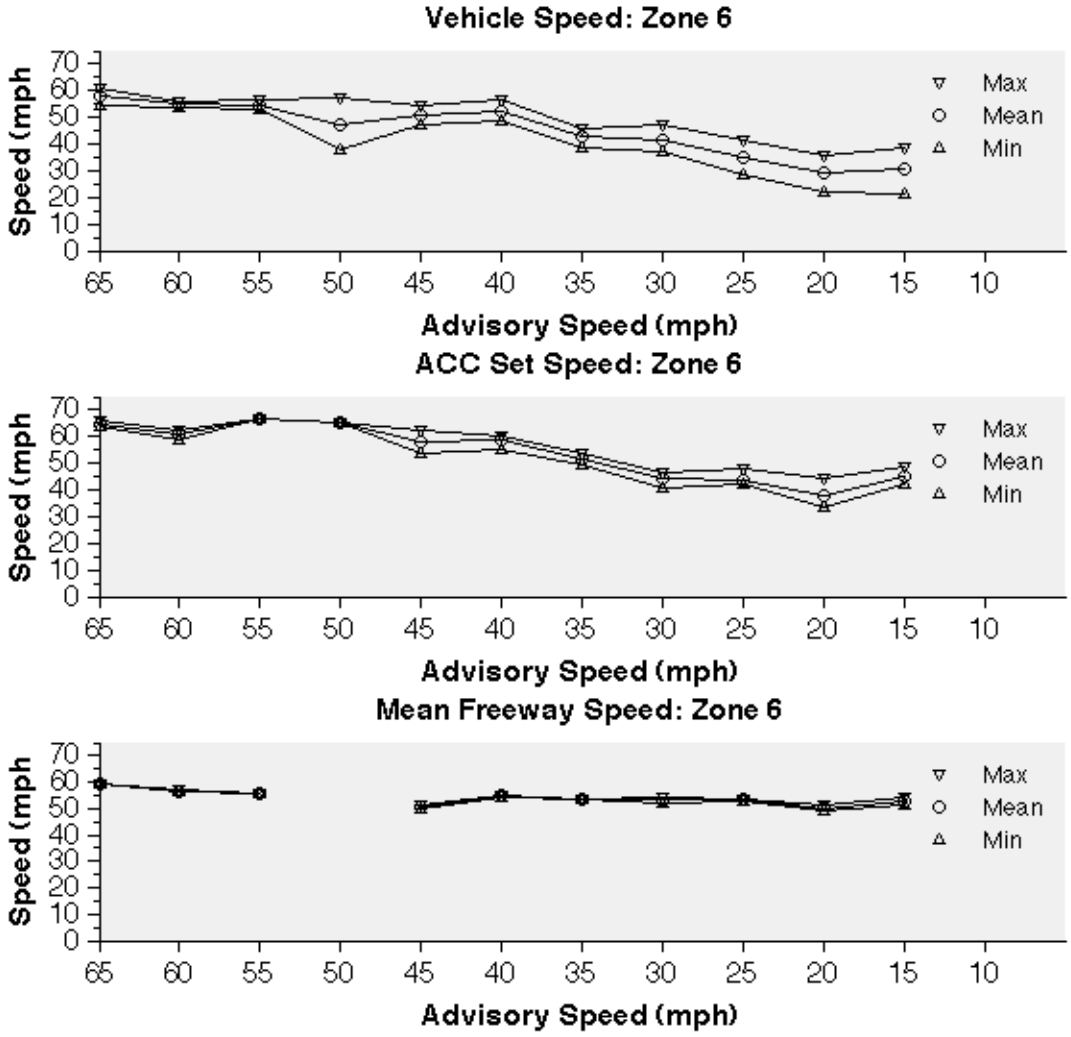

Figure 6.20 Driver Compliance with Advisory Speeds in Zone 6.

Similarly, as the advisory speed dropped into the range of 25 to 35 mph, the participants lowered the ACC set speed, but kept the set speed about 15 mph higher than the advisory speed even though they were only travelling, on average, 10 mph higher than the advisory speed. In these

cases, the ACC Set speed may not be the best metric regarding the driver acceptance of the advisory speed because the system worked too well. The drivers could set a higher ACC set speed and then let the system take care of keeping the vehicle at the prevailing traffic speeds. In essence, once the drivers were in congestion, they did not appear willing to driver slower than the prevailing traffic speed. Similar patterns were seen in Figure 6.21 in Zone 7.

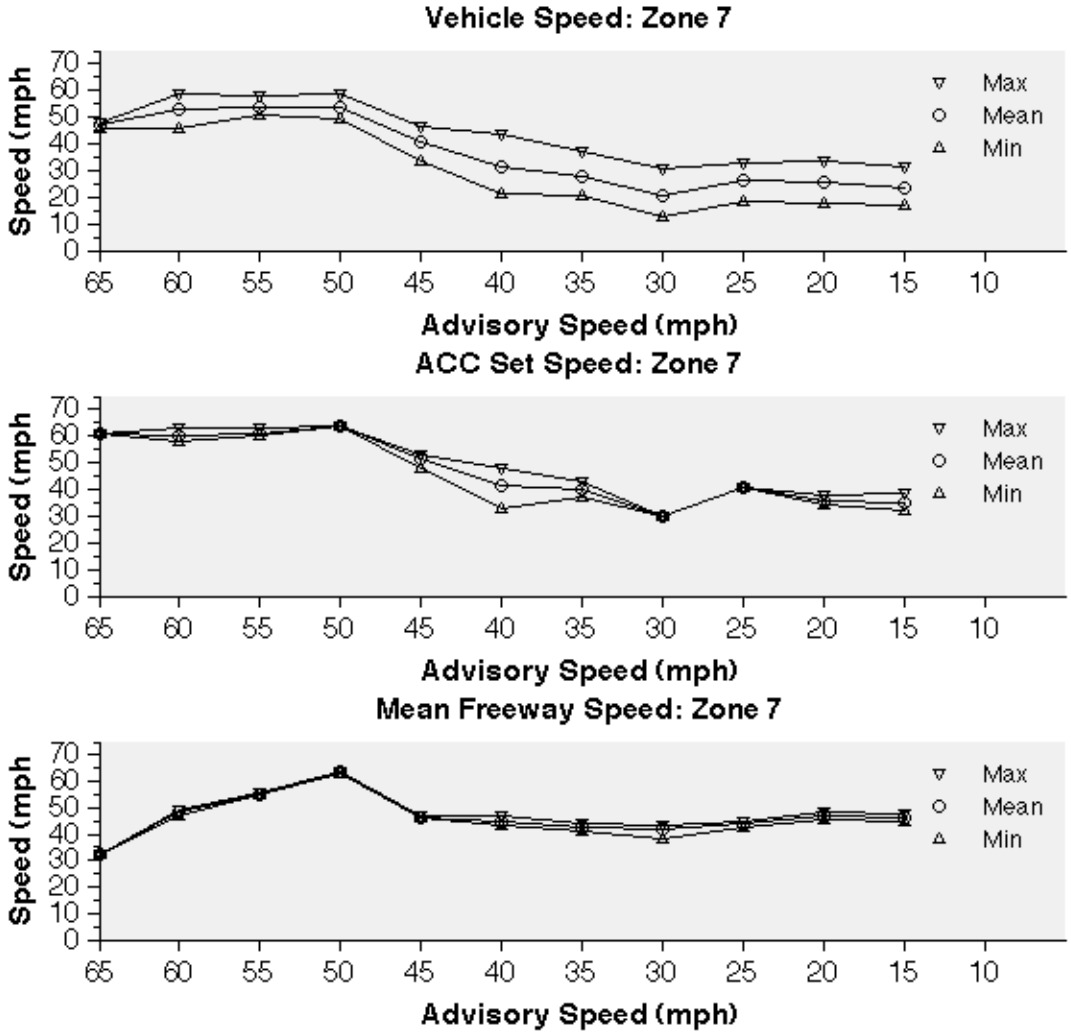

Figure 6.21 Driver Compliance with Advisory Speeds in Zone 7.

In Zone 7, the freeway segment where traffic congestion typically started, the mean ACC set speeds actually matched the advisory speeds when the advisory speeds ranged from 30 to 45 mph, even though the mean vehicle speeds tended to track 5 to 10 mph lower than the advisory speeds. Thus, if the advisory speeds were close to the prevailing traffic speeds, then the drivers were willing to set the advisory speed in the ACC system and follow it. However, as the advisory speed dipped to 25 mph or below (speeds too low for the ACC system used in this

experiment), the mean vehicle speed remained steady at 25 mph. Again, at low speeds in heavy congestion, drivers appeared unwilling to travel at speeds much lower than the prevailing traffic flow. Some drivers even commented that advisory speeds below 25 mph seemed unreasonable and should not be given.

6.2.5 VSL Survey Results

The written survey provided to drivers was open-ended and meant more as a tool to elicit feedback on the VSL concept, rather than on the actual system that was implemented. Only about one-quarter of the participants were familiar with the VSL concept before participating in the experiment; however, once the concept was explained to the participants almost all of them reported positive or favorable feelings towards it on the survey.

The first set of questions focused on the how comfortable the drivers were when maintaining a recommended advisory speed that was slower than the prevailing traffic speed. The participants reported that either sometimes or most of the time, the recommended advisory speed provided during the experiment was a safe travel speed for the traffic conditions. Furthermore, the participants mostly reported that they would be comfortable with a recommended advisory speed up to 10 mph below the prevailing traffic speeds.

The next set of questions focused on the VSL speed changes. About two-thirds of the participants reported that they were mostly comfortable with the frequency of the VSL speed changes, although several of the participants noted that the system occasionally behaved erratically from their point of view. Suggested update intervals ranged from one-quarter to one mile. As for the speed change increment, most of the drivers agreed that the recommended advisory speed should not change by more than 5 to 10 mph.

The final set of questions focused on VSL implementation issues. Although this experiment only recruited a very small sample size, almost all of the participants stated that they would follow the recommended advisory speed, even if it was not legally enforceable, and half of the participants stated that they were against implementing a VSL system that would be legally enforceable. On the question about where to display the recommended advisory speed, most of the drivers felt that an in-vehicle solution like they had experienced was adequate, but one driver was insistent that the system would only work if the advisory speeds were on roadway signs for all drivers. Only about one-third of the participants were in favor of a system that integrated the recommended advisory speed system with the ACC set speed. However, even the participants who supported this concept were quick to point out that the system would need to be far more reliable than the one tested in the experiment in order for a tightly integrated solution to work.

7. Concluding Remarks about VSL/VSA

The important findings from the VSL/VSA research are:

(a) Based on the simulation results, application of a suitable VSL/VSA strategy to gradually reduce speed upstream of a bottleneck should make it possible to avoid or at least delay traffic flow breakdown at the bottleneck by increasing the effective capacity of the bottleneck. The degree of improvement depends on the overall traffic demand relative to the capacity of the bottleneck.

(b) If all vehicles followed the VSL speed on the approach to the bottleneck, it should be possible to increase the capacity of the bottleneck by 5% ~ 18% (depending on the road geometry and traffic situation). This can lead to savings of as much as 10% ~ 35% (depending on the road geometry and traffic situation) in the vehicle-hours of delay in the corridor that is constrained by the bottleneck.

(c) Compliance with the VSL speed can be achieved if at least 30% of the vehicles follow the VSL speed. This percentage of speed limited vehicles constrains the ability of the rest of the vehicles to go any faster.

(d) VSL has been evaluated with and without coordinated ramp metering (CRM) in order to understand the relative effectiveness of these alternative strategies in mitigating congestion. On the corridor that was selected for evaluation (I-80 from Richmond to Emeryville, CA), the ramps have such small queue storage capacity that CRM can have only limited effectiveness, so VSL was found to be significantly more effective.

(e) Calculation of effective VSL values depends on use of high fidelity traffic condition data. The existing loop detector infrastructure data in the evaluation corridor has significant problems in accuracy and availability, which has necessitated significant effort in data cleaning and massaging in order to make it usable as inputs to the VSL algorithm. With general availability of connected vehicle probe data, these problems should be mitigated.

(f) An in-vehicle display of VSL values was implemented on one of the ACC test vehicles, for use along the I-80 Westbound corridor. As the vehicle traveled along the corridor, it received the VSL values that were computed for the entire corridor, based on existing loop detector data, transmitted from the PATH server where the computations were done over a 3G cellular modem communication link. This demonstrated the technical feasibility of providing the real-time update information to a vehicle, which then decided which VSL value to display to its driver based on its GPS coordinates along the corridor (used to associate the vehicle with the correct network segment).

(g) The VSL displays were provided to 16 drivers recruited from the general public in order to determine their reactions to this new concept. The direct measurements of their reactions were recorded based on the set speeds that they chose for the ACC on the test vehicle, which were then compared with both the recommended VSL values and the prevailing local traffic speeds on

the network segment where they were traveling. The drivers were also surveyed to determine their subjective reactions to the VSL information. This experiment showed the potential for acceptance of the general VSL concept, but indicated the need for a more robust and stable implementation in order to meet driver expectations.

(h) The experiment providing the VSL displays to drivers indicated the need to provide a variety of practical refinements to the basic VSL algorithm to make it more suitable for public use, including:

- filtering to smooth out VSL changes and addition of hysteresis to ensure that the VSL values that any individual driver sees do not oscillate;
- limitations on the magnitude of speed change from one time interval to the next and from one network segment to the next so that drivers can adjust their speeds relatively smoothly;
- lower limits, to ensure that drivers are not confronted with freeway speed limits below those that would be posted on major arterials;
- addition of explanation for the reason for the reduced speed.

(i) The VSL value that is best for traffic flow can also be provided as the reference speed for an infrastructure-cooperative form of CACC, automatically limiting the speed of the vehicle to the VSL value. We planned to test this on the segment of the I-80 corridor where continuous video monitoring is available, so that the interactions between the VSL-limited vehicle and its neighbors could be observed through the vehicle trajectories to check for potential problems (such as excessive lane changing by impatient drivers stuck behind the subject vehicle). It was not possible to do this experiment because the location with the continuous video monitoring turned out to be right at the bottleneck rather than upstream of the bottleneck, and in this location the traffic was either free-flowing or severely congested, with virtually no intermediate conditions when the VSL algorithm would be recommending a speed significantly different from the prevailing traffic speed.

8. Introduction to Adaptive Cruise Control and Cooperative Adaptive Cruise Control Simulation Study

An earlier phase of this project included a field test of Adaptive Cruise Control (ACC) and Cooperative Adaptive Cruise Control (CACC), driven by 16 drivers from the general public. Those drivers were encouraged to select the time gap settings that they preferred for each system, and their selections of time gap were recorded, along with many other parameters, for subsequent analysis. They were also surveyed to determine their subjective opinions about the ACC and CACC systems. The results of this experiment were very encouraging about the potential market acceptance of ACC and CACC when they are made available to the general public. These results were reported in two prior project reports (53, 54) and two technical papers (55, 56).

The C/ACC field test produced quantitative results indicating the relative preferences of the driving population for driving at the different available time gap settings. These time gap preferences can have a significant influence on traffic flow and highway lane capacity. The current work reported here uses a traffic microsimulation, combined with the C/ACC field test results, to produce the first authoritative quantitative estimates of the impacts that these systems could have on highway capacity.

The maximum traffic flow is determined by admissible time gaps between vehicles. The admissible time gap is determined by the means of controlling the vehicle's car following: manual driving, Adaptive Cruise Control, or Cooperative Adaptive Cruise Control. In manual driving, the acceptable time gap is determined based on the driver's perception of what is safe, including his or her perception and reaction time, and is influenced by the driver's experiences, including expectations about the behaviors of other drivers, especially the driver of the leading vehicle. Vehicles with ACC or CACC have discrete time gap settings, which the driver can select based on his or her perceptions of the capabilities of the system. The net effect on traffic depends on whether drivers have sufficient confidence in the C/ACC systems to select time gaps that differ significantly from the gaps they use in manual driving.

This research evaluates the effects of the use of ACC and CACC on freeway capacity by microscopic simulation, based on the actual gaps that the drivers selected in our field testing of these systems. The simulation platform for this study is the commercially available traffic microsimulation program Aimsun, which was selected because it was the only simulation platform in which we could implement the NGSIM over-saturated freeway flow model, to provide the most realistic representation of normal drivers' car following and lane changing behavior in dense traffic.

9. Vehicle Types to be Simulated

There are four vehicle types represented in the simulation, to accommodate all possible combinations of vehicles that could be interacting with each other in ways that would influence freeway traffic flow and capacity:

(a) Manual vehicle - driven manually by a driver, with car following behavior represented by the NGSIM oversaturated flow model

(b) Adaptive cruise control (ACC) - car following is determined based on a simple first-order control law representing the behavior of a typical ACC system, with relatively slow, gentle responses to changes by the car ahead.

(c) Here I am! (HIA) - driven manually just like the Manual vehicle, but it is equipped with a DSRC radio that frequently broadcasts a "here I am" message giving its location and speed. If it is being followed by a CACC vehicle, that following vehicle can use CACC.

(d) Cooperative adaptive cruise control (CACC) - if it is following an HIA vehicle or another CACC vehicle, it can use its CACC car-following capability. If it is following a manual vehicle or an ACC vehicle, it acts like another ACC vehicle. The CACC car-following capability includes a faster response to changes by the car ahead and permits following at significantly shorter time gaps.

10.The Microsimulation Platform

The simulation is done on the platform of Aimsun, which is a transportation simulation environment developed by TSS (57). It contains microscopic and mesoscopic simulators, dynamic traffic simulator, macroscopic and static assignment models. It also offers extended tools for advanced investigation, like the Aimsun SDK (Software Development Kit), Aimsun API, and Aimsun MicroSDK. We used the Aimsun Microscopic Simulator, API, and microSDK in this project.

The Aimsun Microscopic Simulator (58) is the tool to construct traffic networks, define vehicle types and their basic properties, specify traffic demand and traffic control, and run the simulations. In this project, the geometry of the freeway and its speed limit, the four vehicle types and their properties, such as length and width, are defined in the Aimsun Microscopic Simulator.

The Aimsun API module (59) is an interface that allows external applications to access the internal data of Aimsun during simulation. The user can obtain all of the information during simulation, like the measurements of a detector or the state of a particular vehicle. The user can also control the traffic, like determining when and how a new vehicle enters the network. Thus Aimsun API is used to record the measurements of traffic flow and to control the entering of new vehicles to the network during simulation.

The Microscopic Model SDK (60) is the tool to implement new behavior models in the Aimsun simulation, replacing the default driver model in Aimsun. The new driver behavior is implemented by the plug-in, which is a DLL file generated after building some C++ files. During each simulation step, Aimsun calls the functions in the plug-in and updates the driver behavior based on the user-defined model. So the new detailed driver behavior models that we had to develop to represent manual driving, ACC and CACC vehicles were programmed in MicroSDK.

11. Control Algorithm of ACC/CACC Vehicles

The following variables are used to define the vehicle-following control algorithms for ACC or CACC vehicles in this section. It should be noted that these are simplified representations of the ACC and CACC car-following rules that were actually implemented on the test vehicles for the field test. The ACC car-following rules are proprietary to Nissan, while the CACC car following behavior has been described in the technical paper by Bu, Tan and Huang (61). Simpler representations were needed here for computational efficiency, because they need to be executed many times in each simulation, and also because the finer details of the actual car following dynamics of these systems were implemented for driver comfort but probably have little influence on traffic flow dynamics.

v : the speed of the controlled ACC/CACC vehicle (m/s).
v_d : the desired speed set by the driver, or the speed limit of the road (m/s).
v_e : the speed error (m/s).
a_{sc} : the acceleration by speed control (m^2/s).
s : the spacing between the controlled vehicle and its leading vehicle (m).
s_d : the desired spacing (m).
s_e : the spacing error (m).
h_d : the desired time gap (s).

Basically ACC and CACC vehicles have the same control algorithm. The only difference is they have different desired time gaps. There are two modes, speed control and gap control, in the ACC/CACC control algorithm. The goal of speed control is to keep the vehicle speed close to the speed limit, and that of gap control is to maintain the gap between the controlled vehicle and its leading vehicle to be the desired gap. Speed control is activated when the spacing to the preceding vehicle in the same lane is larger than 120 meters, and gap control is activated when the spacing is smaller than 100 meters. If the spacing is between 100 meters and 120 meters, the controlled vehicle retains the previous control strategy to provide hysteresis to avoid dithering between the two strategies.

In speed control, the control law is

$$v_e = v - v_d$$
$$a_{sc} = bound(-0.4 \cdot v_e, 2, -2)$$
$$a = a_{sc}$$

Where the function $bound()$ is defined as $bound(x, x_{ub}, x_{lb}) := \max(\min(x, x_{ub}), x_{lb})$. The values +2 and -2 are the maximum acceleration and deceleration of the vehicle under C/ACC control. This control law tries to eliminate the error between the vehicle speed and the speed limit of the road if the vehicle is in the speed control mode.

In gap control, the control law is

$$v_e = v - v_d$$
$$a_{sc} = bound(-0.4 \cdot v_e, 2, -2)$$
$$s_d = h_d \cdot v$$
$$s_e = s - s_d$$
$$a = bound(\dot{s} + 0.25 \cdot s_e, a_{sc}, -2)$$

The +2 and -2 here have the same meaning as in speed control. This control law forces the vehicle to approach its desired time gap set point in gap control. But the vehicle will still obey the speed limit in gap control, because if the commanded vehicle speed is larger than the speed limit, this law asks the vehicle to slow down, even if the current gap is larger than its desired gap.

12.Manual Driving Model

The following variables are used to explain the manual driving model in this section.

x_n^U and x_n^L : the upper bound and lower bounds for the driving distance (m).
τ : the wave travel time (s).
g_n^{jam} : the jam gap (m).
l : the length of the vehicle (m).
a : the acceleration of the vehicle (m^2/s).
v : the speed of the vehicle (m/s).
x : the position of the vehicle (m).
v^f : the free flow speed (m/s).

The manual driver behavior model is the NGSIM oversaturated freeway flow model developed by Yeo (62, 63). The NGSIM oversaturated freeway flow model contains the car-following model and lane-changing model. But we only use the car-following model, the CF mode in (62, 63), because there is no lane changing in the simulation. The basic car-following model of this model comes from Newell's linear model. It can be described as follows:

$$x_n(t+\Delta t) = \max\{x_n^U(t+\Delta t), x_n^L(t+\Delta t)\}$$
$$x_n^U(t+\Delta t) = \min\{x_{n-1}(t+\Delta t-\tau_n) - l_{n-1} - g_n^{jam}, x_n(t) + v_n(t)\Delta t + a_n^U \Delta t^2, x_n(t) + v_n^f \Delta t, x_n(t) + \Delta x_n^s(t+\Delta t)\}$$
$$x_n^L(t+\Delta t) = \max\{x_n(t) + v_n(t)\Delta t + a_n^L \Delta t^2, x_n(t)\}$$
$$\Delta x_n^s(t+\Delta t) = \Delta t\left(a_n^L \tau_n + \sqrt{(a_n^L \tau_n)^2 - 2a_n^L(x_{n-1}(t) - x_n(t) - (l_{n-1} + g_n^{jam}) + d_{n-1}(t)}\right)$$
$$d_{n-1}(t) = -\frac{v_{n-1}^2(t)}{2a_{n-1}^L}$$

This NGSIM oversaturated freeway flow model was calibrated by using the NGSIM data (64).

13.A Freeway Section Model with Simplified Road Geometry

The tested road is a one-lane straight freeway with speed limit of 120 km/h (73 mph). The freeway is 6.5 km long, and there is a detector located 6 km from the entrance. This location is selected to make sure all the flow measurements are in steady state. The freeway is empty before the simulation. During the simulation, the entering of new vehicles is controlled by the algorithm written in the API file, which will be described in the next paragraph. The total simulation length is 1 hour, and the simulation step is 0.1 second. The flow is recorded at intervals of 5 minutes, but the first measurement is discarded because the first 5 minutes are viewed as the warm-up time. The capacity is the average flow over the remaining 55 minutes.

The four types of vehicles have the same physical characteristics. The length is 4.7 meters and width is 1.9 meters. The maximum acceleration is 2 m/s^2 and maximum deceleration is -2 m/s^2.

In the simulation, the type of the next entering vehicle is randomly chosen, but follows the percentages defined in the simulation cases we want to test. The desired time gap of the entering vehicle is also random. For manual driving, the randomness is introduced by the randomness of g_n^{jam}.

We know that the maximum flow for manually driven vehicles on this type of simple freeway link should be about 2200 veh/h, so we assume the desired headway for manual driving is 1.64 sec (≈3600/2200). The desired time gaps of the ACC or CACC vehicles were selected based on the results of the field test (1-4), as shown in Figure 13.1:

ACC: 31.1% at 2.2 s time gap, 18.5% at 1.6 s time gap, 50.4% at 1.1 s time gap

CACC: 12% at 1.1 s time gap, 7% at 0.9 s time gap, 24% at 0.7 s time gap, 57% at 0.6 s time gap.

Note that the difference between headway and time gap needs to be accounted for by incorporating the incremental time needed to travel the vehicle length at the defined operating speed.

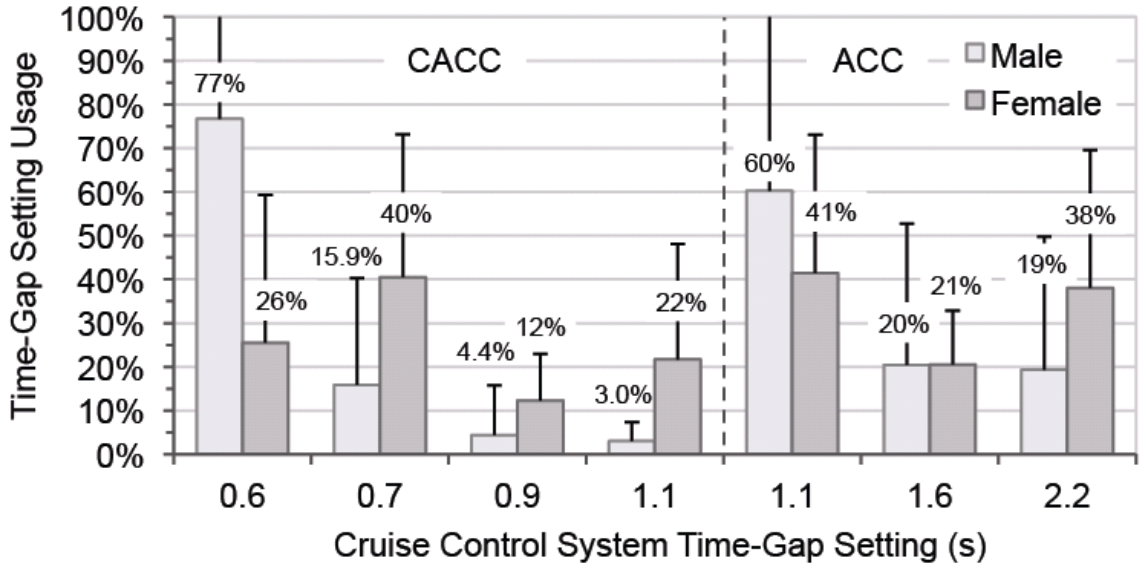

Figure 13.1 Distribution of time gap settings for CACC and ACC chosen by drivers while car following in field test

The desired entering headways for the ACC and CACC vehicles are chosen based on these time gaps, with the addition of the time increment to account for vehicle length. The gap for manual driving is selected randomly during the simulation, within a +/- 10% error range of 1.64 s, that is, from 1.48 to 1.8 sec. At each simulation step, we check the travel time from the entrance to the location of the last entering vehicle, based on the speed of that vehicle at that step. If this travel time is larger than the desired entering time gap, we let a new vehicle enter the freeway at the same speed as its leading vehicle at that step. By this algorithm, the vehicles enter the freeway at an interval and speed that will not generate a measured maximum flow lower than the real capacity due to insufficient demand, while preventing vehicle collision because of entering at too high a speed or too small a time gap.

Because the entering time gap for manually driven vehicles usually does not match its desired time gap, the manually driven vehicles need to adjust their speeds after they enter the freeway. This causes the vehicles following them, whether they are manual, ACC or CACC, to also need to adjust speeds. By this, we introduce small disturbances into the simulation. This means that the measured maximum flow should be achievable and stable in traffic with small disturbances.

14.Simulation Scenarios and Results

Simulation scenarios have been defined to represent diverse combinations of manually driven, ACC, CACC and HIA vehicles so that the effects of changes in market penetration of each kind of vehicle can be determined. For each scenario, three simulations were run with different random number seeds and the results of those simulations were averaged to produce the estimates of achievable traffic flow.

The all-manual case was already referenced as a base case with a nominal capacity of 2200 veh/hr per lane. When basic ACC vehicles are incorporated into the traffic stream, the achievable traffic flow appears to be remarkably insensitive to the market penetration of ACC vehicles, as shown in Figure 14.1. Note that the flow remains within the narrow range from 2031 to 2101 vehicles per hour regardless of the market penetration. This is a consequence of the driver preferences for ACC time gap settings being very similar to the time gaps that they adopt when they drive manually. It is important to note that this refutes the assumptions in some published papers (65) that contend that ACC could substantially increase highway capacity.

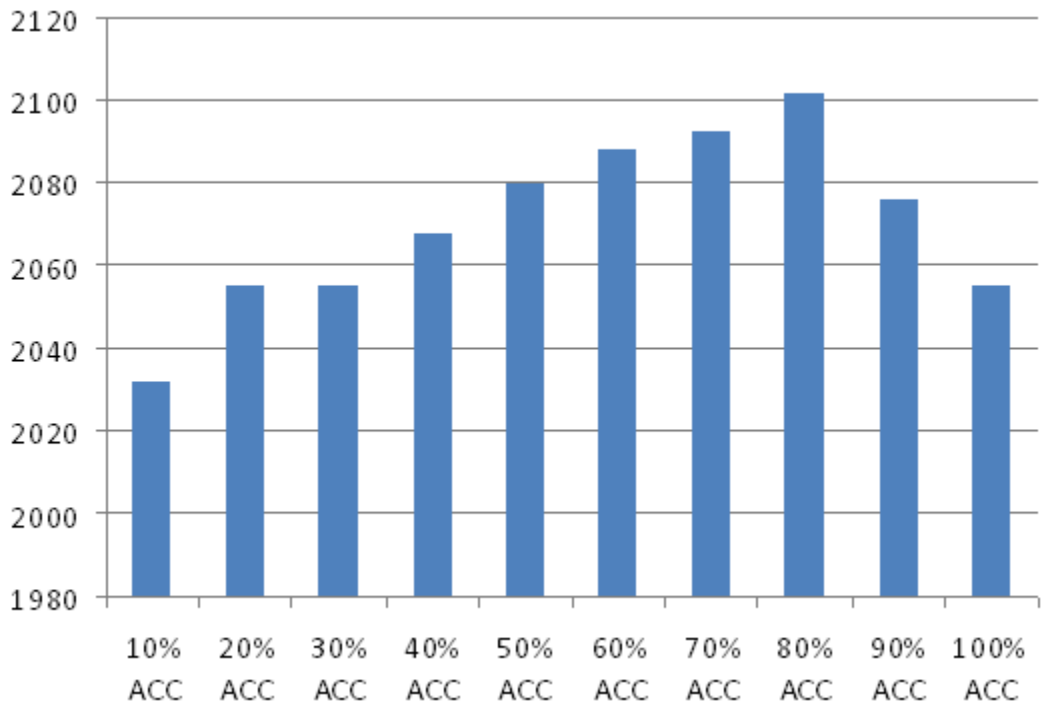

Figure 14.1 Highway Lane Capacity (Vehicles/Hour) as a Function of Changes in ACC Market Penetration

If we consider only the combinations of manually driven and CACC vehicles, the trend in highway lane capacity with respect to CACC market penetration is as shown in Figure 14.2. This has an obvious quadratic shape, based on the fact that the CACC vehicle can only use its CACC capability when it is following another CACC vehicle (or an HIA vehicle), but when it is following a manual vehicle it must revert to conventional ACC control. As a result of this, the capacity grows very slowly until the CACC market penetration becomes substantial, and then it grows much more rapidly. If all vehicles in a lane were equipped with CACC capability and the

drivers chose the same distribution of CACC time gaps as they chose in our field test, the lane capacity would increase to 3970 vehicles per hour, a very dramatic improvement.

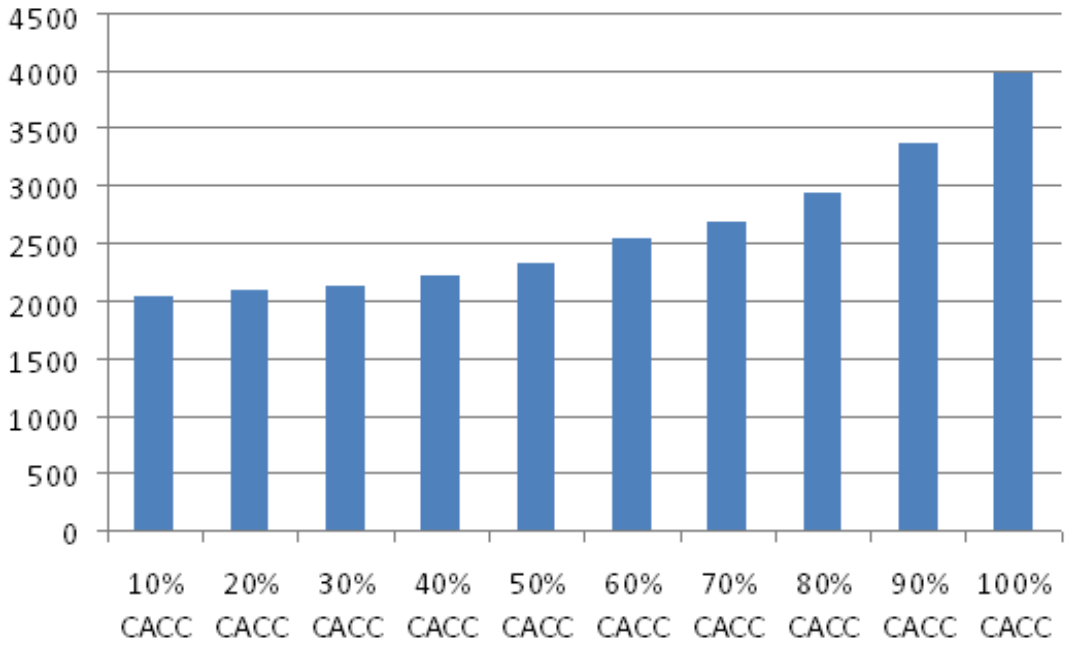

Figure 14.2 Highway Lane Capacity (Vehicles/Hour) as a Function of Changes in CACC Market Penetration Relative to Manually Driven Vehicles

One of the strategies being proposed in the Connected Vehicles initiative to improve performance of cooperative systems at low market penetrations is to equip as many existing vehicles as possible with a simple and inexpensive aftermarket positioning and communication Onboard Unit (OBU) that can broadcast a "Here I Am" (HIA) message. This message provides the basic GPS coordinates and vehicle speed and heading information so that the OBUs on other vehicles can detect the trajectory of the vehicle. This information, if it is sufficiently accurate, would enable and HIA equipped vehicle to be the leader for a CACC vehicle to follow at a short time gap. The effects of replacing the manually driven vehicles in the simulation cases of Figure 14.2 with HIA vehicles are shown in Figure 14.3. In this case, all the vehicles that do not have CACC are equipped with the HIA devices and can therefore serve as leaders for the CACC vehicles. With this change, the quadratic growth in Figure 14.2 becomes more nearly linear, and the capacity of the highway lane can be increased more significantly even at modest CACC market penetrations. At a 20% market penetration, the HIA addition increases capacity by 7%, at 30% market penetration it increases by more than 10% and in the 50% to 60% market penetration range the increase is in the range of 15% compared to the cases without HIA devices.

In our earlier studies of CACC, prior to the current project, we simulated the effects of the different combinations of ACC and CACC market penetrations, based on the assumption that the CACC vehicles would be driven at 0.5 s time gaps (66, 67). This produced a 3-D plot of achievable highway lane capacity that has been widely cited, and is reproduced here as Figure 14.4. The new simulation results, based on the time gaps that drivers actually chose in our field

test, are shown in Figure 14.5 and Table 14.1. These capacity estimates are somewhat lower, with the 80% CACC/20% ACC result now in the range of 3000 rather than 3500 vehicles per hour, for example.

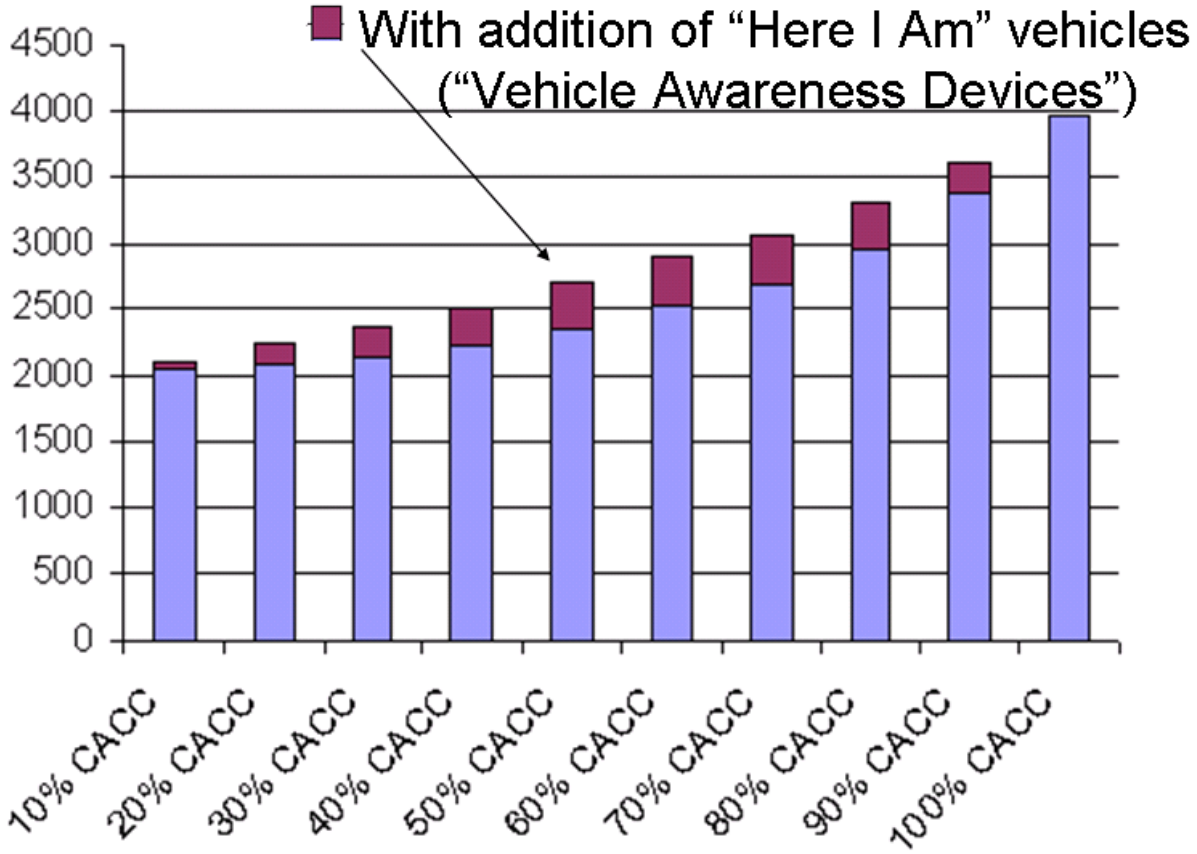

Figure 14.3 Highway Lane Capacity (Vehicles/Hour) as a Function of Changes in CACC Market Penetration Relative to "Here I Am" Vehicles and Unequipped Vehicles

The capacity effects of different combination of CACC vehicles and HIA vehicles (with the rest being manually driven) are shown in Figure 14.6 and Table 14.2. As the market penetration of CACC increases, the increasing capacity attributable to the additional HIA vehicles can be seen, but it is a relatively subtle effect. For completeness, the analogous results for different combinations of CACC vehicles and HIA vehicles (with the rest being conventional ACC vehicles) are shown in Figure 14.7 and Table 14.3. Since the effects on capacity of ACC and manually driven vehicles are very similar, these results do not differ much from the previous results.

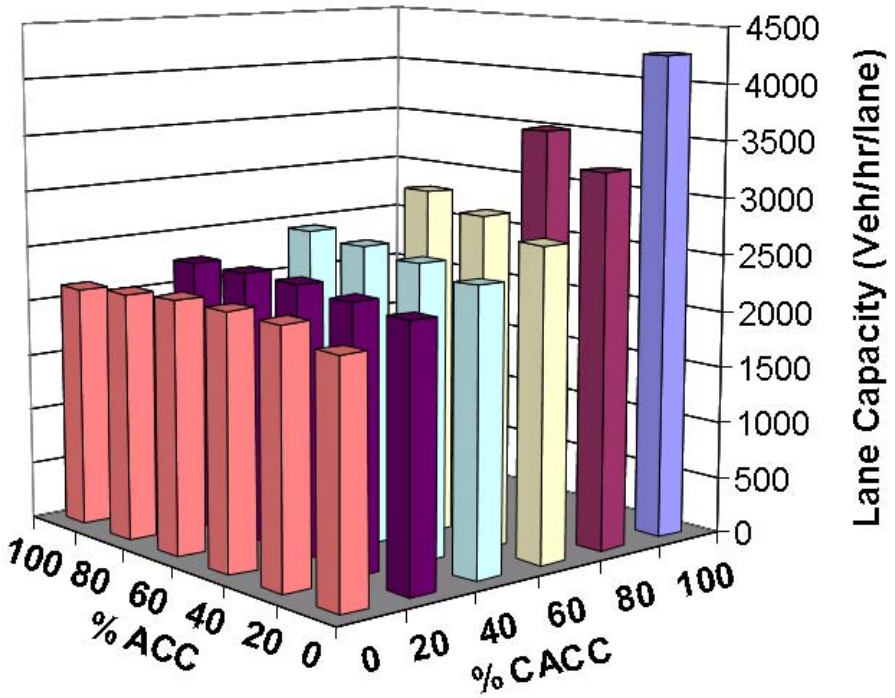

Figure 14.4 Original Prediction of Lane Capacity Effects of ACC and CACC Driven at 0.5 s Time Gap from 2001

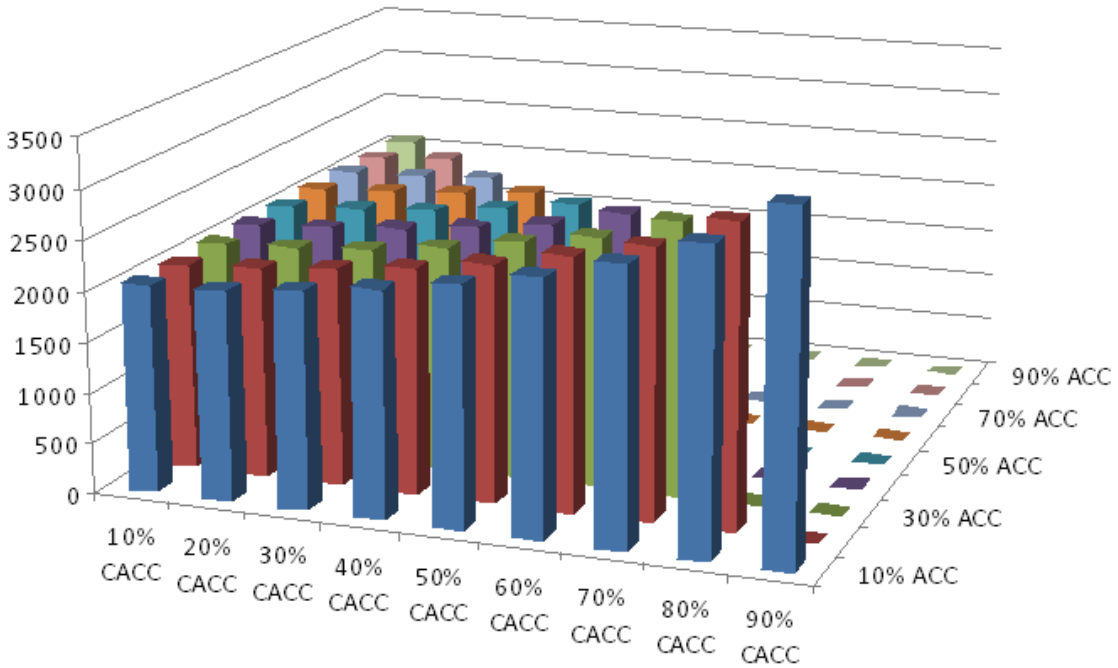

Figure 14.5 Updated Prediction of Lane Capacity Effects of ACC and CACC Driven at Time Gaps Chosen by Drivers in Field Test (With remaining vehicles manually driven)

Table 14.1 Updated Prediction of Lane Capacity Effects of ACC and CACC Driven at Time Gaps Chosen by Drivers in Field Test (With the remaining vehicles manually driven)

		Percentage of CACC Vehicles								
		10%	20%	30%	40%	50%	60%	70%	80%	90%
Percentage of ACC	10%	2065	2090	2170	2265	2389	2458	2662	2963	3389
	20%	2065	2110	2179	2265	2378	2456	2671	2977	0
	30%	2077	2127	2179	2269	2384	2487	2710	0	0
	40%	2088	2128	2192	2273	2314	2522	0	0	0
	50%	2095	2133	2188	2230	2365	0	0	0	0
	60%	2101	2138	2136	2231	0	0	0	0	0
	70%	2110	2084	2155	0	0	0	0	0	0
	80%	2087	2101	0	0	0	0	0	0	0
	90%	2068	0	0	0	0	0	0	0	0

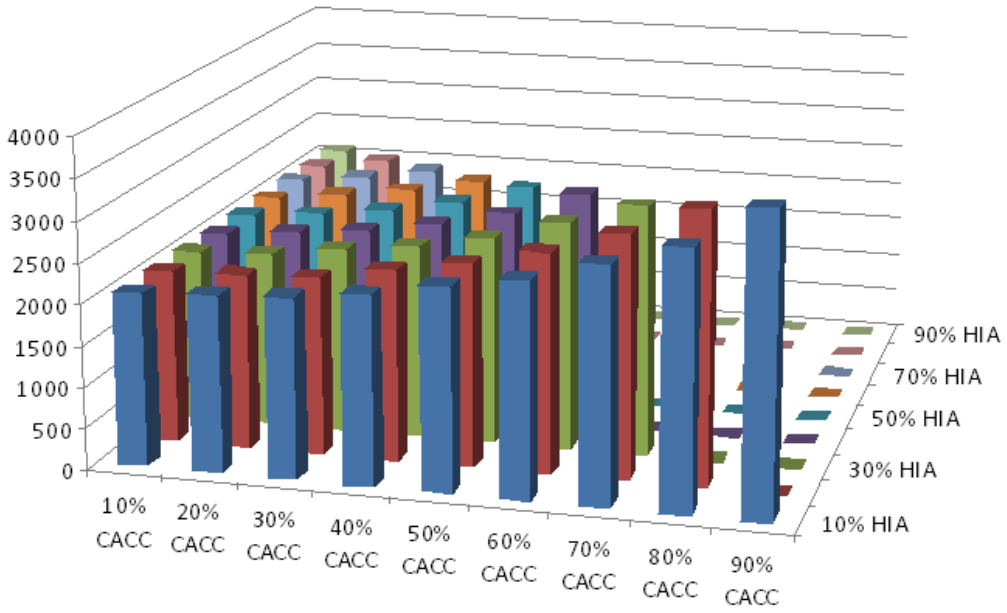

Figure 14.6 Prediction of Lane Capacity Effects of HIA and CACC Driven at Time Gaps Chosen by Drivers in Field Test (With the remaining vehicles manually driven)

Table 14.2 Prediction of Lane Capacity Effects of HIA and CACC Driven at Time Gaps Chosen by Drivers in Field Test (With the remaining vehicles manually driven)

		Percentage of CACC Vehicles								
		10%	20%	30%	40%	50%	60%	70%	80%	90%
Percentage of HIA Vehicles	10%	2086	2132	2168	2278	2443	2567	2831	3108	3624
	20%	2135	2164	2207	2366	2446	2669	2941	3303	0
	30%	2137	2193	2291	2364	2533	2775	3041	0	0
	40%	2128	2206	2302	2439	2588	2891	0	0	0
	50%	2139	2220	2324	2499	2685	0	0	0	0
	60%	2134	2239	2373	2545	0	0	0	0	0
	70%	2137	2245	2395	0	0	0	0	0	0
	80%	2132	2252	0	0	0	0	0	0	0
	90%	2123	0	0	0	0	0	0	0	0

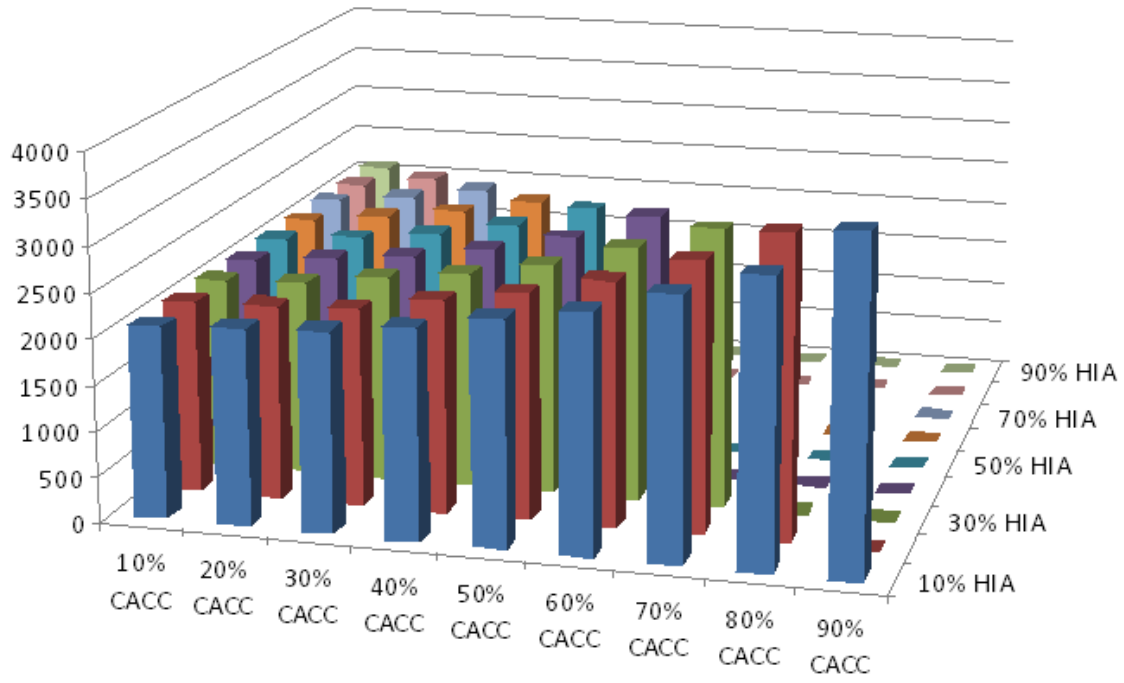

Figure 14.7 Prediction of Lane Capacity Effects of HIA and CACC Driven at Time Gaps Chosen by Drivers in Field Test (With the remaining vehicles being ACC)

Table 14.3 Prediction of Lane Capacity Effects of HIA and CACC Driven at Time Gaps Chosen by Drivers in Field Test (With the remaining vehicles being ACC)

		Percentage of CACC Vehicles								
		10%	20%	30%	40%	50%	60%	70%	80%	90%
Percentage of HIA Vehicles	10%	2045	2110	2179	2288	2447	2576	2760	3111	3624
	20%	2054	2125	2211	2323	2512	2671	2893	3303	0
	30%	2064	2148	2246	2378	2519	2787	3041	0	0
	40%	2073	2165	2282	2434	2611	2891	0	0	0
	50%	2084	2187	2318	2503	2685	0	0	0	0
	60%	2097	2206	2362	2545	0	0	0	0	0
	70%	2102	2227	2395	0	0	0	0	0	0
	80%	2114	2252	0	0	0	0	0	0	0
	90%	2123	0	0	0	0	0	0	0	0

15. Concluding Remarks about Cooperative Adaptive Cruise Control

The results reported here represent the first predictions of the effects of ACC and CACC on highway lane capacity that are founded on real experimental data, from drivers who have driven the suitably equipped vehicles and selected the time gap settings with which they were comfortable. These results show that conventional ACC is unlikely to produce any significant change in the capacity of highways, but CACC has the potential to substantially increase highway capacity when it reaches a moderate to high market penetration.

These results showed a maximum lane capacity of about 4000 vehicles per hour if all vehicles were equipped with CACC. If the vehicle population consists of CACC and HIA vehicles, meaning that all vehicles have been equipped with DSRC radios, the lane capacity increases approximately linearly from 2000 to 4000 as the percentage of CACC vehicles increases from zero to one hundred. On the other hand, if the vehicle population consists of manual and CACC vehicles, without any mandate for non-CACC vehicles to be equipped with DSRC, the increase in lane capacity follows a quadratic profile, lagging significantly behind at the intermediate market penetration values. Therefore, the capacity benefits of CACC can be accelerated, or obtained at somewhat lower market penetrations, if the rest of the vehicle population is equipped with HIA devices so that they can serve as the lead vehicles for the CACC vehicles.

References

1. Banks, J. H. The Two-Capacity Phenomenon: Some Theoretical Issues. *TRR 1320,* TRB, 1991, pp234–241.
2. Bertini, R. L., and M. T. Leal, Empirical Study of Traffic Features at a Freeway Lane Drop, *J. of Trans. Eng.*, 131(6), June 1, 2005, pp397-407
3. Cassidy, M. and R. Bertini, Some traffic features at freeway bottlenecks, *Transportation Research Part B*, 33, 1999, pp25-42
4. Hall, F. L., and K. Agyemang-Duah. Freeway Capacity Drop and the Definition of Capacity. *TRR 1320,* TRB, 1991, pp91–98.
5. Persaud, B., S. Yagar, and R. Brownlee. Exploration of the Breakdown Phenomenon in Freeway Traffic, *TRR 1634*, TRB, 1998, pp61-69
6. Zhang, L., and D. Levinson. Ramp Metering and Capacity of Active Freeway Bottlenecks, *83rd TRB Annual Meeting*, Washington, D.C., Jan. 2004.
7. Winick, R. M., D. Matherly, and D. Ismart, Examining the Speed-Flow-Delay Paradox in the Washington, DC Region: Potential Impacts of Reduced Traffic on Congestion Delay and Potential for Reductions in Discretionary Travel during Peak Periods, Final Report, FHWA-09-017, December, 2008
8. Brinckerhoff, P., Synthesis of Active Traffic Management Experiences in Europe and the United States, Final Report, Pub. #FHWA-HOP-10-031, March 2010
9. Lu, X. Y., T. Z. Qiu, P. Varaiya,R. Horowitz, and S. E. Shladover. Combining Variable Speed Limits with Ramp Metering for freeway traffic control, *American Control Conference*, Baltimore, Maryland, June 30 - July 2, 2010
10. Bogenberger, K., and A. May, Advanced Coordinated Traffic Responsive Ramp Metering Strategies, *California PATH Working Paper*, UCB-ITS-PWP-99-19, 1999
11. Zhang, M., T. Kim, X. Nie, W. Jin, L. Chu, and W. Recker. Evaluation of On-ramp Control Algorithms. *California PATH Research Report*, UCB-ITS-PRR-2001-36, Berkeley, CA., 2001
12. Scariza, J. R.. Evaluation of Coordinated and Local Ramp Metering Algorithms using Microscopic Traffic Simulation, *MSc. Thesis*, MIT, 2003
13. Papamichail I. and Papageorgiou M., Traffic-responsive linked ramp-metering control, *IEEE Transactions on Intelligent Transportation Systems*, Vol. 9, 2008, pp. 111-121
14. Papamichail I., Papageorgiou M., Vong V., and Gaffney J., HERO coordinated ramp metering implemented at the Monash Freeway, *CD 89th TRB Annual Meeting*, Washington, D.C. Jan. 10-14, 2010.
15. Papamichail I., Kotsialos A., Margonis I. and Papageorgiou M., Coordinated ramp metering for freeway networks - A model-predictive hierarchical control approach, *Transportation Research Part C* , Vol. 18, 2010, pp311-331
16. Lin, P.-W., K.-P. Kang, and G.-L. Chang. Exploring the effectiveness of Variable Speed Limit controls on highway work-zone operations, *Int. J. of Intelligent Transportation Systems*, vol. 8, 2004, pp155–168
17. Alessandri, A., A. D. Febbraro, A. Ferrara, and E. Punta. Nonlinear optimization for freeway control using variable-speed signaling, *IEEE Trans on Veh. Tech*, 48(6), 1999, pp2042-2052
18. Hegyi, A., B. D. Schutter, and H. Hellendoorn. Optimal coordination of variable speed limits to suppress shock waves, *IEEE Trans. on Intelligent Trans. Syst.*, vol. 6, 2005, pp102–112

19. Wang, H., W. Wang, X. Chen, J. Chen, and J. Li. Experimental features and characteristics of speed dispersion in urban freeway traffic, *86th TRB Annual Meeting,* Jan 2007, Washington D. C.
20. Papageorgiou, M., E. Kosmatopoulos, and I. Papamichail. Effects of Variable Speed Limits on motorway traffic, *TRR No. 2047, TRB*, 2008, pp37-48
21. Spiliopoulou, A. D., I. Papamichail, I., and M. Papageorgiou. Toll Plaza merging traffic control for throughput maximization, *J. of Transportation Engineering , ASCE*, 2010, pp67
22. Papageorgiou, M., (1983). Applications of Automatic Control Concepts to Traffic Flow Modeling and Control. Lect. *Notes in Control and Inf. Sc*., Berlin, Germany: Springer
23. Abdel-Aty, M., and A. Dhindsa. Coordinated use of Variable Speed Limits and Ramp Metering for Improving Safety on Congested Freeways, *86th TRB Annual Meeting*, Washington, D.C., January 21-25, 2007
24. Caligaris, C., S. Sacone, and S. Siri. Optimal ramp metering and variable speed signs for multiclass freeway traffic, *Proc. of European Control Conference*, Kos Greece, July 2-5, 2007
25. Alessandri, A., A. Di Febbraro, A. Ferrara, and E. Punta. Optimal control of freeways via speed signaling and ramp metering, *Control Engineering Practice*, vol. 6, 1998, pp771–780
26. Papamichail, I., K. Kampitaki, M. Papageorgiou, A. Messmer. Integrated Ramp Metering and Variable Speed Limit Control of Motorway Traffic Flow. CD-ROM of *17th IFAC World Congress*, Seoul, Korea, 2008
27. Hegyi, A., B. D. Schutter, and H. Hellendoorn. Model predictive control for optimal coordination of ramp metering and variable speed limits, *Transportation Research C*, vol. 13, 2005, pp185–209
28. Carlson R.C., Papamichail I., Papageorgiou M. and Messmer A., Optimal mainstream traffic flow control of large scale motorway networks, *Transportation Research Part C* , Vol. 18, 2010, pp193-212
29. Carlson R.C., Papamichail I., Papageorgiou M. and Messmer A., Optimal motorway traffic flow control involving variable speed limits and ramp metering, *Transportation Science* , Vol. 44, pp.238-253, 2010.
30. Brackstone, M., M. McDonald. Car-following: A Historical Review. *Transportation Research Part F: Traffic Psychology and Behaviour*, Volume 2, Issue 4, December 1999, P181-196
31. Ossen, S., S.P. Hoogendoorn, B.G.H. Gorte. Interdriver Differences in Car-Following A Vehicle Trajectory-Based Study. *Transportation Research Record #1965: Journal of the Transportation Research Board*, Washington D.C., 2006, P121-129
32. Brockfeld, E., R.D. Kuhne, P. Wagner. Calibration and Validation of Microscopic Models of Traffic Flow. *Transportation Research Record #1876: Journal of the Transportation Research Board*, Washington D.C., 2005, P179-187
33. Wilson, R.E.. An Analysis of Gipps's Car-following Model of Highway Traffic. *IMA Journal of Applied Mathematics*, 2006, P509-537
34. Rakha, H., W. Wang. Procedure for Calibration Gipps Car-following Model. *Transportation Research Record: Journal of the Transportation Research Board #2124*, Washington D.C., 2009, P113-124
35. Abdel-Aty, M., J. Dilmore, and A. Dhindsa. Evaluation of variable speed limits for real-time freeway safety improvement. *Accident Analysis and Prevention*, Vol. 38, 2006, pp 335-345

36. Park, B., and S. Yadlapati. Development and Testing of Variable Speed Limit Logics at Work Zones Using Simulation. Presented at *82nd Annual Meeting of the Transportation Research Board*, Washington, D.C., 2003.
37. Hasan, M., M. Jha, and M. Ben-Akiva, Evaluation of ramp control algorithms using microscopic traffic simulation, *Transportation Research Part C* 10, 2002, pp229–256
38. Daganzo, C. F. The Cell Transmission Model: A Dynamic Representation of Highway Traffic Consistent with the Hydrodynamic Theory. *Transportation Research, B*, 28(4), 1994, pp. 269-287.
39. Lu, X. Y., and A. Skabardonis, Freeway Traffic Shockwave Analysis: Exploring the NGSIM Trajectory Data, *TRB 86th Annual Meeting,* Washington, D.C., Jan 21-25, 2007
40. Lu, X. Y., P. Varaiya, and R. Horowitz. Fundamental Diagram modeling and analysis based NGSIM data, *12th IFAC Symposium on Control in Transportation System*, Redondo Beach, CA, Sept 2 - 4, 2009
41. X. Y. Lu, T. Z. Qiu, P. Varaiya, R. Horowitz, and S. Shladover, Combining Variable Speed Limits with Ramp Metering for freeway traffic control, *CD ROM of 2010 American Control Conference*, Baltimore, Maryland, June 30 - July 2, 2010
42. Chow, A. H. F., X. Y. Lu, Z. J. Qiu, S. Shladover, and H. Yeo. An empirical study of traffic breakdown for Variable Speed Limit and Ramp Metering control, *89th TRB Annual Meeting*, Jan10-14, 2009
43. Su, D., X. Y. Lu, P. Varaiya, R. Horowitz and S. E. Shladover, Integrated microscopic traffic control simulation and macroscopic traffic control design, accepted to *90th TRB Annual Meeting*, Washington, D. C., Jan. 23-27, 2011
44. J.F. Bonnans, J.Ch. Gilbert, C. Lemaréchal, and C.A. Sagastizábal. *Numerical Optimization: Theoretical and Practical Aspects* (second edition). Springer, 2006.
45.SQPLab:http://wwwrocq.inria.fr/~gilbert/modulopt/optimizationroutines/sqplab/sqplab.html, accessed on September 2009.
46. Coifman, B., Lyddy, D., and Sabardonis, A. The Berkeley Highway Laboratory- Building on the I-880 Field Experiment, Proc. IEEE ITS Council Annual Meeting, IEEE, 2000, pp 5-10.
47. Gipps, P. G.. A Behavioural Car-following Model for Computer Simulation. Transportation Research Part B: Methodological, Volume 15B, 1981, pp. 105-111.
48. Next Generation Simulation. http://ops.fhwa.dot.gov/trafficanalysistools/ngsim.htm. Accessed July 26, 2010.
49. Aimsun. http://www.aimsun.com/site/. Accessed July 26, 2010.
50. Freeway I80-W. *PeMS 10.3*.
51. Varaiya, P. (2009). *The Freeway Performance Measurement System (PeMS), PeMS 9.0: Final Report* (Technical Report UCB-ITS-PRR-2009-25). Berkeley, CA: California PATH, Institute of Transportation Studies, University of California, Berkeley.
52. Nowakowski, C., Shladover, S., Cody, D., Bu, F., O'Connell, J., Spring, J., Dickey, S., and Nelson, D. (2011). *Cooperative Adaptive Cruise Control: Testing Drivers' Choices of Following Distances* (Technical Report UCB-ITS-PRR-2011-01). Berkeley, CA: California PATH, Institute of Transportation Studies, University of California, Berkeley.
53. S.E. Shladover, X.-Y. Lu, D. Cody, C. Nowakowski, Z. Qiu, A. Chow, J. O'Connell, J. Nienhuis and D. Su, "Development and Evaluations of Selected Mobility Applications for VII", PATH Research Report UCB-ITS-PRR-2010-25. Available online at: http://database.path.berkeley.edu/reports/index.cgi?reqtype=displayrecord&record=1011

54. C. Nowakowski, S. E. Shladover, D. Cody, F. Bu, J. O'Connell, J. Spring, S. Dickey, and D. Nelson, "Cooperative Adaptive Cruise Control: Testing Drivers' Choices of Following Distances", PATH Research Report UCB-ITS-PRR-2011-01. Available online at: http://database.path.berkeley.edu/reports/index.cgi?reqtype=displayrecord&record=1032
55. Steven E. Shladover, Christopher Nowakowski, Jessica O'Connell and Delphine Cody, "Cooperative Adaptive Cruise Control: Driver Selection of Car-Following Gaps", *ITS World Congress,* Busan, Korea, November, 2010.
56. C. Nowakowski, D. Cody, J. O'Connell and S. E. Shladover, "Cooperative Adaptive Cruise Control: Driver Acceptance of Following Gap Settings Less Than One Second", *Human Factors and Ergonomics Society 54th Annual Meeting*, San Francisco, September 2010.
57. "Aimsun Users Manual", Transport Simulation Systems, July 2009.
58. "Microsimulator and Mesosimulator in Aimsun 6 User's Manual", Transport Simulation Systems, April 2009.
59. "Aimsun Microsimulator API Manual", Transport Simulation Systems, July 2009.
60. "Aimsun Microscopic Simulator Behavioural Models SDK, Transport Simulation Systems", May 2008.
61. F. Bu, H.-S. Tan and J, Huang, "Design and Field Testing of a Cooperative Adaptive Cruise Control System", *2010 American Control Conference*, Baltimore, MD.
62. Yeo, H. (2008). Asymmetric Microscopic Driving Behavior Theory, PhD thesis, University of California, Berkeley.
64. Yeo, H. et al. (2008). "Oversaturated freeway flow algorithm for use in next generation simulation", *Transportation Research Record, No. 2088*, Transportation Research Board, Washington, D.C., pp. 68–79.
64. Yeo, H. and Skabardonis, A. (2008). "Parameter estimation for NGSIM freeway flow algorithm", *ASCE AATT 2008*, Athens, Greece.
65. A. Kesting, M. Treiber, M, Schönhof and D. Helbing, "Adaptive Cruise Control Design for Active Congestion Avoidance", *Transportation Research Part C, Volume 16C*, No. 6, Dec. 2008, pp. 668-683.
66. J. VanderWerf, S.E. Shladover, M.A. Miller and N. Kourjanskaia, "Effects of Adaptive Cruise Control Systems on Highway Traffic Flow Capacity", *Transportation Research Record No. 1800*, Transportation Research Board, Washington DC, 2002, pp. 78-84.
67. Shladover, S; VanderWerf, J.; Miller, MA; Kourjanskaia, N; Krishnan, H, *Development and Performance Evaluation of AVCSS Deployment Sequences to Advance from Today'sDriving Environment to Full Automation*, California PATH Research Report UCB-ITS-PRR-2001-18. Available online at: http://database.path.berkeley.edu/reports/index.cgi?reqtype=displayrecord&record=619

Appendix A – Consent Materials

Informed Consent for Testing Driver Willingness to Follow
Traffic Control Center Recommendations to Aid in Smoothing Traffic Flow and Preventing Congestion

Welcome to the California PATH Research Program. PATH stands for Partners for Advanced Transit and Highways. We are part of the University of California at Berkeley and this project is under the direction of Professor Alex Skabardonis who is a Professor of Civil Engineering. I would appreciate your participation in my research study on driving behavior. In this research study, we wish to collect data about the way people drive when approaching traffic congestion, and we wish to test several strategies that have been shown in simulation to help reduce or prevent traffic congestion.

During this study you will be driving an Infiniti FX 45 on local roadways using an OEM Adaptive Cruise Control system that regulates both the vehicle's speed and the distance from your car relative to the car directly in front of you (this distance is called gap). The vehicle also contains a system that links to our traffic management center which will be monitoring traffic conditions on the freeway. This system will display recommendations about what speed and gap settings you should be using via a small display mounted on the dashboard. At no time during this study will you be asked to perform any driving actions that you feel are unsafe. When you receive a recommendation, you are only encouraged to follow the recommendation as closely as you feel is safe or prudent.

As a prerequisite to take part in this research, I will ask permission to inspect your driving record. Your record will be obtained either by having you fill out and mail a record request form to the California DMV or by consenting to an electronic check using a third party provider. I will look only for information about moving violations less than three years old and Driving Under the Influence (DUI). The driving records will be destroyed after the screening procedure regardless of whether or not you are selected (or choose) to participate in the research.

If you agree to take part in this research the study will last approximately 3 hours and will be conducted on weekdays between approximately 1 PM and 4 PM. For this research study you will meet a California PATH researcher at the Richmond Field Station on the day of the test. There are 5 phases to the experiment.

Phase 1: The first approximately 15 minutes of the study will be devoted to the pre-experiment paperwork, such as verifying your information and reading and answering questions about this consent form.

Phase 2: The second phase of the experiment will also require about 15 minutes. During this time, an experimenter will familiarize you with the test vehicle, the experimental systems, and protocol while sitting in the parking lot at California PATH.

Phase 3: The next phase of the experiment will take approximately 30 minutes. You will be given a chance to drive the vehicle and use the ACC system while driving on roads with light traffic. (Typically this will be a loop on I-80 from El Cerrito to Hercules and back.)

Phase 4: The main experiment will proceed once you are comfortable using the ACC system and will last for approximately 90 minutes. During this time you will make several loops through an area of higher density traffic. (Typically this will be a loop on I-80 from El Cerrito to Emeryville and back.) As you approach heaver traffic, the traffic control center will broadcast recommended gap and speed settings to your vehicle. According to our research, if enough vehicles were to follow these recommended settings, then it should prevent the traffic flow from breaking down into stop and go traffic. You are only asked to conFigure the vehicle to as close to the recommended settings as you feel are both safe and comfortable.

Phase 5: The final part of the experiment will be conducted after we return to California PATH and take approximately 15 minutes. You will be asked to fill out a short survey.

At the end of the test, you will receive a total of $55 in cash for your participation. There is no direct benefit to you from the research. We hope that the research will benefit society by improving our knowledge about driver behavior and using this knowledge to improve the development of advanced transportation concepts and prototypes.

During the experiment, video cameras will record the front and rear scene as well as your face, hands, and feet at all times. We will use these video recordings in order to assess the type of traffic you were in, and to verify actions that

were taken by you. You have the right to restrict the use of the video recordings made during this experiment, and you have the right to change your mind as to the extent of those restrictions or limitations. You can specify the authorized uses of your video recordings by filling out the attached video release form. Release of your recorded images is not a requirement to participate in this test; however, if consent is granted there is the chance that someone may be able to identify you based on your image.

All of the information that I obtain about you during the research will be kept confidential. I will not use your name or identifying information in any reports of my research. I will protect your identity and the information that I collect from you to the full extent of the law (this does not include subpoena). Unfortunately, with all research, there is a risk of a breach of confidentiality. Furthermore, should you be involved in an accident while driving the study car, the videotapes taken may be subpoenaed as evidence.

After this project is completed, I may make the data collected during your participation available to other researchers or use the data in other research projects of my own. If so, I will continue to take the same precautions to preserve your identity from disclosure. Your identity will not be released to other researchers.

This study presents minimal risk to you. The driving situations presented in this study will not be any more difficult or dangerous than one would encounter on a typical day. However, since the study involves driving a car, there is always the potential for a crash. If you are injured as a result of taking part in this study, care will be available to you. The costs of this care may be covered by the University of California depending on a number of factors. If you have any questions regarding this assurance, you may consult the Committee for Protection of Human Subjects, University of California, 2150 Shattuck Avenue, Rm. 313, Berkeley, CA 94704-5940, PH: 510-642-7461, email: subjects@berkeley.edu.

Vehicle insurance coverage will be provided by the University of California as long as the vehicle is used as described above. If you violate any of the laws of California or the terms outlined above while driving the Infiniti, the University's vehicle insurance coverage will not be in effect and you will be held liable for any damages. Passengers other than the experimenter will not be covered, which means that you cannot carry any passenger other than the experimenter while driving the research vehicles.

Your participation in this research is voluntary. You are free to withdraw from the study at any time without penalty/loss of any benefits to which you are otherwise entitled. If you decide to withdraw from the study before the completion, you will be paid a prorated amount based on the extent of your participation. If you have any questions about the research, you may contact the lead investigator, Christopher Nowakowski, at (510) 665-3673. You may also request a copy of this consent form for you records.

I have read and understood this consent form, and I agree to take part in the research.

_____
Participant's Name (*Please Print*)

_____ _____
Participant's Signature Date

_____ _____
PATH Researcher Obtaining Consent Date

Consent for Electronic DMV Records Check

By providing California PATH with the information below, I authorize California PATH, UC Berkeley, to use my personal information to check my DMV record using the online, third-party service, Volunteers Select Plus, offered by Choice Point. The company's privacy policies are available for you to review at the following websites:

http://www.volunteerselectplus.com/	http://www.privacyatchoicepoint.com/

The DMV record report generated by ChoicePoint will only be used to verify your eligibility to volunteer for this study. The researchers at California PATH can, at your request, provide you with a copy of the results of your electronic DMV records request. You also have the right under Section 1786.22 of the California Civil Code to contact ChoicePoint directly during normal business hours to obtain your file for your review. You may obtain such information as follows:

1. In person at a ChoicePoint office. You will need to furnish proper identification prior to receiving your file. You may have someone accompany you and should inform such person that they will also have to present reasonable identification. If you want ChoicePoint to disclose to or discuss your information with this third party, you may be required to provide a written statement granting ChoicePoint permission to do so.

2. By certified mail, if you make a written request (and provide proper identification) to have your file sent to a specified addressee.

3. By telephone, if you have previously made a written request and provided proper identification.

Electronic copies of our DMV records stored on ChoicePoint's servers are deleted 30 days after being requested. The information that you provided below and any electronic or paper copies of your DMV records held by California PATH will be destroyed 30 days after your participation in this research has been completed.

Name	
Address	
Date of Birth	
Social Security Number	
Driver's License Number	

_____ _____

Participant's Signature Date

☐ The participant provided the information above and consented to allow California PATH to perform the DMV record screening either by email (attached) or verbally over the phone.

_____ _____

PATH Researcher Obtaining Consent Date

Photographic, Audio, and/or Video Records Release Consent Form

As part of this project we will have made photographic, audio, and/or video recordings of you while you participated in the research. You have the right to restrict the use of the recordings made during this experiment, and you have the right to change your mind as to the extent of those restrictions or limitations. Release of your recorded images (beyond question 1) is not a requirement to participate in this test.
Please indicate below, the authorized uses of your photographic, audio, and video recordings. Although your name and personal information will always be kept confidential, whenever consent is granted to release your recordings, there is the chance that someone may be able to identify you based on your image. When possible, if the participant's face is not crucial to the point being made in the report or presentation, we will blur your face.

1. The records can be studied by research teams for use in this research project and future research projects.

   Photo: _____ Audio: _____ Video: _____
   initials *initials* *initials*

2. The records can be shown to subjects in other experiments.

   Photo: _____ Audio: _____ Video: _____
   initials *initials* *initials*

3. The records can be used for scientific publications.

   Photo: _____ Audio: _____ Video: _____
   initials *initials* *initials*

4. The records can be shown at meetings of scientists interested in the study of driving behavior

   Photo: _____ Audio: _____ Video: _____
   initials *initials* *initials*

5. The records can be shown in classrooms to students.

   Photo: _____ Audio: _____ Video: _____
   initials *initials* *initials*

6. The records can be shown in public presentations to nonscientific groups.

   Photo: _____ Audio: _____ Video: _____
   initials *initials* *initials*

7. The records can be used on television and radio.

   Photo: _____ Audio: _____ Video: _____
   initials *initials* *initials*

I have read the above descriptions and given my consent for the use of the records as indicated above.

_____ _____
Participant's Signature Date

Appendix B – Post-Experiment Questionaire

Congestion Speed Advisory Questionnaire

-Did you perceive the speed advisory to be safe to follow?
Always | Most of the Time | Sometimes | Never

-Were you able to follow the speed suggestions in the lane you were in?
Always | Most of the Time | Sometimes | Never

-Did you have to change lanes to follow the speed suggestions?
Always | Most of the Time | Sometimes | Never

-Using the Adaptive Cruise Control, which setting did you prefer?
Longest | Middle | Shortest

-How was the timing of the advisory in comparison to when the traffic slowed?

-How much slower were you comfortable going in relation to traffic?

-Were you familiar with adaptive cruise control prior to this study? Yes | No

-Were you familiar with variable speed limits prior to this study? Yes | No

-What are your thoughts on the concept of congestion variable speed advisory?

-How likely are you to comply with variable speed advisory information?

-How comfortable were you with the frequency of speed advisory?

-As a driver what preference in the frequency of speed increment steps would you prefer?

-If this information was available to you in your car would you use it…
-If it was optional to follow the speed advisory, not legally required? Yes | No
-If it was legally enforceable? Yes | No

-Do you have a preference on how the speed advisory information could be displayed?

-How would you feel about the recommended variable speed information automatically adjusting the set speed on the ACC system rather than as a separate speed advisory?

Appendix C – Driver Compliance with Advisory Speeds in Zones 1, 3, and 5

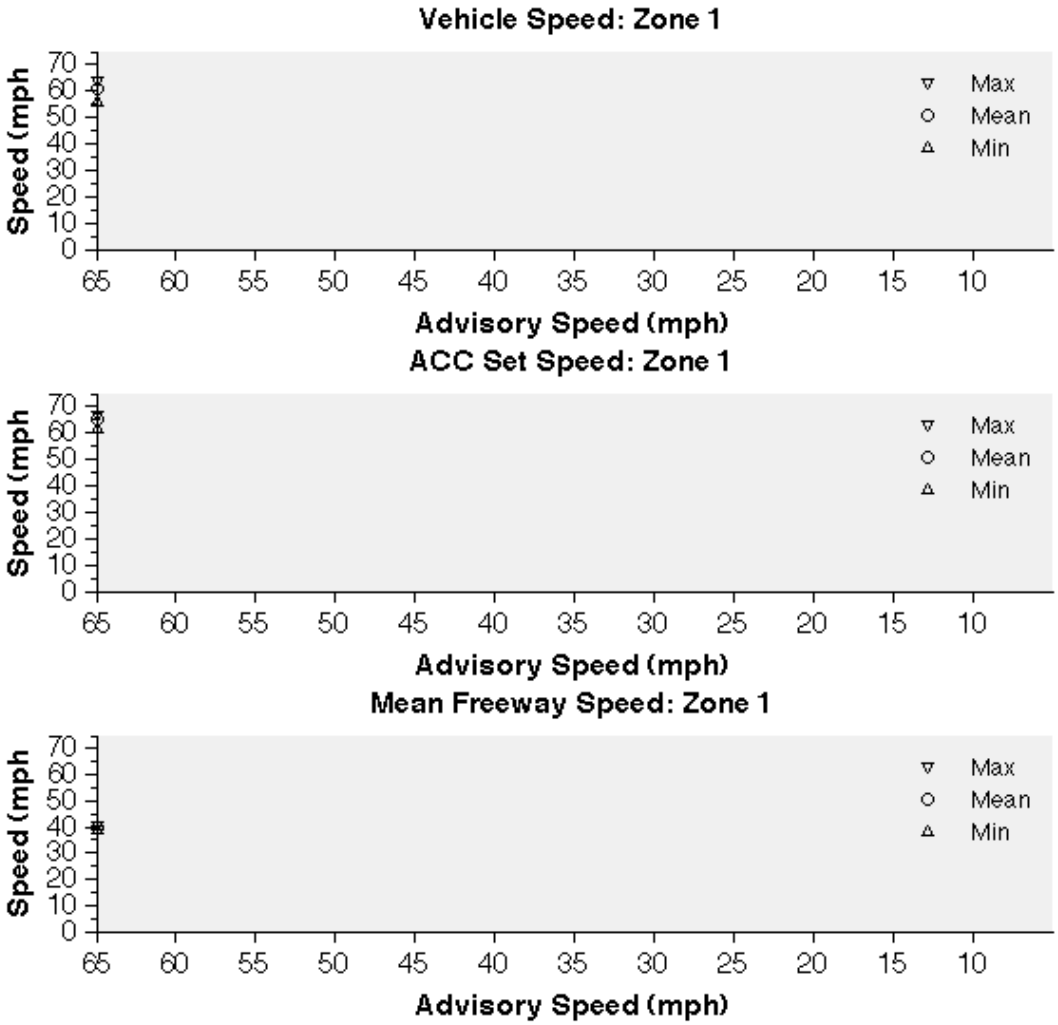

Figure C.0.1 Driver Compliance with Advisory Speeds in Zone 1.

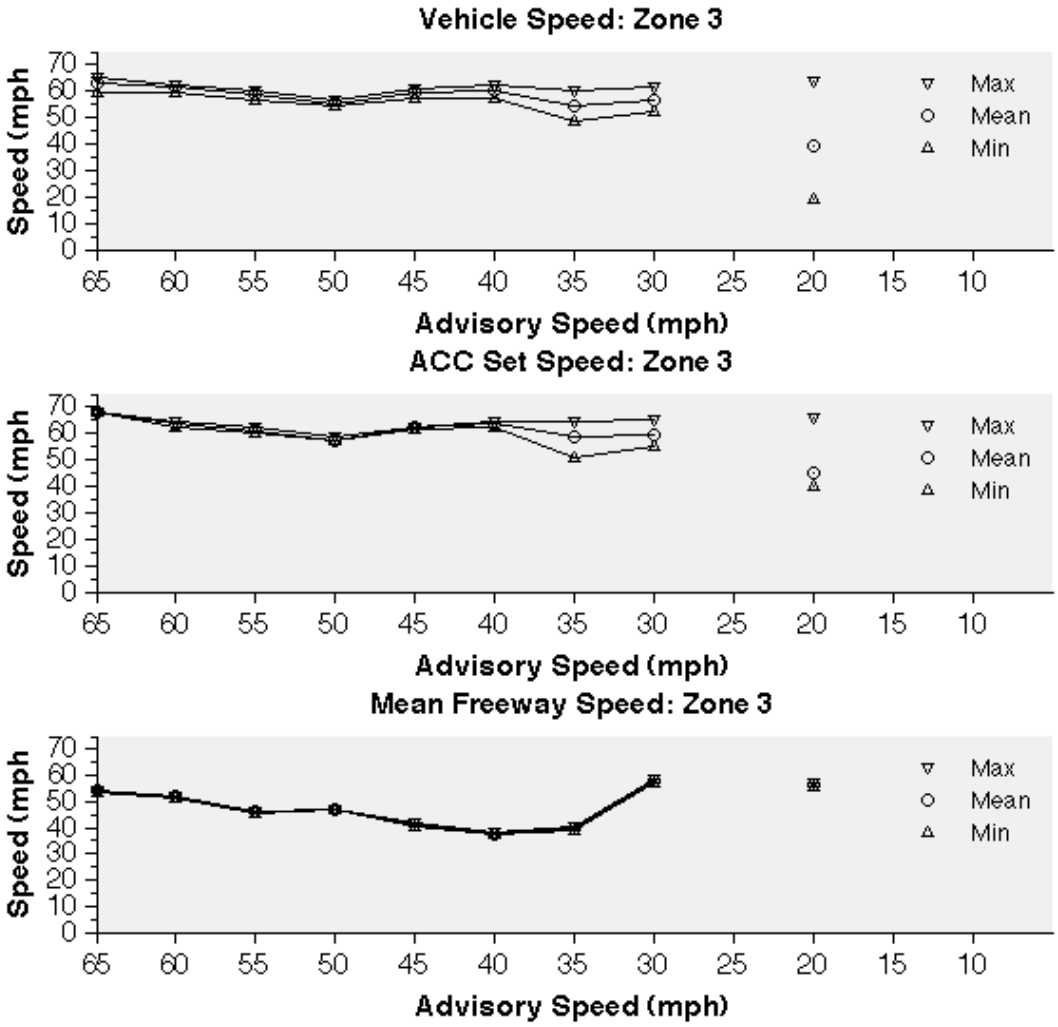

Figure C.0.2 Driver Compliance with Advisory Speeds in Zone 3.

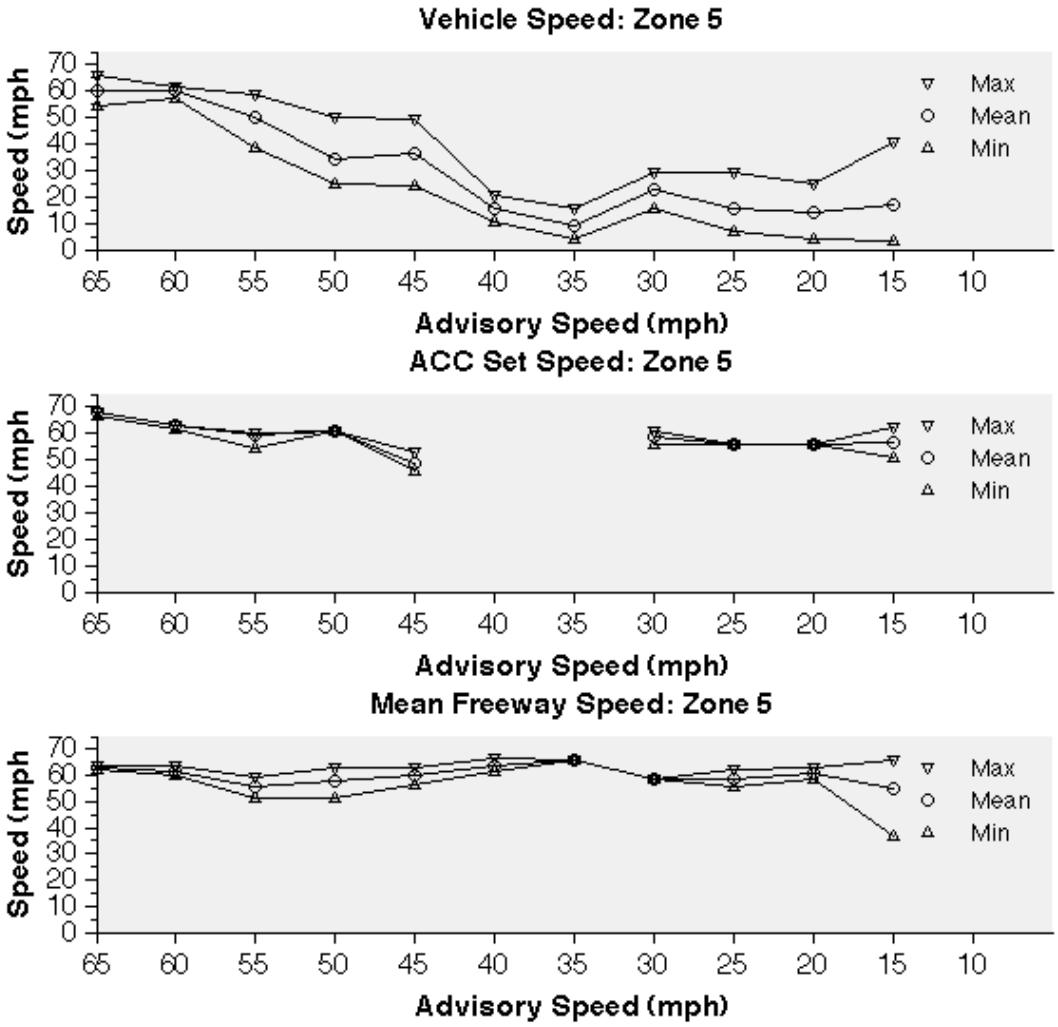

Figure C.3 Driver Compliance with Advisory Speeds in Zone 5.